

PRESSURE TRANSIENT ANALYSIS OF DATA FROM PERMANENT DOWNHOLE GAUGES

BY

MESHAL MOHAMMAD AL BURAIKAN

A Thesis Presented to the
DEANSHIP OF GRADUATE STUDIES

KING FAHD UNIVERSITY OF PETROLEUM & MINERALS

DHAHRAN, SAUDI ARABIA

In Partial Fulfillment of the
Requirements for the Degree of

MASTER OF SCIENCE

In

PETROLEUM ENGINEERING

December 2011

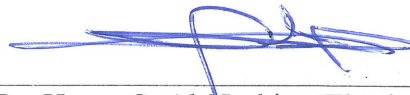
KING FAHD UNIVERSITY OF PETROLEUM & MINERALS

DHAHRAN31261, SAUDI ARABIA

DEANSHIP OF GRADUATE STUDIES

This thesis, written by **Mr. Meshal Mohammad Al Buraikan** under the direction of his thesis advisor and approval by his thesis committee, has been presented to and accepted by the Dean of Graduate Studies, in partial fulfillment of the requirements for the degree of **MASTER OF SCIENCE IN PETROLEUM ENGINEERING**.

Thesis Committee



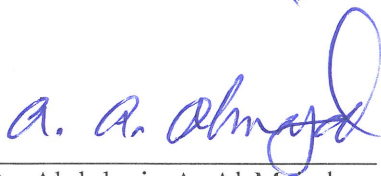
Dr. Hasan S. Al-Nashim (Thesis Advisor)



Dr. Hasan Y. Al-Yousef (Member)



Dr. Mohammad B. Issaka (Member)



Dr. Abdulaziz A. Al-Majed
(Department Chairman)



Dr. Salam A. Zummo
(Dean of Graduate Studies)



21/1/12

Date

DEDICATION

I would like to dedicate this work to my wife and my baby girl who filled my heart with joy.

ACKNOWLEDGEMENT

I would like to express my gratitude to Dr. Hasan S. Al-Hashim for his continuous guidance, advice and encouragement throughout the course of the study. Also, I would like to thank Dr. Hasan Y. Al-Yousef and Dr. Mohammed B. Issaka for their valuable support and advice.

TABLE OF CONTENTS

Acknowledgement	iv
Table of Contents	v
List of Figures	vii
List of Tables	x
Thesis Abstract (English)	xi
Thesis Abstract (English)	xiii
CHAPTER 1: Introduction	1
CHAPTER 2: Literature Review	4
CHAPTER 3: Mathematical and Physical Background	7
3.1: Pressure Transient Analysis	7
3.2: Digital Oil Field of the Future	12
3.3: Permanent Downhole Measurement Systems	14
3.4: Wavelvet Filtration	17
CHAPTER 4: Dynamic Pressure Transient Analysis Workflow	25
4.1: Field Setup	26
4.2: Automated Processes	27
4.2.1: <i>Mirroring</i>	27
4.2.2: <i>Data Reduction</i>	28
4.2.3: Event Detection and Alarming	29
4.3: <i>Manual Processes</i>	30
4.3.1: <i>Shut-in Detection</i>	31
4.3.2: <i>Data Quality Control</i>	33
4.3.3: <i>Analysis and Interpretation</i>	35
4.3.4: <i>Results Retention</i>	37

CHAPTER 5: Case Descriptions	38
5.1 Case 1: X-1	38
5.1.1 <i>Field Description</i>	38
5.1.2 <i>Well Description</i>	38
5.1.3 <i>Data</i>	38
5.1.4 <i>Analysis</i>	43
5.1.5 <i>Assessment of Data Interruption Effects</i>	55
5.2 Case 2: Y-2	62
5.2.1 <i>Field Description</i>	62
5.2.2 <i>Well Description</i>	62
5.2.3 <i>Data</i>	62
5.2.4 <i>Analysis</i>	65
5.2.5 <i>Assessment of Long Rate Stabilization Effects</i>	74
5.2. <i>Assessment of Minimum Duration Effects</i>	76
5.3 Case 3: Z-3	78
5.3.1 <i>Field Description</i>	78
5.3.2 <i>Well Description</i>	78
5.3.3 <i>Data</i>	78
5.3.4 <i>Analysis</i>	82
5.3.5 <i>Assessment of Minimum Duration Effects</i>	88
CHAPTER 6: Conclusion	94
REFERENCES	95
APPENDIX A: Data and Detailed Analysis Results	98
CURRICULUM VITAE	120

LIST OF FIGURES

<u>FIGURE</u>	<u>TITLE</u>	<u>PAGE</u>
Figure 3.1	Simplest example of scaling and wavelet functions.....	18
Figure 3.2	Schematic of a single-frequency wavelet algorithm	20
Figure 3.3	Schematic of complete wavelet algorithm	21
Figure 3.4	Real scaling and wavelet functions.....	22
Figure 4.1	Dynamic PTA workflow.....	25
Figure 4.2	Example of initial field setup for PTA workflow	27
Figure 4.3	Example of PDHMS data noise and outlier removal using wavelet algorithm.....	29
Figure 4.4	Example of alarm setup	30
Figure 4.5	Semi-automatic method that detects multiple pressure buildup periods	32
Figure 4.6	Quick-look diagnostic plots for pressure buildup analysis	33
Figure 4.7	Setup for recreating production rate data to synchronize with shut-in	34
Figure 4.8	Setup composite plot showing rate before and after applying shut-in condition	35
Figure 4.9	Multiple pressure buildup analysis using PDHMS data	36
Figure 5.1	Formation analysis and directional logs for X-1	40
Figure 5.2	Cross section of X-1	41
Figure 5.3	Rate and pressure data obtained from well X-1	42
Figure 5.4	Well parameters	51
Figure 5.5	Reservoir parameters	52
Figure 5.6	Rate and pressure data obtained from well X-1 and compared to the model	53
Figure 5.7	Log-log analysis of the last buildup compared to ideal horizontal well response	54

<u>FIGURE</u>	<u>TITLE</u>	<u>PAGE</u>
Figure 5.8	Semilog analysis of the last buildup for X-1	55
Figure 5.9	X-1 frozen data	56
Figure 5.10	Effect of data interruption on X-1 log-log analysis	57
Figure 5.11	Overlay of X-1 buildups in log-log analysis	58
Figure 5.12	Data loss in the early time of pressure buildup	59
Figure 5.13	Effect on log-log analysis of data loss in the early time of pressure buildup	59
Figure 5.14	Data loss in the middle time of pressure buildup	60
Figure 5.15	Effect on log-log analysis of data loss in the middle time of pressure buildup	60
Figure 5.16	Data loss in the late time of pressure buildup	61
Figure 5.17	Effect on log-log analysis of data loss in the late time of pressure buildup	61
Figure 5.18	Y-2 well trajectory, formation tops, and formation analysis logs	63
Figure 5.19	Y-2 well cross section	64
Figure 5.20	Rate and pressure data obtained from well Y-2	65
Figure 5.21	Well parameters	69
Figure 5.22	Reservoir parameters	70
Figure 5.23	Pre-stimulation log-log analysis for Y-2 compared to ideal horizontal well	71
Figure 5.24	Post-stimulation log-log analysis for Y-2 compared to ideal horizontal well	72
Figure 5.25	Comparison of pre- and post-stimulation log-log analysis for Y-2	73
Figure 5.26	Rate changes on Y-2 before shut-in for pre-acid pressure buildup	74
Figure 5.27	Y-2 log-log analysis overlay of original case vs. stabilized rate	75
Figure 5.28	Rate changes on Y-2 before shut-in for post-acid pressure buildup	76
Figure 5.29	Y-2 log-log analysis overlay of original case vs. last production rate	77
Figure 5.30	Z-3 formation analysis logs	79

<u>FIGURE</u>	<u>TITLE</u>	<u>PAGE</u>
Figure 5.31	Z-3 well cross section	80
Figure 5.32	Rate and pressure data obtained from well Z-3	81
Figure 5.33	Z-3 log-log analysis	84
Figure 5.34	Comparison between Z-3 log-log analyses with nearby well A-105	86
Figure 5.35	Well parameters	87
Figure 5.36	Reservoir parameters	88
Figure 5.37	Z-3 Horner plot	89
Figure 5.38	Log-log analysis of Z-3 with Horner approximation	90
Figure 5.39	Log-log analysis of Z-3, with the Cinco approximation 40% + tpe	91
Figure 5.40	Z-3 log-log analysis of the base case, Horner, and Cinco approaches	92
Figure 5.41	Z-3 analysis of base case, Horner, and Cinco, compared with a shorter rate history	93

LIST OF TABLES

<u>TABLE</u>	<u>TITLE</u>	<u>PAGE</u>
Table 3.1	Data Measurement Points	8
Table 3.2	Well Test Objectives	10
Table 5.1	Equations for Analyzing Flow in Horizontal Well	44

THESIS ABSTRACT

NAME: MESHAL MOHAMMAD AL BURAIKAN
TITLE: PRESSURE TRANSIENT ANALYSIS OF DATA FROM
PERMANENT DOWNHOLE GAUGES
MAJOR FILED: PETROLEUM ENGINEERING
DATE OF DEGREE: DECEMBER 2011

In the recent years there has been a significant growth in the number of Permanent Downhole Measurement System (PDHMS) installations in oil and gas fields around the world, as PDHMS prices have been falling steadily and their reliability has also been increasing.

However, the full benefits of this investment can only be realized when it is taken from simple surveillance and monitoring to a source for reservoir characterization. This study assess systems and workflows that have been put in place to transform the massive amounts of data, including pressure, flow rate and temperature, into actionable information to improve field development and performance. This study presents a dynamic real-time well testing workflow using data from real cases from intelligent fields discuss the applicability of pressure transient analysis utilizing I-Field real-time data from Permanent Downhole Gauges to characterize reservoir and well performance.

The study investigates the following aspects:

1. Develop a workflow for efficient utilization of the real-time data for pressure transient analysis.
2. Assess the rate effects on establishing reliable analysis;
 - Minimum duration
 - Long stabilization
 - Data Interruptions

Actual real-time PDHMS and Multi-Phase Flow Meters (MPFM) data was used and analyzed to determine reservoir parameters and evaluate well performance. This study highlights some of the challenges in using real-time data from PDHMS and MPFM. Diamant[®] application has been used to filter, and manage the real-time data and Saphir[®] application was used for modeling and analysis.

خلاصة الرسالة

اسم الطالب : مشعل محمد ناصر البريكان

عنوان الرسالة : تحليل معلومات المجسات الدائمة لأغراض إختبار الآبار

التخصص : هندسة البترول

تاريخ الدرجة : صفر 1433هـ

شهدت السنوات القليلة الماضية إعتتماداً متزايداً من شركات النفط والغاز لتثبيت مجسات دائمة في أعماق آبارها , حيث تحسنت وازدادة إعتماضية هذا النوع من المجسات وفي نفس الوقت إنخفضت أسعارها بشكل ملحوظ مما شجع على الإستثمار بتركيبها بشكل موسع في حقول النفط لمراقبة التغير بضغط المكامن بشكل عام. وزيادة على ذلك , تكمن الفائدة الأكبر من الأستثمار بتجهيز الحقول بهذا النوع من المجسات بإستخدامها لتشخيص أداء الآبار وتوصيف المكامن.

هذه الدراسة تعرض الأنظمة وطرق العمل المتبعة لمعالجة كمية البيانات الهائلة الواردة من تلك المجسات الدائمة وتحويل المعلومات إلى قرارات لتحسين أداء الحقول. تقدم هذه الدراسة مقترحات لأنظمة عمل ديناميكية للإستفادة من تلك المجسات لإختبار الآبار , وتعرض هذه الدراسة حالات واقعية لإستخدام هذه الأنظمة.

وتهدف الدراسة إلى تقديم الجوانب التالية:

- تقديم طريقة عمل للإستفادة من المعلومات الواردة من المجسات دائمة في أعماق الآبار في مجال إختبار الآبار.
- دراسة تأثير معدلات الإنتاج على نتائج إختبارات الآبار من نواحي المدة الزمنية اللازمة و ثبات معدلات الإنتاج و إنقطاع المعلومات أثناء الأختبار.

وفي هذه تم إستخدام بيانات واقعية لضغط الآبار المزودة بالمجسات الدائمة وكذلك لقراءات عدادات الإنتاج المصاحبة في الحقول التي تمت دراستها لتقييم أداء تلك الآبار وتشخيص مكانها. وأوضحت هذه الدراسة بعض التحديات والصعوبات في إستغلال وتحليل تلك المعلومات. تم إستخدام برنامج Diamant لإدارة ومعالجة البيانات و برنامج Saphir لإجراء تحاليل إختبارات الآبار.

درجة ماجستير العلوم

جامعة الملك فهد للبترول والمعادن

الظهران – المملكة العربية السعودية

التاريخ: صفر 1433

CHAPTER 1

INTRODUCTION

The last several years have seen an explosion in the number of permanent downhole measurement system (PDHMS) installations in oil and gas fields around the world. While PDHMS prices have been falling steadily, their reliability has also been increasing. Major exploration and production (E&P) companies have been investing heavily in the acquisition of real-time data from their fields. Many more installations are scheduled in the coming years.

The history of PDHMS installations worldwide dates back to the 1960s, when they were used mostly for operational purposes such as monitoring pumps and downhole equipment (Nestlerode, 1963). However, PDHMS installations were not very common until the early 1990s, when early stage applications in the North Sea showed that PDHMSs could be a good source of information for reservoir surveillance and management. As the reliability of PDHMS installations increased, their use became more widespread.

However, the full benefits of this investment can only be realized when it is taken from simple surveillance and monitoring to a source for reservoir characterization. Systems and workflows need to be put in place to transform the massive amounts of data—including pressure, flow rate, and temperature—into actionable information to improve field development and performance.

PDHMSs are becoming an integral part of new intelligent field (I-Field) development plans, but the actual real-time data collected through these systems are not fully utilized. To evaluate and analyze these data to characterize reservoir evaluation and well performance, a dynamic real-time well testing workflow was developed using data from actual I-Fields. Some data quality issues were encountered, and many benefits were realized. Also, a methodology was developed for pressure transient analysis (PTA) utilizing I-Field data from permanent downhole gauges.

With the wide adaptation of I-Fields, PDHMSs became a significant source of information to capture real-time reservoir pressure response. PDHMSs, coupled with multiphase flow meters (MPFMs), can also provide far more value by translating their data into reservoir characterization information. Occasional field and well shut downs result in buildups that may be called "free well tests," which can be utilized to provide vital information about the field and well performance and evolution through time. An established workflow is required to manage the real-time data in terms of denoising, filtering, storage, and retrieval, which are essential to attaining the maximum benefit from the instrumentation investments.

Cases were investigated to reveal the use of permanent downhole pressure gauges for reservoir characterization and well performance evaluation with PTA. The following steps were taken:

1. Develop a workflow for efficient utilization of the real-time data for PTA.
2. Assess the rate effects on establishing reliable analysis:
 - i. Minimum duration
 - ii. Long stabilization

iii. Data interruptions

Actual real-time PDHMS and MPFM data were used, and field, reservoir, and well data were assessed and validated, during which challenges were encountered. These data were then analyzed to determine reservoir parameters and evaluate well performance. The Diamant[®] application was used to filter and manage the real-time data, and the Saphir[®] application was used for modeling and analysis.

CHAPTER 2

LITERATURE REVIEW

Probably the first paper to discuss the use of permanently installed bottomhole pressure gauges is by W.A. Nestlerode (1963). Nestlerode aims to identify potential operation problems and to get some necessary reservoir data for effective control with less than one pressure point per day. More recent literature is summarized in the following paragraphs.

Athichanagorn et al. (1999) present a methodology and sequential steps for data acquired with permanent downhole pressure gauges. A variety of wavelet algorithms are discussed to denoise the data and provide reliable pressure transient identification.

Ortiz et al. (2009) tested several wavelet denoising techniques on a large volume of PDHMS data. The effect of several factors, such as wavelet type, threshold, and resolution level, are discussed. The paper classifies and rates each technique and variation for efficiency comparison.

Chorneyko (2006) presents the operational perspective of permanent downhole pressure gauges. The author presents practical cases of information obtained and reservoir management decisions derived from the PDHMS. The author also highlights the ever-increasing number of gauge installations in his company, specifically, and across the industry as a whole. The author stresses the fact that such a sizeable investment requires active stewardship to realize effective utilization.

de Oliveira Silva and Kato (2004) present a successful case of utilizing a PDHMS to identify barrier and inter-reservoir connectivity, which eliminated the need for workovers or survey services. This paper illustrates how a PDHMS can be a vital tool to achieve sound reservoir management, completion, and production decisions. More can be attained with more improvement in PDHMS data management and treatment tools.

From a publication in the SPE Distinguished Author Series, Horne (2007) discusses methods and algorithms to manage and interpret permanent downhole pressure gauge data for the industry to make the best use of these abundant sources of data. The author highlights the need to store the PDHMS data in a manner that allows efficient access and recovery. Also, the author stresses that the problems are not yet fully solved, and research in this area is appropriately active, where the need for a set of reliable automated algorithms will be necessary to gain maximum advantage.

Ouyang and Kikani (2002) discuss some improvement to PDHMS data processing. A new formula to automatically identify pressure transient periods is proposed, and polytope regression for noise level identification and outlier removal techniques are discussed.

Suzuki and Chorneyko (2009) presented a new method for automatic pressure buildup detection from PDHMSs. The new method analyzes the pressure response for specific patterns and the change of specific pressure over the change of a specific time window to identify the start of the buildup or drawdown. The authors tested this new method on field cases with positive results.

Yang Liu, and Roland N. Horne (2011) presented an interpretation approach for pressure and flow rate data from permanent downhole gauges using data mining. The aim was to

obtain a reservoir model using pressure and flow rate data from the PDHMS and nonparametric data mining algorithm. Noisy synthetic data and the real field data were used to test this approach. The method was able to recover the reservoir model successfully. Even at the extreme cases when the flow rate data are very noisy and changing frequently, and in the absence of any shut-ins, the method was still able to extract the reservoir models

Olivier Houzé, Olivier Allain, Bruno Josso (2011) presented the use of a new generation of wavelets, allowing a more accurate processing. The objectives were to reduce the volume of data without losing valuable information, remove outliers, and identify build-ups and re-allocate production. This paper also presents a new method using tangents crossing, which successfully replaces the failing wavelets for identify build-ups and re-allocate production.

In the literature, there is evident focus on PDHMS data denoising, filtration, and events detection. There are very limited publications on the utilization of these data in reservoir characterization and well performance evaluation, which this study focuses on.

CHAPTER 3

MATHEMATICAL AND PHYSICAL BACKGROUND

To provide general knowledge and a wide perspective on subjects directly related to this study, technical details are presented in abstracted and simplified forms.

3.1 Pressure Transient Analysis

Well testing, or PTA, has come a long way since the first drill stem test was run in 1926. From a simple composite packer and valve run on drill string, the scope of well testing has blossomed into a broad array of sophisticated downhole and surface technologies.

Every E&P company wants to know what type of fluids its well will produce, what flow rates the well will deliver, and how long production can be sustained. Given the right planning, technology, and implementation, well testing can provide many answers to these important questions. In one form or another, well testing has been used to determine reservoir pressures, distance to boundaries, areal extent, fluid properties, permeability, flow rates, drawdown pressures, formation heterogeneities, vertical layering, production capacity, formation damage, productivity index, completion efficiency, and more (Al-Dhubaib et al., 2008a)

By measuring in-situ reservoir conditions and fluids as they flow from the formation, the testing process gives access to a variety of dynamic and often unique measurements.

Depending on the scale of a test, some parameters are measured at multiple points along the flow path, allowing engineers to compare downhole pressures, temperatures, and flow rates against surface measurements (**Table 3.1**). Through well testing, operators can extract reservoir fluid samples, both downhole and at the surface, to observe changes in fluid properties and composition between the perforation and the wellhead. This information is vital to predict the future behavior of a reservoir or well completion (de Oliveira Silva and Kato, 2004).

Table 3.1: Data Measurement Points

Wellhead		Pressure, temperature, and rate (if equipped with flow meter)
Choke manifold		Pressure and temperature
Downhole recording		Pressure and temperature
Wireline tools		Pressure, temperature, flow rates, and samples across single- or multiple-depth portfolios
Separator		Pressure, temperature, rates (oil, water, and gas), shrinkage factors, specific gravities (oil and gas), and fluid samples

In its most basic form, a well test records changes in downhole pressure that follow a change in flow rate. Often, downhole pressures and temperatures, surface flow rates, and samples of produced fluids are obtained (Horne, 1990).

Well testing using PTA objectives changes with each stage in the life of a well and its reservoir. During the exploration and appraisal phase, well testing helps ascertain the size of a reservoir and its permeability and fluid characteristics. This information, along with pressures and production rates, is used to assess the deliverability and commercial viability of a prospect, and it is critical for booking reserves. Fluid characteristics are particularly important during the early stages of a prospect's evaluation, when E&P

companies need to determine the type of process equipment they must install to treat and move produced fluids from the wellbore to the refinery. During development, the focus shifts from assessing deliverability and fluid type to evaluating pressure and flow and ascertaining compartmentalization within the reservoir. This information is needed to refine the field development plan and optimize placement of subsequent wells. During the production phase, well tests are conducted to evaluate completion efficiency and diagnose unexpected change in production. These tests assist in determining whether production declines are caused by the reservoir or by the completion. Later in the life of the reservoir, these results will prove crucial for assessing subsequent secondary recovery strategies (de Oliveira Silva and Kato, 2004).

PTA for well testing can be generally classified as either productivity or descriptive tests. Productivity tests are carried out to obtain representative samples of reservoir fluids and to determine fluid-flow capacity at specific reservoir static and flowing pressure. On the other hand, descriptive tests are needed to estimate a reservoir's size and flow capacity, analyze horizontal and vertical permeability, and determine reservoir boundaries (**Table 3.2**). Productivity testing typically seeks to obtain stabilized bottomhole pressures over a range of different flow rates. Successive rate changes are made by adjusting choke size, which is not done until continual measurements have determined that bottomhole pressures and temperatures have stabilized.

Unlike testing to obtain stabilized bottomhole measurements, descriptive tests require transient pressure measurements. Pressure transients are induced by step changes in surface production rates and can be measured by a bottomhole pressure sensor or permanent downhole pressure gauges. The changes in production cause pressure

perturbations that propagate from the wellbore to the surrounding formation. These pressure pulses are affected by fluids and geological features within the reservoir. While they might travel straight through a homogeneous formation, these pulses may be hindered by low-permeability zones or may vanish entirely when they enter a gas cap. By recording wellbore pressure response over time, the operator can obtain a pressure curve that is influenced by the geometry of geological features and the particular fluids contained within the reservoir (Aghar et al., 2007).

Table 3.2: Well Test Objectives

Productivity Tests		Obtain and analyze representative samples of produced fluids
		Measure reservoir pressure and temperature
		Determine inflow performance relationship and deliverability
		Evaluate completion efficiency
		Characterize well damage
		Evaluate workover or stimulation treatments
Descriptive Tests		Evaluate reservoir parameters
		Characterize reservoir heterogeneities
		Assess reservoir extent and geometry
		Evaluate hydraulic communication between wells

The behavior of reservoir fluids and their interactions with reservoir rock and completion and production systems must be thoroughly characterized to produce a reservoir efficiently. This characterization is accomplished through reservoir modeling, and well test data provide a driving force for running model simulations. Reservoir models are developed on a framework of geophysical, geological, and petrophysical data. Dynamic well test data are integrated into this static framework to simulate and predict reservoir behavior. Data from PTA are particularly useful in detecting

heterogeneities, permeability barriers, structural boundaries, fractures, fluid contacts, and gradients that can be incorporated into the model.

Once a reservoir model is built, it is calibrated by comparing results of a test simulation against measured data to check its parameters. To achieve a good match between real and modeled data, the user may need to fine-tune certain assumptions in the model concerning the well and its reservoir, such as permeability, distance to a fault, or other such parameters.

Production histories from wells in this field are then entered into the model. Another simulation is carried out to model pressures at the wellbore and across the reservoir. Simulation-derived fluid ratio and wellbore pressures are run through a history-matching process for comparison with measured production ratios and pressures. It is not unusual for initial results to disagree, in which case the model parameters are again changed. This iterative procedure continues until a good match is obtained between actual and simulated results. The reservoir model can then be used in predicting future production, well location, and completion scenarios.

Perhaps one of the most useful applications of well test data is achieved through PTA. By generating a log-log plot of measured pressure over time, when plotted along with the derivative of changing pressure, analysts are able to study pressure changes in great detail. The derivative of the pressure change provides a characteristic signature of reservoir pressure response to well testing that can be interpreted in terms of flow regimes, boundaries, permeability, formation damage, heterogeneities, and reservoir volumes. PTA data, when integrated into these and other advanced interpretation techniques, help production teams understand their reservoirs and achieve their engineering and business objectives (Horne, 1990).

3.2 Digital Oil Field of the Future

The E&P industry has a long history of exploiting the growing power of digital technology. The accelerating performance of digital devices (e.g., processors, storage, and bandwidth) is leading to waves of technological innovation that promise significant new capabilities for E&P firms. As a result, the industry is standing on the crest of the digital oil field of the future (DOFF), which will enable petro-professionals and field workers to benefit from total asset awareness on the ability to monitor and manage all operational activities in real time or near real time, regardless of location (Al-Dhubaib et al., 2008b).

It is believed that this state-of-the-art technology for finding, developing, and producing oil and gas will likely play an important role in allowing E&P companies to realize the full economic potential of their assets. The following are the primary benefits offered by the DOFF:

- **Enhanced recovery:** The DOFF has the potential to provide better data, enhance decisions, and improve execution in production planning and operations, leading to additional hydrocarbon recovery. Potential extra recovery due to the DOFF could be as much as 125 billion bbl—a figure that is equivalent to the whole of Iraq’s current estimated reserves (de Oliveira Silva and Kato, 2004).
- **Lower operating costs:** Labor-saving automation, revamped work processes, and more efficient maintenance and operations practices—all DOFF-related—

lead to greater operational efficiency. Companies could realize operating savings of billions magnitude per year (Chorneyko, 2006).

- **Increased production rates:** Reducing equipment failures and improving well management increases production volumes, with debottlenecking and optimization efforts delivering additional gains. The industry currently operates at 80 to 90% of its technical capacity. The DOFF could increase this utilization rate by 2 to 6% (de Oliveira Silva and Kato, 2004).
- **Reduction in capital costs:** The DOFF concept represents the next step in a migration toward using computing systems to monitor and control remote machinery. DOFF-enabled facilities can be designed to operate with fewer onsite staff, translating into lower initial capital investments. Current trends indicate that DOFF implementations may lower facility costs by 5 to 10% over the next 3 to 5 years, with a potential for larger reductions by the end of the decade as unmanned and subsea processing facilities become widespread. Additionally, real-time drilling technology is leading to reductions in drilling costs by 5 to 15%, as drilling engineers are able to react to problems in a more informed and timely manner (Chorneyko, 2006).

These benefits do not exist independent of one another, but rather rely on a strong interdependence to achieve their maximum gains. The technologies and processes that enable greater production volumes also control water and gas handling, strongly influencing ultimate recovery capabilities. Discovering and exploiting additional reserves increases facility throughput and the need for optimization.

DOFF benefits will not materialize simply by acquiring more and better data from all aspects of oil and gas operations. Transformative work processes and organizational changes will likely be needed to take full advantage of new technologies, one of which is the utilization of real-time data from PDHMSs into the well testing and PTA process (Saleri et al., 2006).

3.3 Permanent Downhole Measurement Systems

Over the past 100 years, petroleum exploration and development has evolved from simple techniques, such as digging a hole into a suspected reservoir, to complex production monitoring and control methods. The petroleum industry has since then grown into a multibillion dollar industry. In addition, exploration and development techniques have become increasingly complex as reserves have become more difficult to find. The need for accurate downhole data is now a necessity for successful reservoir monitoring and production because the petroleum reservoirs available today are located in environments that pose a great deal of technical challenges when it comes to development. Today, petroleum is found in offshore environments, and those located on land still require improved oil recovery techniques in order to maximize profitability. To successfully apply improved recovery techniques—such as water flooding, vertical lift performance, hydraulic fracturing, etc.—accurate downhole data are required. Permanent sensors and monitoring systems help to ensure optimization of reservoir monitoring and production techniques by providing the petroleum engineer with real-time data to make timely and accurate decisions. Examples of such decisions are where to place perforations, how best to conduct a waterflood, and whether to fracture a well or acidize it. Data acquired by permanent monitoring systems also enable the petroleum

engineer to diagnose problems such as plugged chokes, leaking valves, etc. This is why the study of sensors and permanent monitoring systems is so important. A great deal of research is being done in the area of sensors to improve them and make them more effective. Permanent monitoring systems have become an important aspect of petroleum technology (Daungkaew et al., 2000).

The need for accurate downhole data first led to the use of surface gauges. It was soon discovered that the data acquired with surface gauges was not sufficiently accurate for oil recovery techniques. In order to acquire accurate data, wireline gauges were invented. This led to further inventions, such as the downhole gauge, from which the permanent monitoring system evolved.

Permanent sensors can be defined as measuring devices that make measurements by exhibiting changes in properties in response to a measured variable such as pressure, temperature, flow rate, etc. They are devices that could be electrical, mechanical, or in the form of an optical fiber. In the petroleum industry, sensors are used to measure physical variables downhole. Measured variables include temperature, pressure, flow rate, density, viscosity, and electrical resistivity (Omotosho, 2004).

Permanent monitoring systems can greatly improve the decisions made during oil production and reservoir development. However, traditional reservoir monitoring methods cannot be completely overruled. Rather, they can be used in conjunction with permanent well monitoring systems as a reference for evaluating the accuracy of the system. That way, a problem with the monitoring system can be easily detected. Permanent well monitoring systems acquire information quicker than conventional methods of data acquisition. As measurements are made, information is relayed through

various means of telecommunication such as satellite communication. Information can reach the petroleum engineer responsible for interpreting the data in real time (Reynolds, 1986).

Technology has made permanent well monitoring systems more than just data collectors. With the recent advent of various kinds of software for communication and interpretation, a well monitoring system can now collect data and interpret it. In some cases, it can take the necessary action required to control the well, such as closing a valve with minimal human intervention. When a permanent well monitoring system is capable of taking certain actions—such as the shutting-in of a gas lift valve based on the data collected by the system—with little or no human input, it is known as an intelligent completion. The intelligent system is a well monitoring system that, to some extent, is able to manage field production with little need for human intervention. It maximizes field production by analyzing the data collected with permanent sensors on a continuous basis. The intelligent completion is designed to last throughout the life of the well, but in reality, 55% of most downhole electronic sensors record failures within less than 4 years (Daungkaew, 2000).

To accomplish this form of automated field management, a feedback loop connects the well monitoring system to subsurface controls. As the data are collected, they are interpreted, and the necessary action is taken without the need for an expensive workover. Because of the high cost of intelligent completions and permanent monitoring systems in general, only offshore wells usually justify such an expense because well interventions for such wells far exceed the cost of an intelligent completion. In addition, high production rates from offshore wells meet similar

conditions. Other wells where intelligent completion technology may be applied are high-rate production land wells in very remote areas. Again, this is because a workover operation in such wells will be more expensive than an intelligent completion, therefore making intelligent completions an economic option. The ability to monitor downhole variables in real time provides a better picture of what is actually happening downhole. In addition, the wealth of data collected is much greater than the data collected using methods that are more traditional. All these factors help the production or reservoir engineer to make effective decisions during production or reservoir development (de Oliveira Silva and Kato, 2004; Van Gisbergen and Vandeweyer, 2001).

3.4 Wavelet Filtration

The main challenge in the processing of permanent gauge data is to implement a smart filter that would drastically reduce the number of data points without losing either high-frequency or low-frequency data. Permanent gauge data is naturally noisy. For the low-frequency information (i.e., the production period), an efficient reduction requires some denoising before the reduction in number of points. This is the typical task of a low-pass filter. The problem is the opposite when we want to keep the high-frequency data. Whenever we have a shut-in, we do not want the break in the pressure response to be masked by a low-pass filter. At the time of the shut-in, we want a high-pass filter. So depending on the part of the information we are interested in, we need a low-pass filter or a high-pass filter. The solution would be a filter that identifies the relevant break of high-frequency data and acts as a high-pass filter on these breaks to keep them intact, but acts as a low-pass filter anywhere else in order to smooth producing phase responses and allow an efficient data reduction. This must be done based on the

pressure data only, without knowing the well producing history a priori. This specification is successfully met by wavelet algorithms. For the engineer, it acts as a filter with a threshold. Any noise below a certain level is considered noise and is filtered out. This will be, hopefully, the case for most noisy signals during the producing phase. On the other hand, any noise above a certain level of threshold will be considered a representative break in the data and will be preserved. This will be, hopefully, whenever the well is shut in. The break in the pressure data will act as local, high-level noise (Ouyang and Kikani, 2002; Houzé et al., 2008).

Wavelet algorithms are multi frequency processes. We will start by showing what happens on a given frequency, corresponding to a time period “a.” We use two basic tools: a normalized scaling function ϕ , used to define a low-pass filter, and a corresponding wavelet function ψ , used to define a high-pass filter. These functions must respect the following conditions:

$$\int_{-\infty}^{\infty} \phi(x) dx = 1 \quad (\text{Eq. 3.1})$$

and

$$\int_{-\infty}^{\infty} \psi(x) dx = 0 \quad (\text{Eq. 3.2})$$

A simple example for functions ϕ and ψ is shown in **Fig. 3.1**.

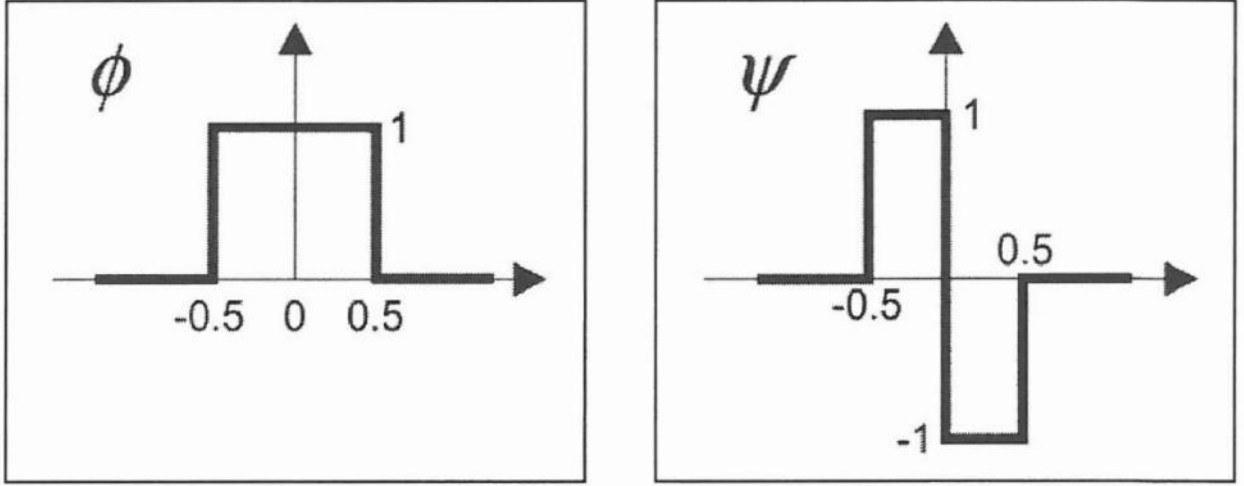


Figure 3.1: Simplest example of scaling and wavelet functions (Houzé et al., 2008).

These functions are used to decompose a given signal (our original data or some transformed data) into two component signals: the complementary transform C_a and the wavelet transform W_a , by respective convolution of the original data with the scaling and wavelet functions.

$$C_a(t) = \frac{1}{a} \int_{-\infty}^{\infty} f(x) \phi\left(\frac{x-t}{a}\right) dx \quad (\text{Eq. 3.3})$$

$$W_a(t) = \frac{1}{a} \int_{-\infty}^{\infty} f(x) \psi\left(\frac{x-t}{a}\right) dx \quad (\text{Eq. 3.4})$$

One remarkable property of these transforms is that there is a numerical way to make these transformations reversible. If we decompose a signal into a wavelet transform and a complementary transform, we will be able to recreate the original signal from these two transforms by a reverse operation. So these dual transforms act as a projection of the signal into two complementary spaces. This is only possible because the operators ϕ and ψ have been carefully chosen. One operator ϕ will correspond to one operator ψ , and vice versa.

The process for a single frequency is schematized in **Fig. 3.2**. The numerical implementation of this algorithm requires that original data are evenly sampled in time,

with the time interval being a . Original raw data is generally not evenly sampled. The required initial interpolation may have a large impact on the process, as any information in the raw data lost in this initial interpolation will be lost for good. This is why the frequency choice is important. The function $W_a(t)$ depends on the level of noise of frequency $1/a$ around time t . If the noise is high, or if there is a break in the data at time t , the value of $W_a(t)$ will be strongly negative or positive. We select a threshold value THR , which defines the value of W_a , above which we consider the signal should be kept. We then define a modified wavelet function:

$$|W_a(t)| > THR \Rightarrow W'_a(t) = W_a(t) \quad (\text{Eq. 3.5})$$

$$|W_a(t)| > THR \Rightarrow W'_a(t) = 0 \quad (\text{Eq. 3.6})$$

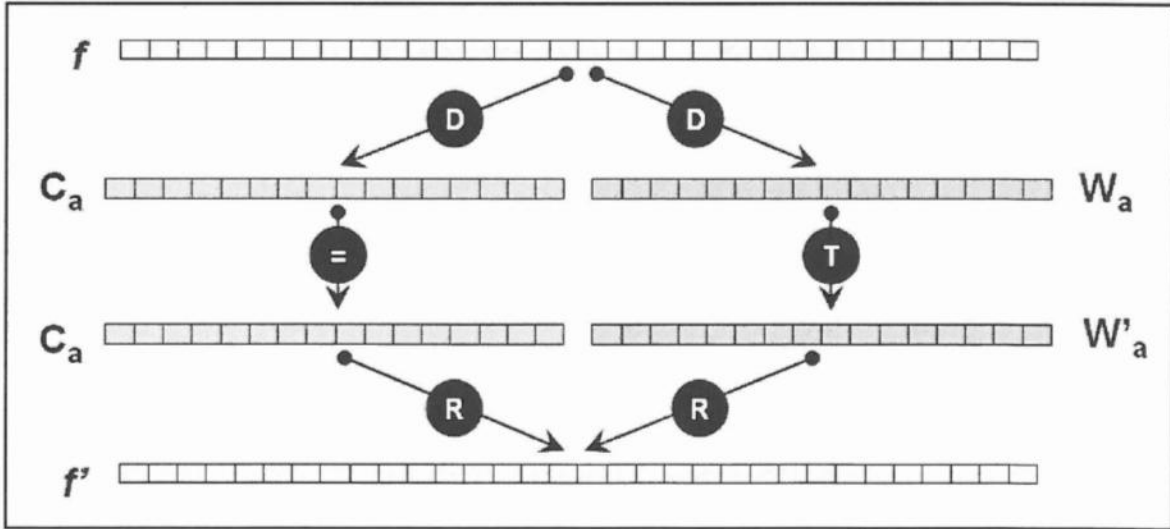


Figure 3.2: Schematic of a single-frequency wavelet algorithm: D = decomposition, T = threshold, R = recombination (Houzé et al., 2008).

Instead of recombining $C_a(t)$ with the original wavelet transform $W_a(t)$ and arriving back at the original signal, we recombine $C_a(t)$ with the modified wavelet transform $W'_a(t)$.

When the noise level corresponding to the frequency $1/a$ is small (i.e., when the wavelet

transform is below threshold), the function $W'_a(t)$ is set to zero, and after recomposition, the data will have been smoothed out. When the wavelet transform is above threshold, the function $W'_a(t)$ is not truncated, and after recomposition, the noise/break is kept. If we had N evenly sampled data points on the original signal f , we now have $N/2$ evenly sampled data points in each of the transforms after decomposition. The total number of points remains N , but as we have two signals, the time interval is now $2a$ (Ouyang and Kikani, 2002; Houzé et al., 2008).

Comprehensive wavelet denoising is a multiple-frequency process, as shown in **Fig. 3.3**. In this example, there are four such frequencies. This is a parameter that will be controlled in the filtering application. The process must first interpolate the raw data to start with a set of points C_a with a uniform time spacing a .

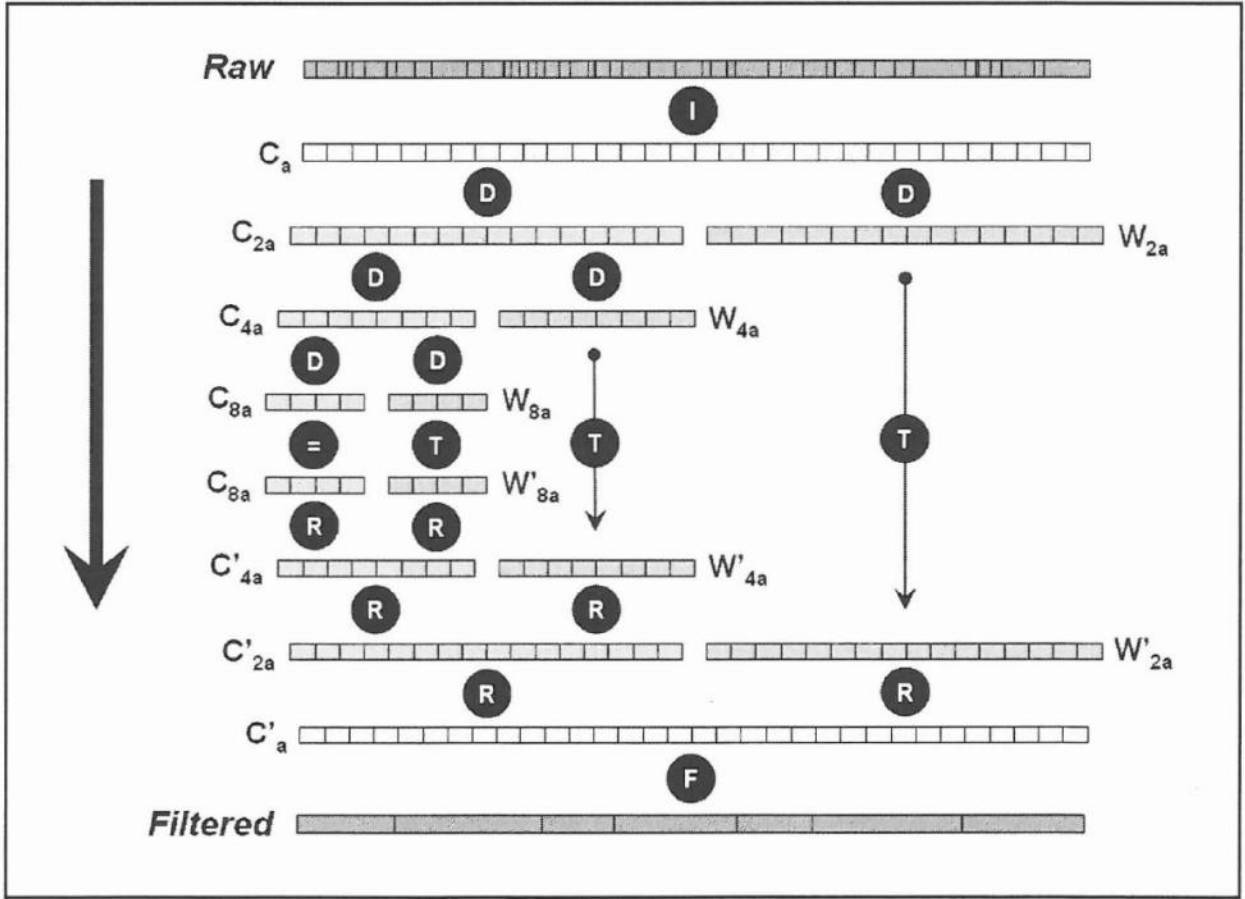


Figure 3.3: Schematic of complete wavelet algorithm: I =interpolation, D=decomposition, T =threshold, R =recombination, F =post-filtration (Houzé et al., 2008).

The signal C_a is decomposed into a complementary transform C_{2a} and a wavelet transform W_{2a} . The total number of points remains the same, half with C_{2a} and half with W_{2a} . The time spacing for each of these series is $2a$, and the frequency is now half the original. The signal C_{2a} is, in turn, decomposed into C_{4a} and W_{4a} , C_{4a} is decomposed into C_{8a} and W_{8a} , and so on until the desired number of decomposition levels is reached. The data are denoised by applying the threshold to the different wavelet transforms. The new signal C'_a will be created by successively recombining C_{8a} with the modified wavelet transforms W_{8a}' , then recombining the resulting C_{4a}' with W_{4a}' , and finally recombining the resulting C_{2a}' with W_{2a}' . This will result in the same number of points, but this time,

large sections of the data—the producing part—will be smoothed, and this will allow data elimination with simple post-filtration. On a typical set of permanent gauge data, the ratio between the number of raw data points and the number of filtered points will range between 100 and 1,000 (Houzé et al., 2008).

The functions ϕ and ψ presented in Fig. 3.1 are the simplest case. However, functions used on real data are smoother in order to avoid numerical effects. **Fig. 3.4** shows another set of functions, more likely to be used on the real data.

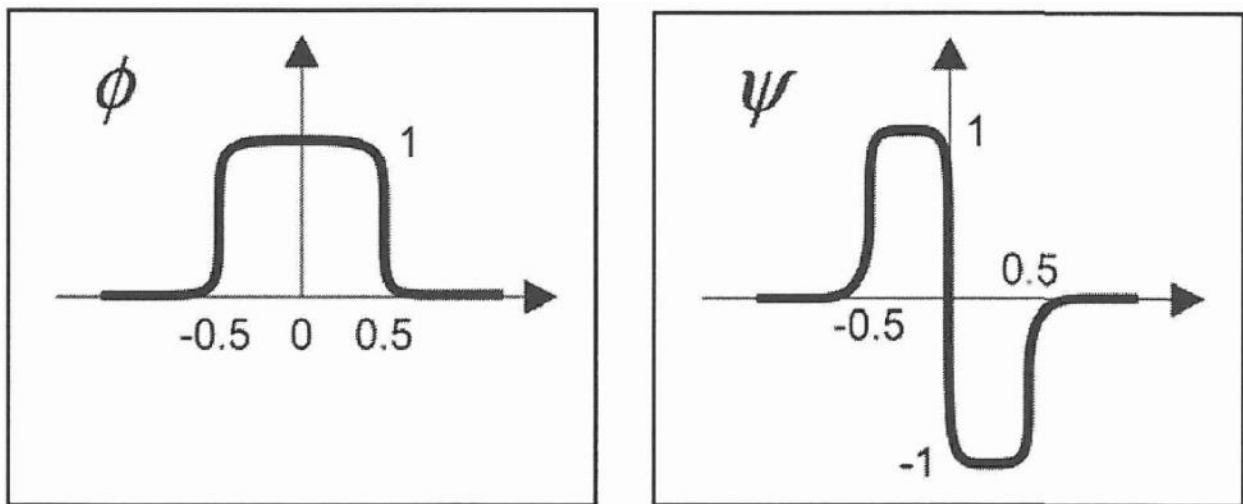


Figure 3.4: Real scaling and wavelet functions (Houzé et al., 2008)

The parameters that define the wavelet process may be automatically set or controlled by the engineer performing the filtration. In the following list, we specify the parameters that will generally be automatic or controlled, and the following sections will describe the influence of the controlled parameters.

- Scaling and wavelet functions ϕ and ψ (automatic)

- Starting data frequency $1/a$ (controlled)
- Number of decomposition levels (automatic)
- Choice of threshold function (controlled)
- Threshold value (controlled)
- Post-filtration parameters (controlled)

The initial time spacing a is very important. $1/a$ will be the highest frequency handled by the wavelet algorithm, and behavior with a higher frequency will be lost in the initial interpolation. Selecting the smallest time interval between consecutive raw data is not a solution, as acquisition times are not regular, and it will not guarantee that the raw data points are taken. The highest possible frequency (i.e., the smallest possible a) filtration with an initial interpolation sampling of one-tenth of a second would guarantee that we will not miss anything, but it would involve one or several billion points. Furthermore, starting with a very high frequency has a major drawback. For each additional level of decomposition, there is only a doubling of the time stepping. As the number of these decomposition layers is limited, we might miss the frequency of the real noise. The solution is to select an initial time stepping that fits the engineer's needs. A time stepping of 1 second will work, but will involve central processing unit (CPU) demands that may not be worth it, and the denoising of the production data may be insufficient. If the interest is not at all in high-frequency data, a time step of 1 minute will be more than enough and very fast. When one wants to pick the high frequency at a reasonable expense, a time step of 10 to 20 seconds will be a good compromise. The exact point of shut-in may not be spotted exactly, but the data will still be usable for PTA, and it will be possible to return to the raw data and selectively reload specific sections of interest (Houzé et al., 2008; Horne, 2007).

CHAPTER 4

DYNAMIC PRESSURE TRANSIENT ANALYSIS WORKFLOW

Fig. 4.1 outlines the dynamic well testing workflow as implemented. The workflow is implemented by a commercially available system designed to manage permanent sensor data from the field through the process of filtering and cleansing for analyzing and interpreting the data for reservoir and well characterization. The workflow consists of an automated part and a manual part. Both of these parts are preceded by the initial field setup, where the field and its associated wells and data are organized in a directory structure.

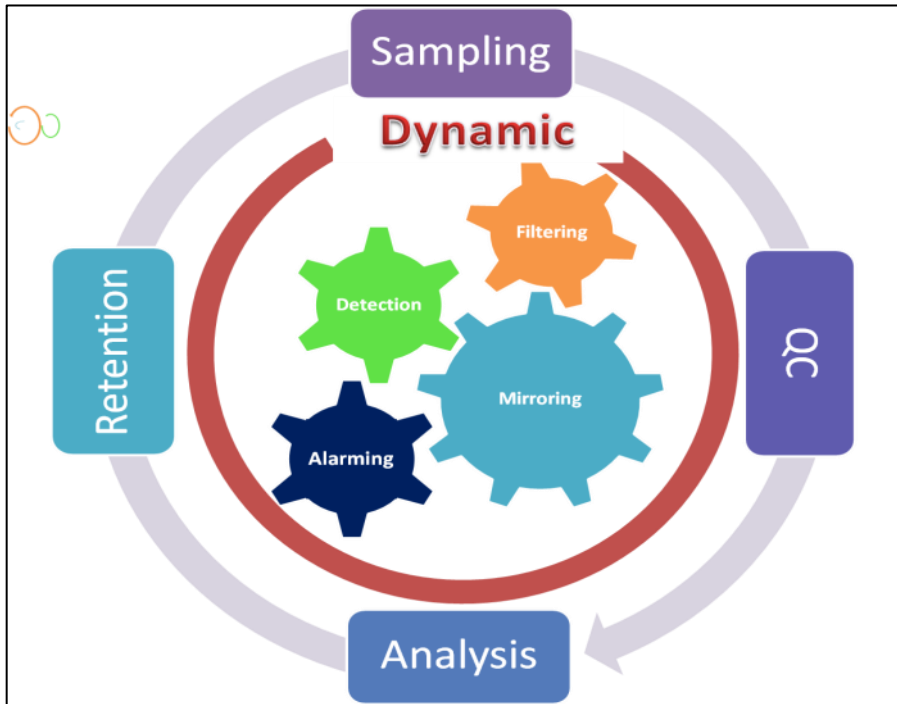


Figure 4.1: Dynamic PTA workflow

4.1 Field Setup

The first task in the workflow requires setting up the field. This task will normally be done only once. During the field setup, information such as name, location, reference date and time for the start of data collection, etc. are entered. Other common field properties, such as pressure/volume/temperature (PVT) and relative permeability data, can also be entered. Here, we can also load in a map of the field showing the various well locations. This map can later be digitized and used for multi well test analysis to study the influence of nearby wells on the pressure behavior of a particular well being tested. The next step is to add all wells in the field and proceed to configuring the data tags for each well. Typical data tags include the downhole pressures, flow rates, and surface pressures. In most of these wells, there are actually two pressure gauges installed. Data tag configuration requires associating each tag name in the field setup with a corresponding tag name in the data repository or historian. The system allows one to connect to any data source. In our case, we connected to an Oracle database that hosts most of the company's data. With the tag configuration completed, the system is now ready to start receiving data from the field sensors via the corporate data repository. **Fig. 4.2** shows a typical field setup, with associated wells and data nodes in a directory structure.

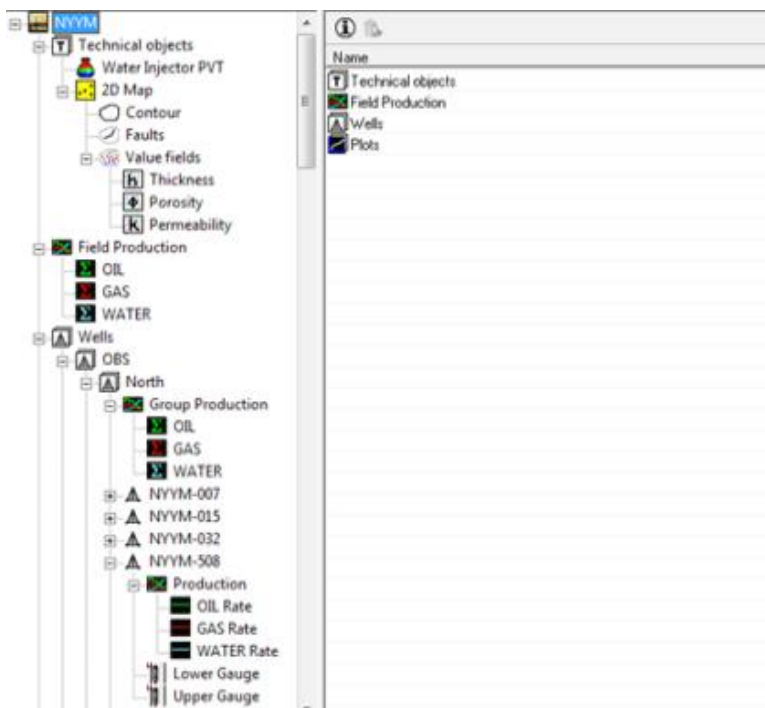


Figure 4.2: Example of initial field setup for PTA workflow

4.2 Automated Processes

4.2.1 Mirroring

Loading pressure and rate data into the system begins with a process called mirroring. During this process, the system interrogates the Oracle data repository for the high-frequency pressure and flow rate data in their original state. An evenly spaced reduced data set is displayed on the screen for inspection, while the original data are compressed, indexed, and stored as a binary file in the system. The data reduction ratio for display purposes is user-defined, with a default set at 1,000. The mirroring process ensures that all the gauge data are available later for fast processing, including smart filtration and cleansing, prior to analysis and interpretation. By default, the mirroring process is repeated every 2 hours, during which any new data received in the data

repository are loaded and appended to the existing data mirrored in the system. This automated update process ensures that permanent sensor data are available in or near real time for the user. The user can set the update process to be carried more or less frequently as required.

4.2.2 Data Reduction

Because the raw data coming from the permanent sensors are very large and often accompanied by noise and outliers, the data need to be denoised and then filtered down to a reasonable size for analysis and interpretation. The system accomplishes this data reduction by using a wavelet-based algorithm for smart denoising and filtration. For noise or outlier removal, the wavelet algorithm determines the trend in the data and provides the user with an adjustable band or ribbon around the data set. All data points outside this band are discarded as noise or outliers. **Fig. 4.3** shows an example of wavelet denoising with the aid of the adjustable ribbon. The wavelet algorithm is also employed for smart data filtration, which ensures that all significant events, such as shut-ins, are preserved. The wavelet data filtration algorithm requires that the original data set be evenly spaced. Otherwise, the system fills in any uneven spaces with interpolated data. The system provides the facility to create and store a filtered data set from the mirrored raw data. During the initial filtration setup, the user has the option to use the system default filter settings or to override them. These settings will automatically be applied to any subsequent raw data received and appended to the existing filtered data set. However, the user may return to any part of the data history and locally repopulate any sequences of interest, such as shut-in periods required for PTA. The availability of the mirrored raw data makes this possible and very fast.

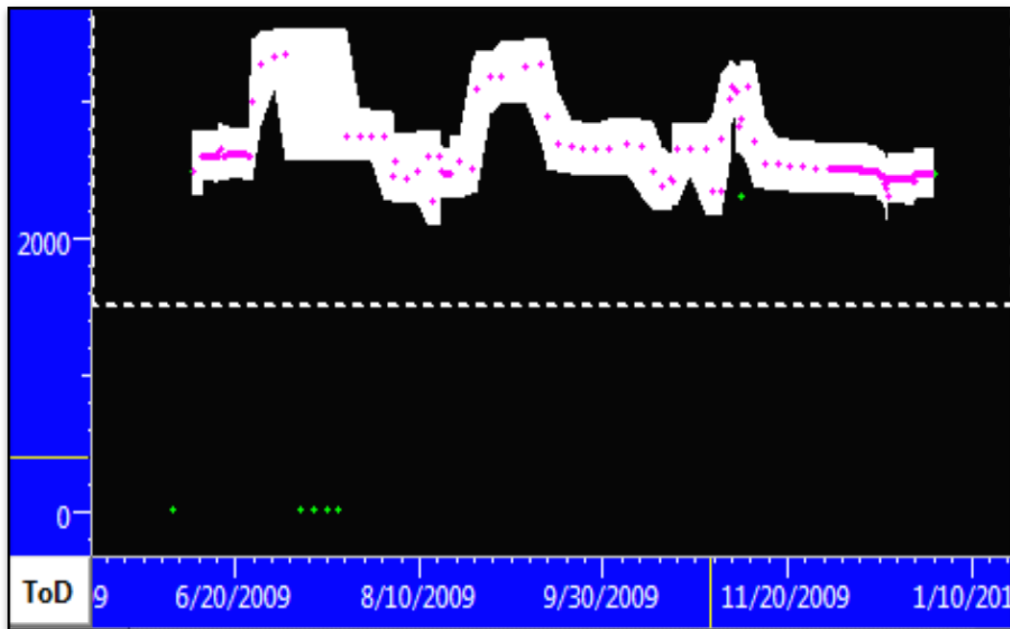


Figure 4.3: Example of PDHMS data noise and outlier removal using wavelet algorithm

4.2.3 Event Detection and Alarming

The system also provides a facility for event detection and alarming (notification). A feature in the system allows the user to set conditions or criteria for which an alarm will be raised and a notification email message sent to the person whose attention is required. Using a formula whose output is logical (true or false), the system can be setup, for example, to send an alarm when an abnormal pressure or flow rate is encountered. Alarms can be set as historical, which allows the system to scan the data back in time to a specified date, or they can be set as instantaneous, in which case the system will only consider newly imported data in the search for the alarm trigger. **Fig. 4.4** shows the setup for an alarm to be raised when the pressure goes above 5,000 psia. In this case, a notification message will be emailed to the address indicated.

The above data processing functions—mirroring, data reduction, and event detection and alarming—need to be set up only once. As new data become available, the system will automatically update itself using whatever conditions were previously set.

The screenshot displays a software interface for configuring an alarm. It is divided into two main tabs: 'Formula' and 'Alarm'. The 'Formula' tab is currently selected, showing a 'Channel name' of 'Higher than 5000' and a formula 'if (a>500, 1, 0)'. Below this, there are 'Save formula' and 'Load formula' buttons. The 'Alarm' tab is also visible, showing a checkbox 'Use this derived channel as an alarm' which is checked. The 'Properties' section includes a 'Type' dropdown set to 'Historical', a 'Mode' section with 'On' selected, and a date/time field showing '11/ 2/2009 9:11:04 PM'. The 'Comments' field contains the text 'Bottom hole pressure above 5000 psia'. The 'Status' section shows 'First checked: 11/2/2009 9:11:04 PM', 'Last triggered: -', and 'Last checked: -'. The 'Action' section shows 'Mail to: mohammed.issaka@aramco.com'. At the bottom, it says 'An email will be send per 1.0 day(s)' and 'Advanced'. The interface also includes a 'Variables' section with a table of variables and an 'Output' section with 'Type: Logical', 'Property: Logical', 'Unit:', and 'Show by: Step'.

Cst	Value	Selected data	Property	Unit
a		Wells - OP - UNYZ-A - North - NYYM-105 - Upper Gu	Pressure	psia

Figure 4.4: Example of alarm setup for notification when pressure goes above 5,000 psia

4.3 Manual Processes

While the data processing functions of the workflow are generally automatic, the data analysis and interpretation aspects are manual and, at best, semi-automated. Once a pressure transient (or a group) has been detected, the user can transfer this subset of the

data to a third-party well test analysis software package for analysis and interpretation. This may be achieved by saving the data as an ASCII file and reading it into the third-party application. In the implementation of this workflow, however, we used a well test analysis package from the same software vendor. As a result, the data transfer was accomplished simply by a mouse click. The data transfer can be done for the whole filtered data set for a particular sensor (gauge) or can be done for portions of a filtered data set that the user chooses.

4.3.1 Shut-In Detection

Another special feature of the workflow is the ability to automatically detect shut-in. The system provides three options to select or indicate a shut-in period:

1. The first option is a completely manual process, where, from visual inspection, the user can select a range or section of the data to be tagged as a shut-in.
2. The second option is a semi-automatic method, where the user simply clicks in any portion suspected to have a shut-in. The system will then automatically select the start and end of the shut-in period. **Fig. 4.5** shows an example where the semi-automatic method was used to detect three buildup periods from PDHMS data spanning 6 months.
3. In the third option, which is fully automatic, an algorithm in the system will automatically find all shut-in periods based on the behavior and shape of the pressure data using time- and pressure-change criteria.

After a shut-in period has been determined and tagged, the system provides a quick-look pressure buildup (or falloff) facility, where the user can perform a preliminary transient analysis using defaulted system input data and automatically generated analysis plots. **Fig. 4.6** presents a quick look at the pressure history and diagnostic plots required for analysis and interpretation. If real analysis is desired, the user can simply input the actual test and PVT parameters.

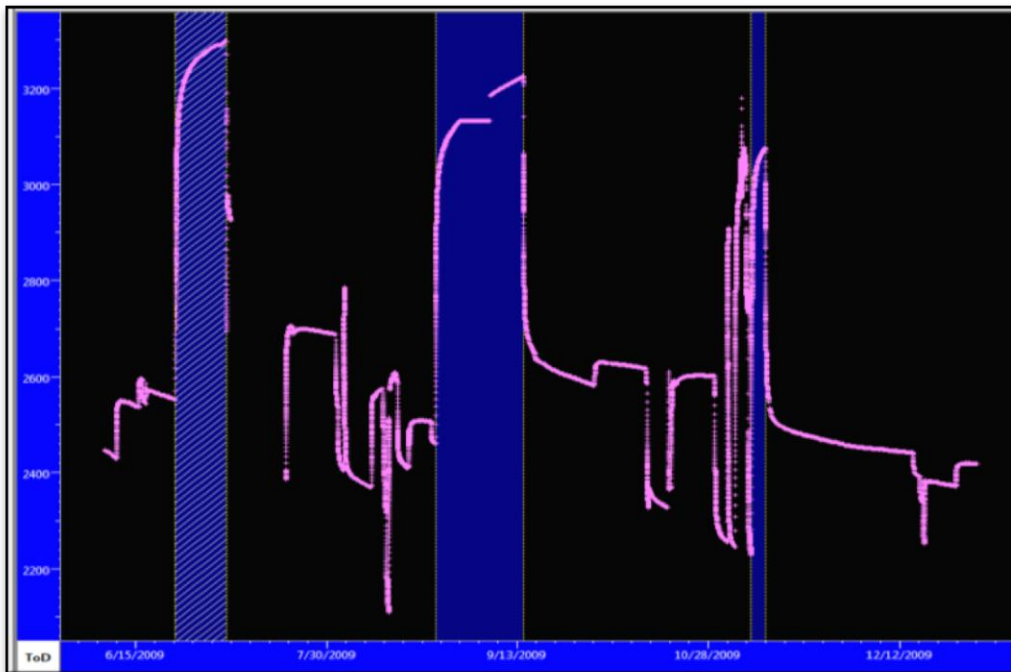


Figure 4.5: Semi-automatic method that detects multiple pressure buildup periods

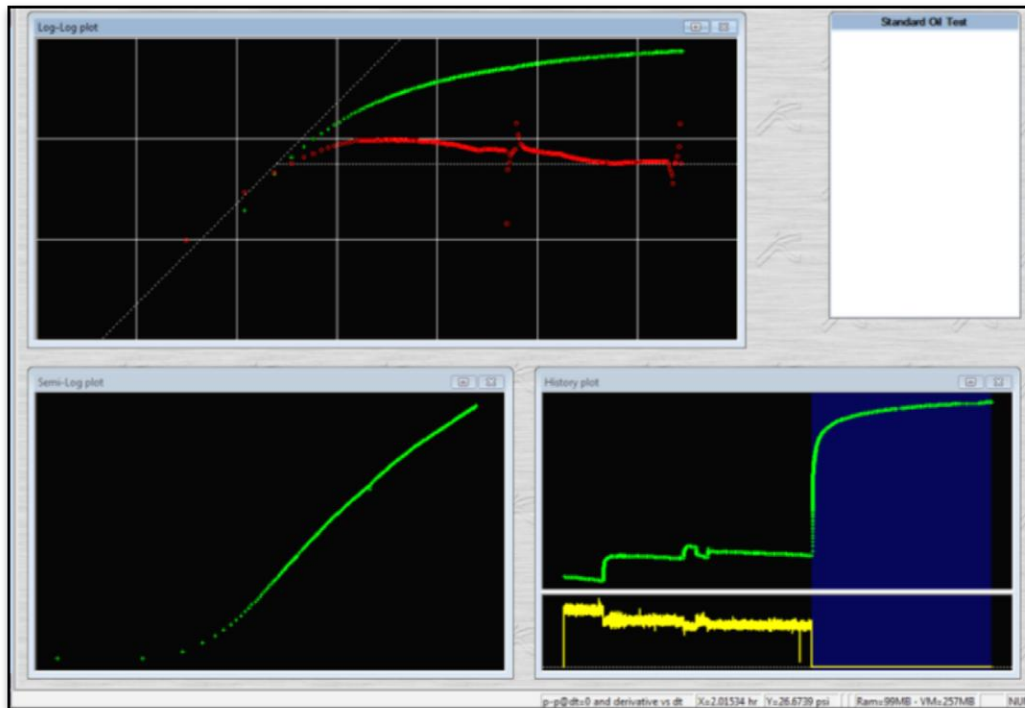


Figure 4.6: Quick-look diagnostic plots for pressure buildup analysis

4.3.2 Data Quality Control

Before any data analysis can begin, however, the data has to be quality-checked for consistency. For PTA to proceed, the pressure data and the flow rate data have to be synchronized. Quite often, shut-in periods are clearly visible on pressure gauge data. However, the flow rate history is not likely to present clear null (zero-rate) sections that are synchronized with the shut-in periods of the pressure data. As a result, some intervention may be required to force the rate to zero, where shut-in is indicated. The system provides a facility to create a secondary or derived channel, where the rate history is recreated to be in synchronized with the pressure data during shut-in. In the recreated production history, the rate is set to zero whenever a shut-in is detected in the pressure data and left in its original values anywhere else. **Fig. 4.7** shows the setup of

the condition where any flow rate below 1,000 STB/D is set to zero to indicate shut-in, while **Fig. 4.8** is a composite plot showing the production rate data before and after application of the condition.

Formula | Alarm

Channel name: Re-created Production History

Formula: if (a<b, 0, a) f(x)

Save formula Load formula

Variables Update list

	Cst		Value	Selected data	Property	Unit
a	<input type="checkbox"/>	<input type="checkbox"/>		Wells - OP - UNYZ-A - North - NYYM-105 - Oil Rate -	Liquid Rate	STB/D
b	<input checked="" type="checkbox"/>	<input type="checkbox"/>	1000.000000			

Output

Type: Oil rate

Property: Liquid Rate

Unit: STB/D

Show by: Step Time step: Original time steps

From: 1/ 2/2010 10:06:04 PM

To: 1/ 2/2010 10:06:04 PM

Advanced settings

Help Cancel OK

Figure 4.7: Setup for recreating production rate data to synchronize with shut-in

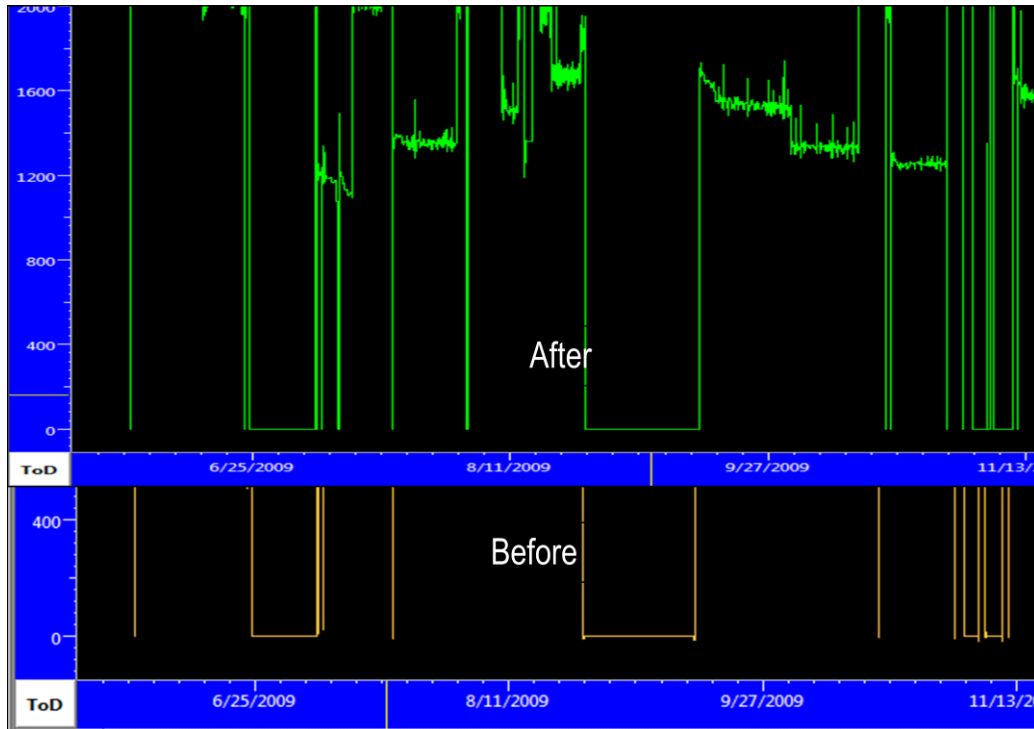


Figure 4.8: Setup composite plot showing production rate before and after applying shut-in condition

4.3.3 Analysis and Interpretation

Once the pressure and production history data have been quality-checked and synchronized, a transient (pressure or rate) analysis and interpretation can begin. As mentioned earlier, the data can be exported to a third-party application for analysis if so desired. In this workflow, the pressure and rate transient analysis applications form part of a suite of interconnected applications that streamlines the data transfer. From the directory tree, the user simply clicks on the desired gauge, followed by a click on another icon to transfer the data. Analysis and interpretation can then be carried out using all the modern tools available, such as pressure derivative diagnostic plots and nonlinear regression for reservoir and well parameter estimation. If the user is not satisfied with the analysis, perhaps because the pressure data has been over-filtered, the

system provides the facility to go back and resample the pressure data again. The user has the option to include more pressure data points or even use all the raw pressure data, if necessary. **Fig. 4.9** shows an example of multiple pressure buildup analysis using PDHMS data over a period of 6 months. Such pressure buildup analysis may be used to track any changes in reservoir properties or wellbore condition (skin) over time. It is also worth mentioning that the third buildup was not a planned shut-in, but the result of plant shutdown for maintenance purposes.

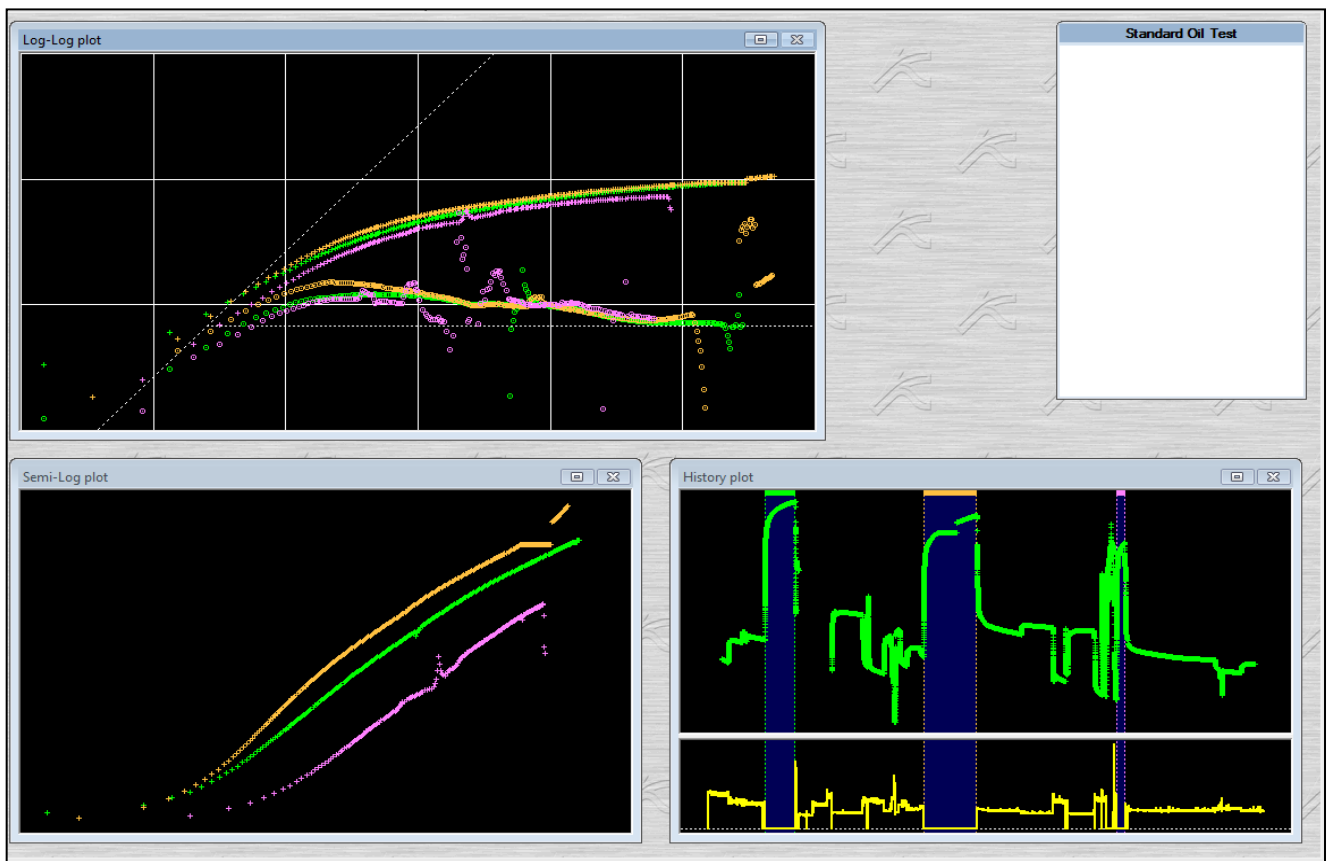


Figure 4.9: Multiple pressure buildup analysis using PDHMS data

4.3.4 Results Retention

Upon completion of the analysis and interpretation, the results of the analysis, as well as the entire analysis file with the accompanying pressure and production history data, can be archived. A pointer to the file location can also be created in the system directory. This ensures that well test analysis files and results are made available in the same system for future reference.

CHAPTER 5

CASE DESCRIPTIONS

For characterizing the reservoir and evaluating well performance with PTA, three case studies were completed using real-time data from permanent downhole pressure gauges.

5.1 Case 1: X-1

5.1.1 Field Description

The field is a north-south–trending anticline 22 mi [37 km] long and 4 mi [7 km] wide. It was discovered in April 1990 and contains two productive sandstone reservoirs: Unayzah-A and Unayzah-B.

5.1.2 Well Description

Well X-1 was completed in June 2008 as a cased-hole horizontal producer in Unayzah-A. Formation analysis logs for X-1 are shown in **Fig. 5.1**. The well was equipped with six premium sand screens from Baker Hughes, with an MP as packer for zonal isolation and a PDHMS for reservoir monitoring. A cross section and detailed downhole schematics are shown for X-1 in **Figs. 5.2**.

5.1.3 Data

Fig. 5.3 shows the downhole pressure and rate readings after applying the workflow described in the previous chapter. These data cover a period of 3,200 hours [133+ days]

with 5,540 pressure points and 1,480 rate points. In this data set, there are three distinct buildups.

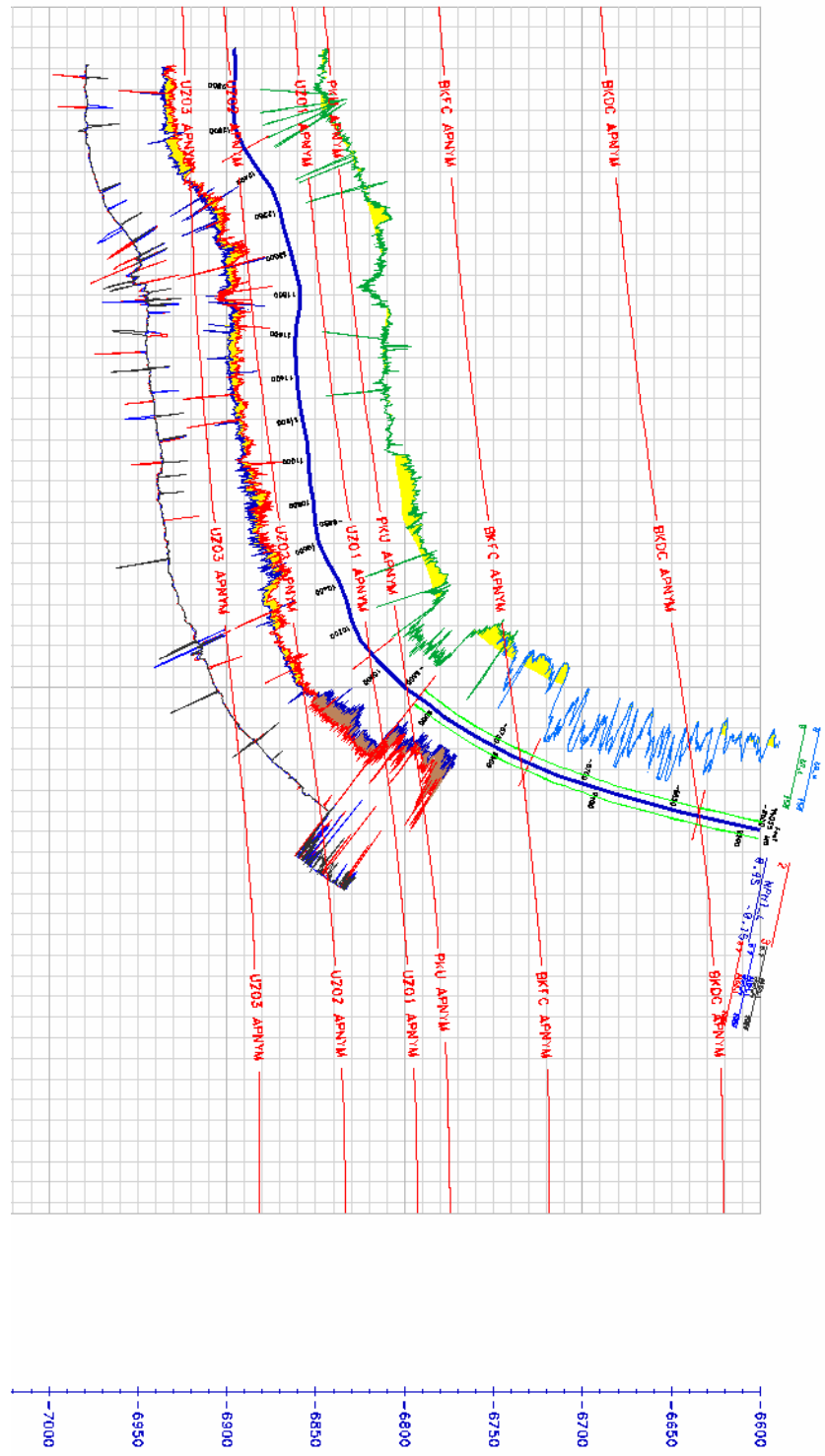
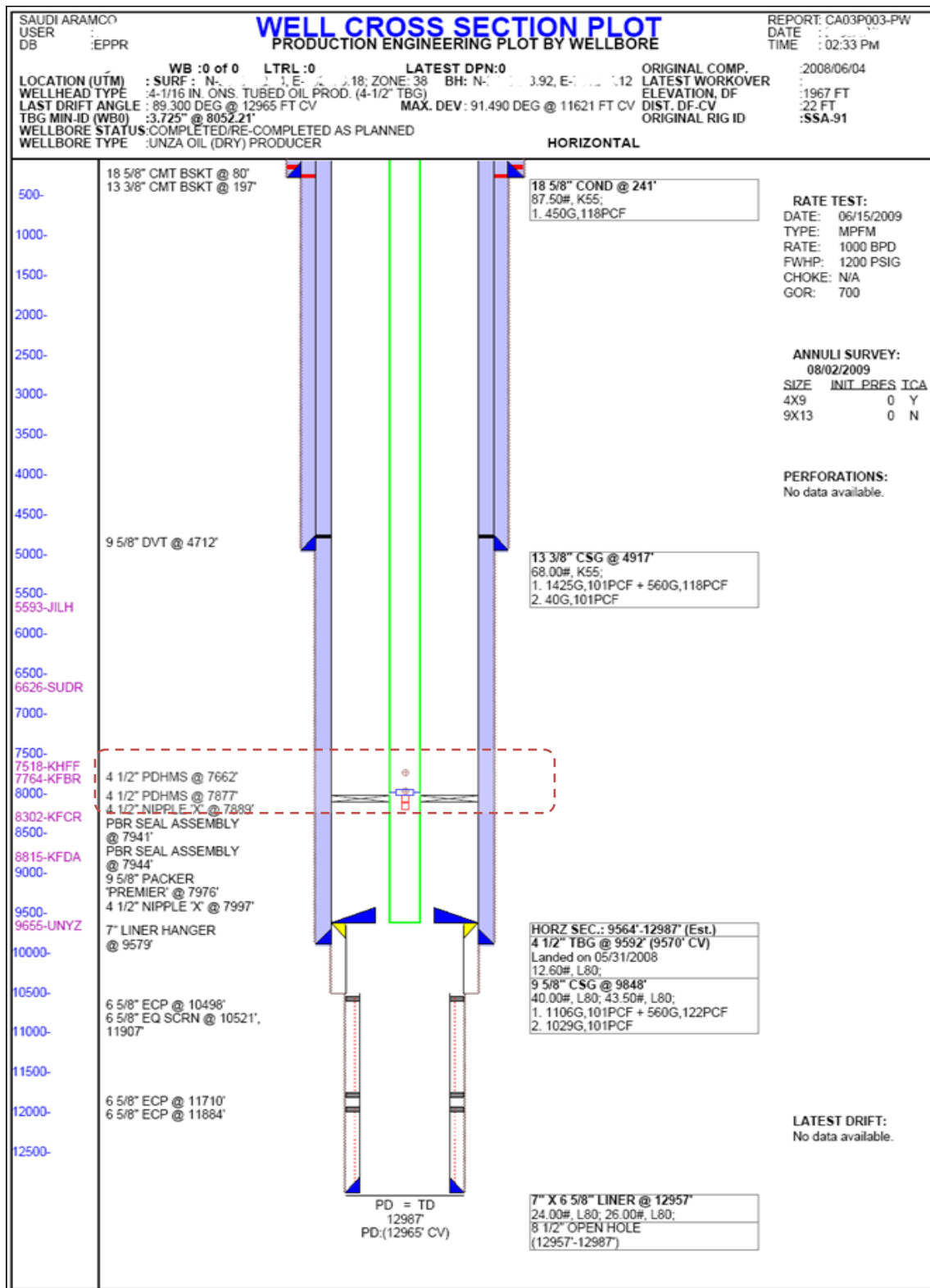
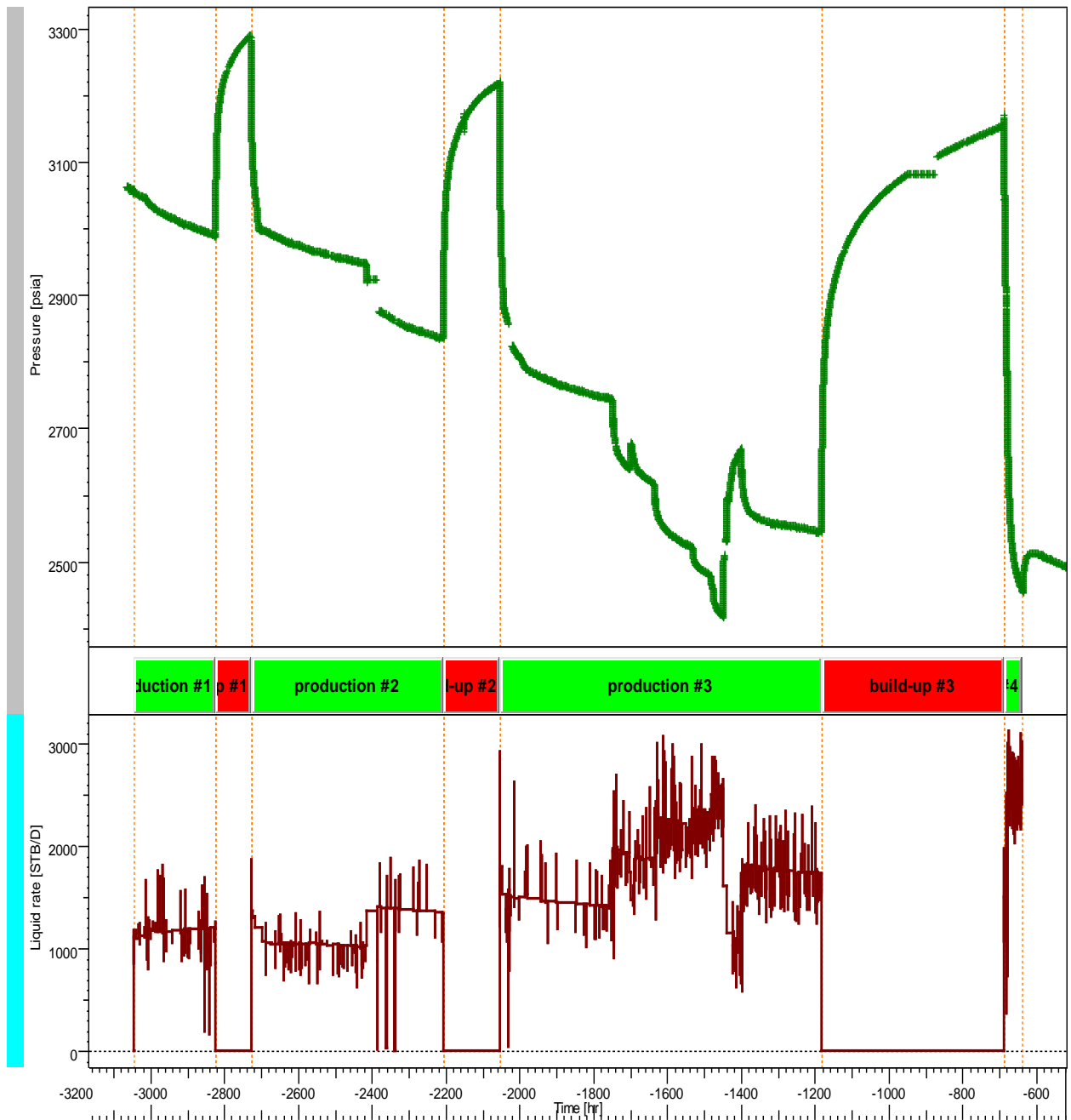


Figure 5.1: Formation analysis and directional logs for X-1





Pressure [psia], Not a unit, Liquid Rate [STB/D] vs Time [hr]

Figure 5.3: Rate and pressure data obtained from well X-1

5.1.4 Analysis

Using **Table 5.1** we calculate the vertical permeability, K_z , from data in the early-radial or hemiradial flow regimes; its calculation requires that we have independent knowledge of K_x . We cannot obtain an explicit expression for K_z alone.

To calculate the permeability in the K_y direction from data obtained from the pseudoradial flow regime; requires that we know K_x , the permeability in the direction perpendicular to the wellbore.

To calculate the value of K_x alone if we have data in the early linear or late-linear flow regimes.

To determine K_x from the early-linear flow regime data, we must know the effective completed wellbore length, L_w ; to determine K_x from the late-linear flow regime, we must know the reservoir length, b_H , parallel to the wellbore. Estimating these quantities can be difficult.

To calculate the effective well bore length, L_w , from data in the early-linear flow regime if we have an independent estimate of K_x .

The length of the boundary, b_H , parallel to the wellbore can be calculated from data in the late-linear flow regime if K_x is known.

If some data (such as L_w or b_H) are unknown or if some of the flow regimes are missing, the analysis procedures based on identifying those flow regimes and making the kinds of calculations that we have been discussing is iterative at best and will result in non unique results. Checks on expected durations of flow regimes using tentative results from the

analysis of the buildup and drawdown tests are helpful to minimize ambiguity in these results.

Assuming $K_x = K_y = K_z$ and simplify the analysis in many cases, but the validity of this assumption is questionable.

The best solution is to use information from the various flow regimes to determine the best estimates possible for reservoir and well properties and then use regression analysis and solutions to the flow equations for horizontal wells (available on most commercial well-test-analysis software) to try to improve the estimates of parameters. Alternatively, numerical models may be used to take into account the non ideal effects of reservoir heterogeneities that are not included in analytical models.

Table 5.1: Equations for Analyzing Flow in Horizontal Well (Horner, 1990)

Parameter	Equations
Wellbore Storage	$t = \frac{(4,000 + 240s_d)C}{\sqrt{K_x K_z} L / \mu}$ $C = V_{wb} C_{wb}$ $C = \frac{25.65 A_{wb}}{\rho_{wb} \cos \theta}$ $C = q B_t / 24 \Delta p$
Early Radial Flow	$\sqrt{K_x K_z} = \frac{162.6 q B \mu}{ m_{erf} L_w}$

$$s_d = 1.151 \left[\frac{\Delta p_{1hr}}{|m_{erf}|} - \log \left(\frac{\sqrt{K_x K_z}}{\phi \mu c_t r_w^2} \right) + 3.23 \right]$$

$$t_{Eerf} = 1,800 d_z^2 \phi \mu c_t / K_z$$

$$t_{Eerf} = 125 L_w^2 \phi \mu c_t / K_y$$

Hemiradial Flow

$$\sqrt{K_x K_z} = 2 \left(\frac{162.6 q B \mu}{|m_{erf}| L_w} \right)$$

$$s_d = 2.303 \left[\frac{\Delta p_{1hr}}{|m_{erf}|} - \log \left(\frac{\sqrt{K_x K_z}}{\phi \mu c_t r_w^2} \right) + 3.23 \right]$$

$$t_{Eerf} = 1,800 D_z^2 \phi \mu c_t / K_z$$

$$t_{Eerf} = 125 L_w^2 \phi \mu c_t / K_y$$

Early Linear Flow

$$\sqrt{K_x} = \frac{8.13qB}{|m_{erf}|L_{wh}} \sqrt{\frac{\mu}{\phi c_t}}$$

$$s_d = \frac{L_w \sqrt{K_x K_z}}{141.2qB\mu} \Delta p_{t=0} - s_c$$

$$\text{where } s_c = \ln\left(\frac{h}{r_w}\right) + 0.25 \ln\left(\frac{K_x}{K_{xz}}\right) - \ln\left[\sin\left(\frac{\pi d_z}{h}\right)\right] - 1.838$$

$$t_{self} = 1,800 D_z^2 \phi \mu c_t / K_z$$

$$t_{self} = 160 L_w^2 \phi \mu c_t / K_y$$

Late Pseudoradial Flow

(requires $L_w/b_H < 0.45$)

$$\sqrt{K_x K_z} = \frac{162.6qB\mu}{|m_{prf}|h}$$

$$s_d = 1.151 \sqrt{\frac{K_z}{K_y}} \frac{L_w}{h} \left[\frac{\Delta p_{1hr}}{|m_{prf}|} - \log\left(\frac{K_y}{\phi \mu c_t L_w^2}\right) + 1.76 \right] + s_c$$

$$t_{sprf} = 1,480 L_w^2 \phi \mu c_t / K_y$$

$$t_{Eprf} = 2,000 \phi \mu c_t (L_w + d_y)^2 / K_y$$

$$t_{Eprf} = 1,650 \phi \mu c_t d_x^2 / K_x$$

Late Linear Flow

$$\sqrt{K_x} = \frac{8.13qB}{|m_{erf}|b_H h} \sqrt{\frac{\mu}{\phi c_t}}$$

$$s_t = \frac{L}{b_H} \left(\frac{b_H \sqrt{K_x K_z} \Delta p_{t=0}}{141.2 q B \mu} - s_p - s_c \right)$$

$$t_{sul} = 4,800 \phi \mu c_t (D_y + L_w/4)^2 / K_y$$

$$t_{ell} = 1,650 \phi \mu c_t d_x^2 / K_x$$

Partial Penetration Skin in
late-Linear Flow and
Productivity Equations

$$p = \left(\frac{b_H}{L_w} - 1 \right) \left\{ \ln \left(\frac{h}{r_w} \right) + 0.25 \ln \left(\frac{K_x}{K_z} \right) - \ln \left[\sin \left(\frac{\pi d_z}{h} \right) - 1.838 \right] \right\}$$

$$\text{Case 1,} \quad \frac{a_H}{\sqrt{K_x}} > \frac{0.75b_H}{\sqrt{K_y}} \gg \frac{0.75h}{\sqrt{K_z}}$$

$$s_p = p_{xyz} + p'_{xy}$$

$$p'_{xy} = \frac{2b_H^2}{L_w h} \sqrt{K_z / K_y} \left\{ F \left(\frac{L_w}{2b_H} \right) + 0.5 \left[F \left(\frac{4y_m + L_w}{2b_H} \right) \right] \right. \\ \left. - F \left(\frac{4y_m - L_w}{2b_H} \right) \right\}$$

$$\text{Where, } y_m = d_y + \frac{L_w}{2}$$

$$F(u) = -u[0.145 + \ln(u) - 0.137(u)^2], u < 1$$

$$F(u) = (2 - u)[0.145 + \ln(2 - u) - 0.137(2 - u)^2], u > 1$$

$$\text{Case 2,} \quad \frac{b_H}{\sqrt{K_y}} > \frac{1.33a_H}{\sqrt{K_x}} \gg \frac{0.75h}{\sqrt{K_z}}$$

$$s_p = p_{xyz} + p_y + p_{xy}$$

$$p_y = \frac{6.28b_H^2}{a_H h} \frac{\sqrt{K_x K_z}}{K_y} \left[\left(\frac{1}{3} - \frac{y_m}{b_H} + \frac{y_m^2}{b_H} \right) + \frac{L_w}{24b_H} \left(\frac{L_w}{b_H} - 3 \right) \right]$$

$$p = \left(\frac{b_H}{L_w} - 1 \right) \left(\frac{6.28a_H}{h} \sqrt{\frac{K_z}{K_x}} \right) \left(\frac{1}{3} - \frac{d_x}{a_H} + \frac{d_x^2}{a_H^2} \right), d_x \geq 0.25a_H$$

Productivity and
Productivity Index

(Uniform Flux Solutions)

$$q = \frac{0.00708 b_H \sqrt{K_x K_z} (\bar{p} - p_{wf})}{B\mu \left[\ln \left(\frac{A^{1/2}}{r_w} \right) + \ln C_H - 0.75 + s_p + \left(\frac{b_H}{L_w} \right) s_d \right]}$$

$$J = \frac{q}{(\bar{p} - p_{wf})} = \frac{0.00708 b_H \sqrt{K_x K_z}}{B\mu \left[\ln \left(\frac{C_H A^{1/2}}{r_w} \right) - 0.75 + s_p + \left(\frac{b_H}{L_w} \right) s_d \right]}$$

$$\begin{aligned} \ln C_H = 6.28 \frac{a_H}{h} \sqrt{\frac{K_z}{K_x}} \left[\frac{1}{3} - \frac{d_x}{a_H} + \left(\frac{d_x}{a_H} \right)^2 \right] \\ - \ln \left(\sin \frac{\pi d_z}{h} \right) - 0.5 \ln \left[\left(\frac{a_H}{h} \right) \sqrt{\frac{K_z}{K_x}} \right] - 1.088 \end{aligned}$$

Dimensionless variables are used to remove the effects of case specificity on the pressure response, defined as

$$p_D = (p_i - p) \frac{kh}{141.2 Q \mu}, \text{ Eq. 5.1}$$

$$t_D = 0.0002637 \frac{kt}{\phi \mu C_t r_w^2}, \text{ Eq. 5.2}$$

$$r_D = \frac{r}{r_w}, \text{ Eq. 5.3}$$

where

t = time (hours)

ϕ = porosity (pore volume/bulk volume)

C_t = total system compressibility (psi⁻¹)

r_w = wellbore radius (ft).

Skin effect, which is a dimensionless parameter that represents the additional (positive or negative) pressure drop, suffered at the sand face by the reservoir fluids flowing into the well on account of near-wellbore flow restriction or flow enhancement, calculated in oilfield units as

$$S = \frac{kh}{141.2qB\mu} \Delta p_s \quad \text{Eq. 5.4}$$

The wellbore storage coefficient C is a parameter used to quantify the volume of fluid that the wellbore itself will produce due to a unit drop in pressure, described as

$$C = \frac{V}{\Delta p} \quad \text{Eq. 5.5}$$

where

V =volume produced (bbl)

Δp = pressure drop (psi).

From the expressions of the dimensionless coordinates t_D , C_D , and P_D and from the pressure match, permeability thickness product kh can be calculated as

$$kh = 141.2Q\mu M_p \quad \text{Eq. 5.6}$$

where

M_p = pressure match.

From the time match, the wellbore storage (WBS) constant C can be calculated as

$$C = 0.000295 \frac{kh}{\mu M_t} \quad \text{Eq. 5.7}$$

where

M_t = time match.

Then, the value of C_D can be calculated from the WBS constant C as

$$C_D = 0.08936 \frac{C}{\phi C_t h r_w^2} \quad \text{Eq. 5.8}$$

From the skin match M_s , the skin factor can be calculated as

$$S = \frac{1}{2} \ln \frac{M_S}{c_D} \quad \text{Eq. 5.9}$$

Given the following conditions, a horizontal well model was used to match the data with changing Wellbore Storage (WBS) in an infinite-boundary homogeneous reservoir with no flow from the top and bottom.

- porosity $\phi = 17\%$
- well radius $r_w = 0.3$ ft
- pay zone $h = 90$ ft
- fluid type is oil
- volume factor $B = 1.66$ B/STB
- viscosity $\mu = 0.362$ cp
- total compressibility $c_t = 2.22 \times 10^{-5}$ psi⁻¹

The main model parameters are as follows (**Fig. 5.4**):

- $M_t = 4.7$ hr⁻¹
- $M_p = 0.00535$ psi⁻¹
- $C = 0.136$ bbl/psi
- total skin = -2.89
- $kh_{\text{total}} = 785$ md.ft
- $k_{\text{avg}} = 8.72$ md
- $P_i = 3,256.03$ psi
- effective well length $L_w = 1,024.51$ ft
- $Z_w = 75.4184$ ft

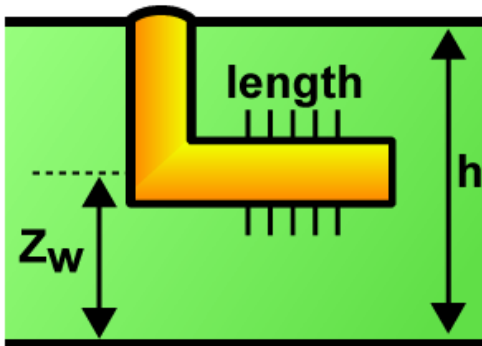


Figure 5.4: Well parameters

The reservoir and boundary parameters obtained from the matched model are as follows (Fig. 5.5):

- $h = 90$ ft
- $kh = 785$ md.ft
- $k = 8.72$ md
- $kz/kr = 0.0146$
- radius of investigation $R_{inv} = 4,410$ ft

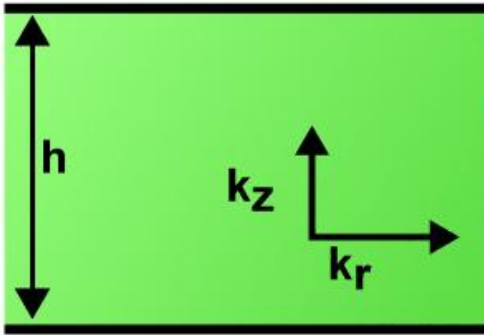


Figure 5.5: Reservoir parameters

Fig. 5.6 shows a comparison between the actual pressure profile and the pressure predicted by the model. Given that no prior stimulation was conducted on this well, the negative skin could possibly be attributed to geoskin or fractures. **Figs. 5.7** and **5.8** show the log-log and semi log analysis, respectively, of the last buildup, where Superposition Time is a time function which will create a common straight line when data from different rates are plotted on the same plot. Detailed analysis for this case is presented Appendix A.

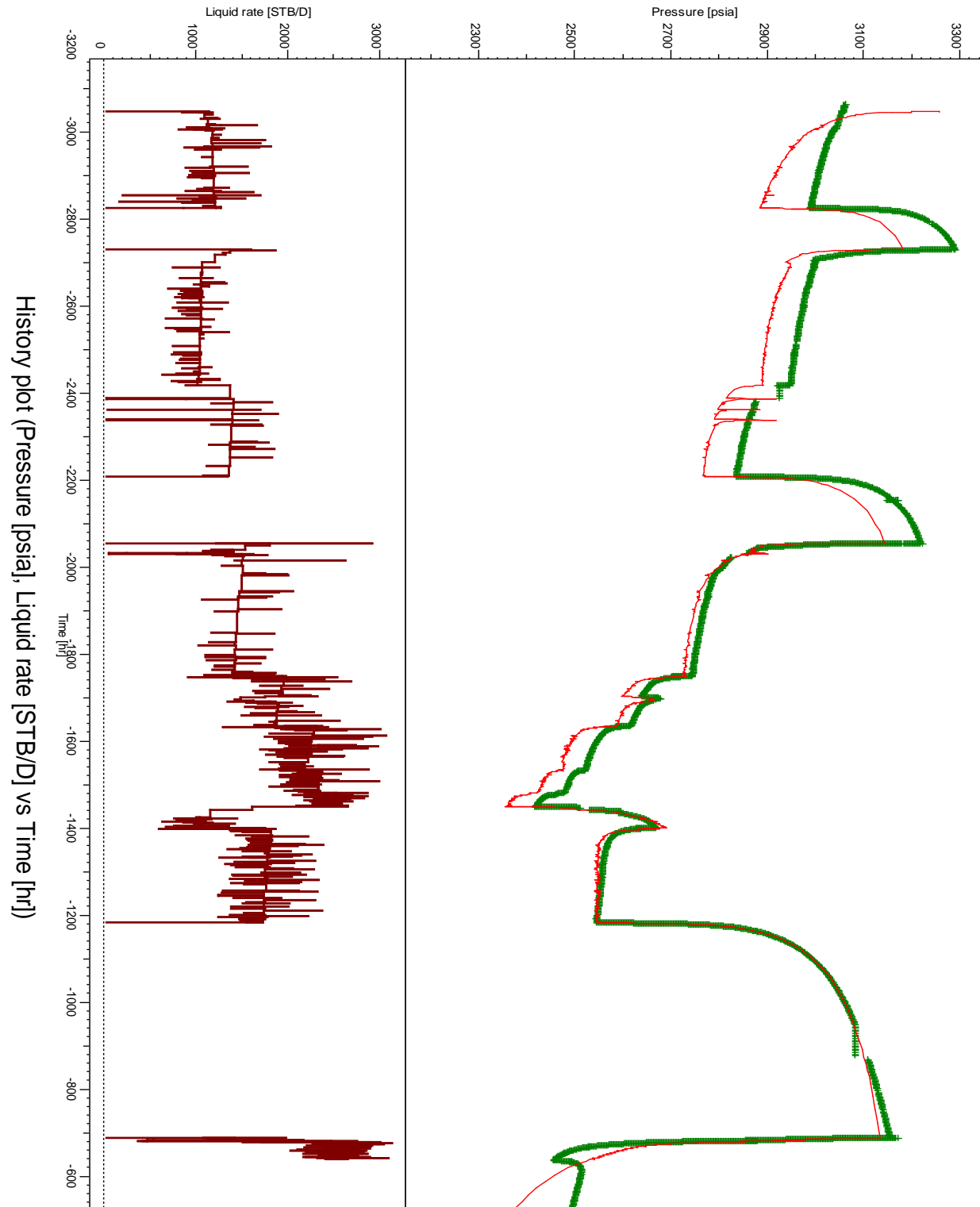
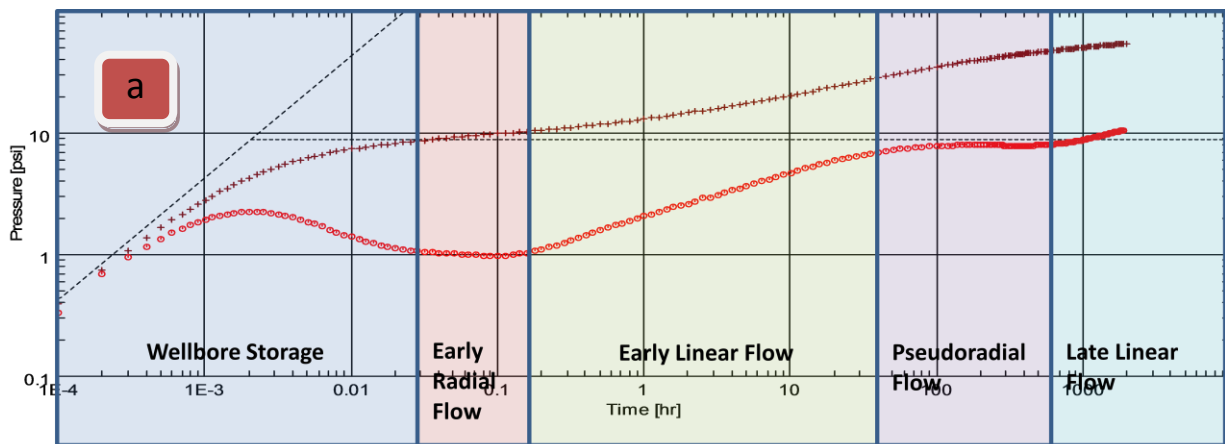
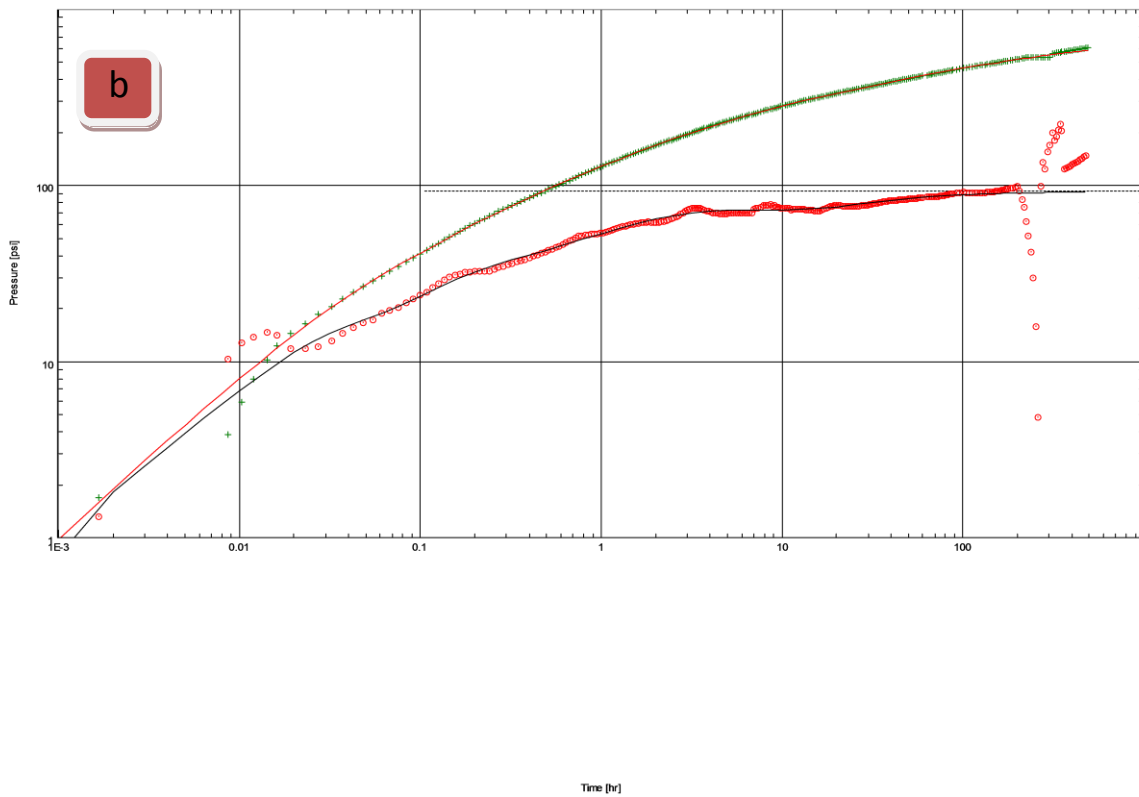


Figure 5.6: Rate and pressure data obtained from well X-1 and compared to the model



Log-Log plot: $p-p@dt=0$ and derivative [psi] vs dt [hr]



Log-Log plot: $p-p@dt=0$ and derivative [psi] vs dt [hr]

Figure 5.7: Log-log analysis of the last buildup for X-1 (b) compared to ideal horizontal well response (a)

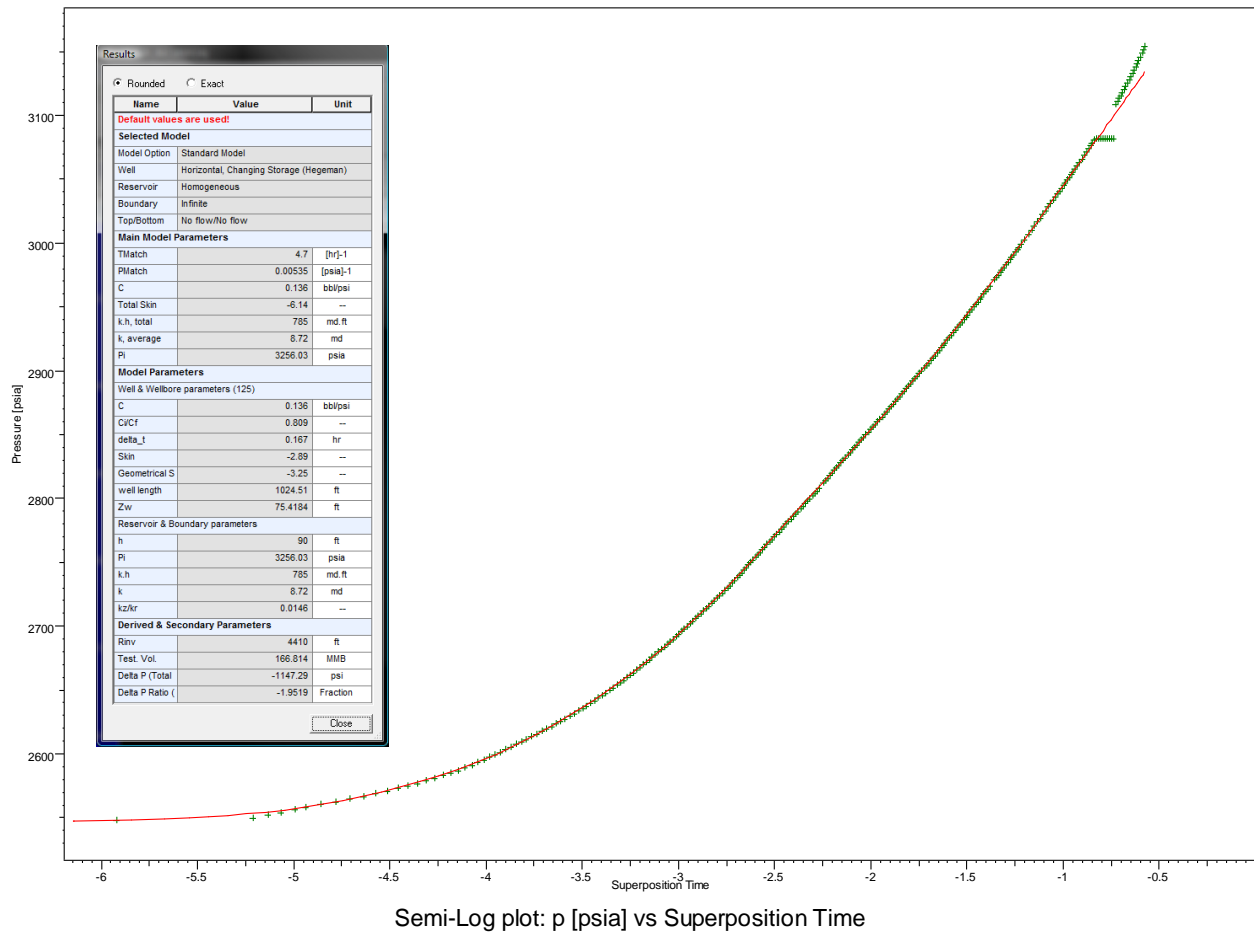
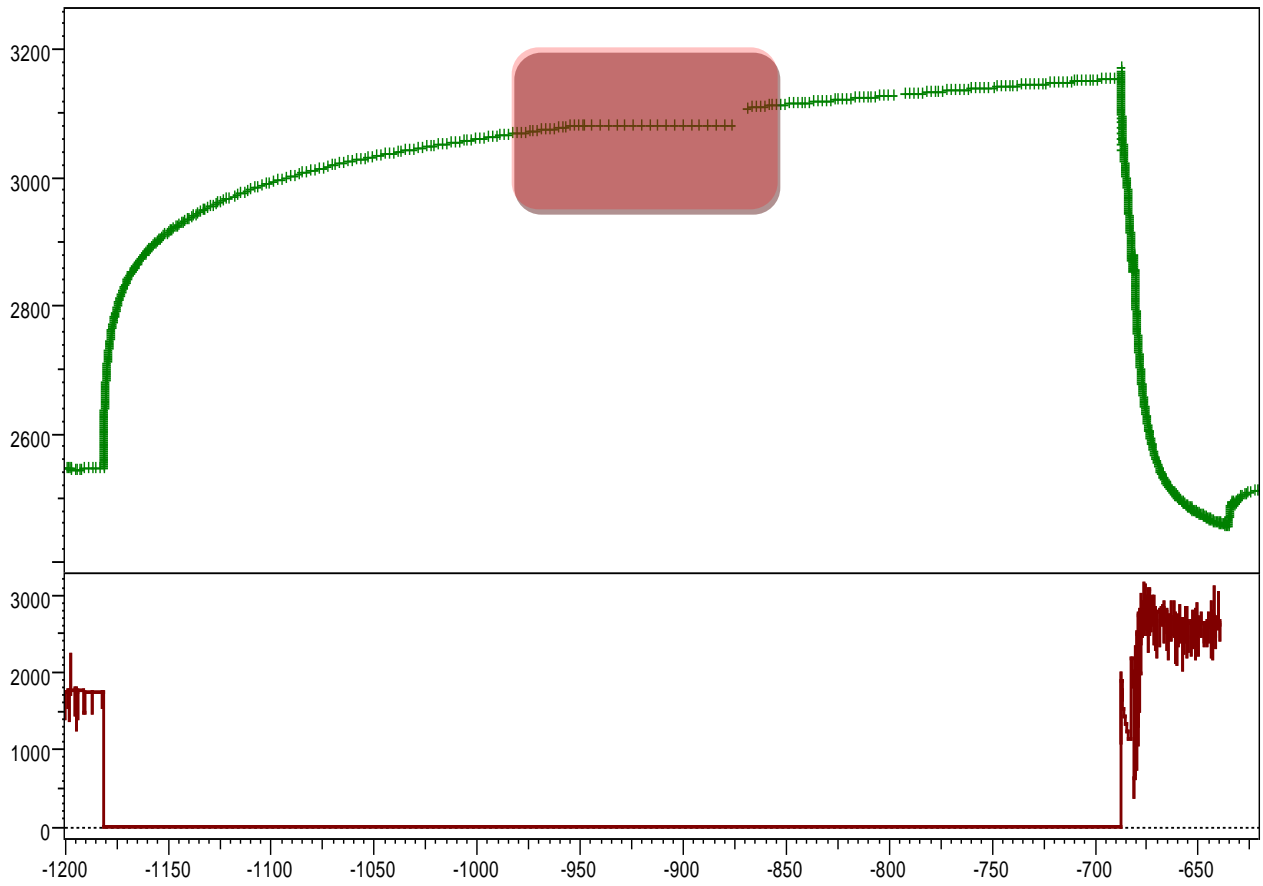


Figure 5.8: Semi log analysis of the last buildup for X-1

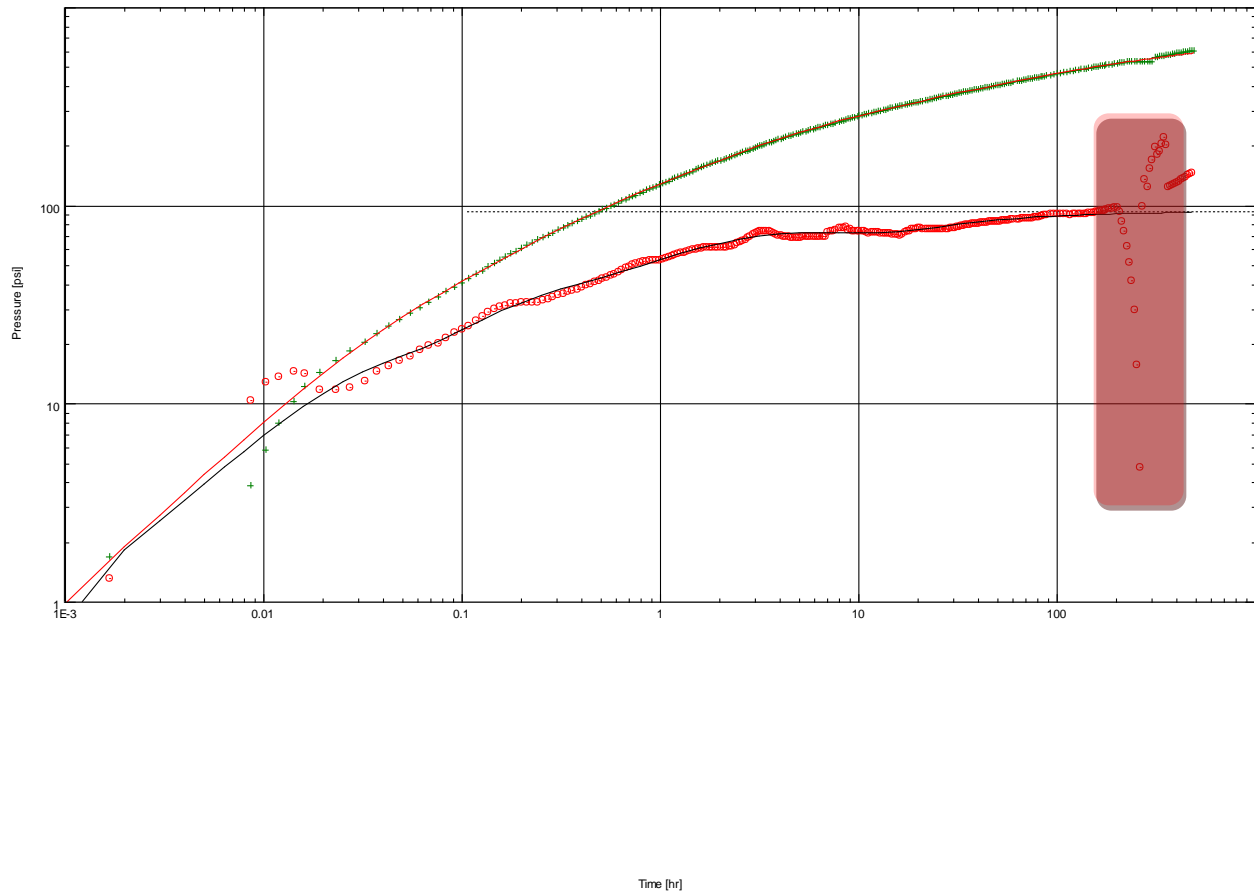
5.1.5 Assessment of Data Interruption Effects

During the last buildup period, there was an error in pressure recording that resulted in a single pressure value for almost 72 hours [3 days] (**Fig. 5.9**). This period of frozen data affects the shape of the pressure derivative of the last buildup at the late time (**Fig. 5.10**). However, the results can be verified by cross-referencing them with previous or later intervals. **Fig. 5.11** shows an overlay of the three buildups in the log-log analysis for X-1.



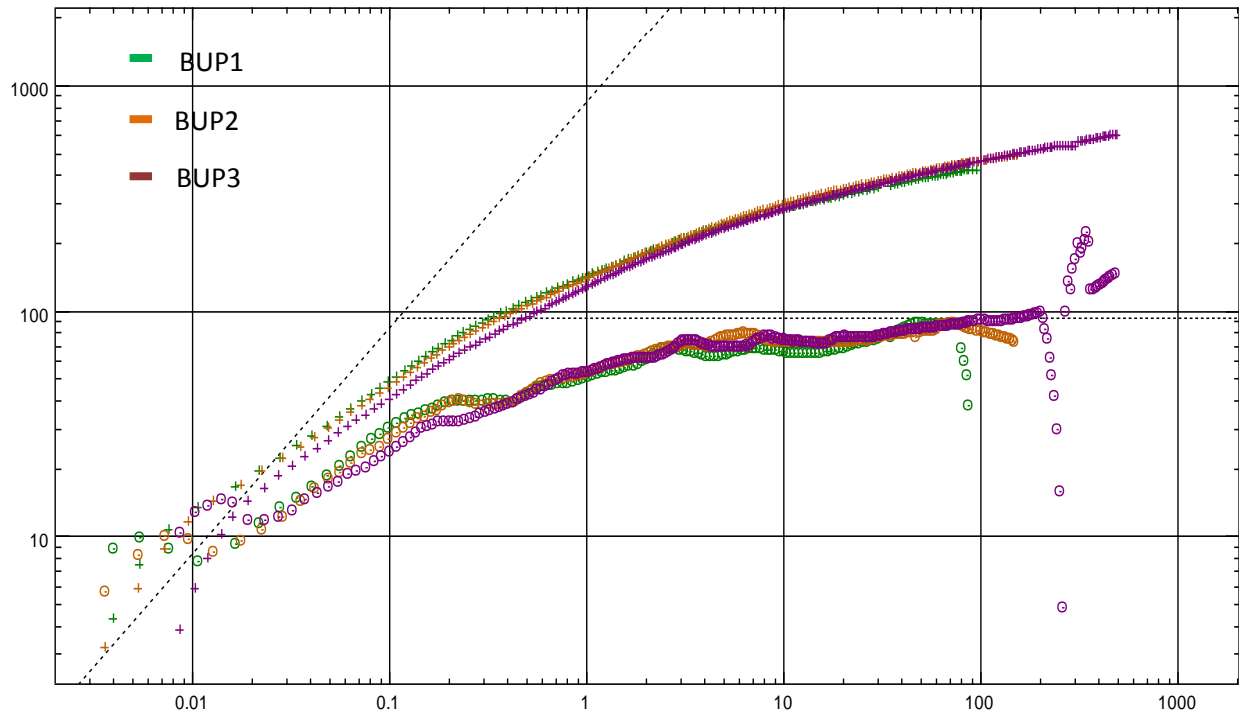
History plot (Pressure [psia], Liquid rate [STB/D] vs Time [hr])

Figure 5.9: X-1 frozen data



Log-Log plot: $p-p@dt=0$ and derivative [psi] vs dt [hr]

Figure 5.10: Effect of data interruption on X-1 log-log analysis



Log-Log plot: dp and dp' normalized [psi] vs dt

Figure 5.11: Overlay of X-1 buildups in log-log analysis

For further investigation of the effect of data interruption during the pressure buildup, different data interruptions on multiple stages of the pressure buildup times and projected their effect imposed on the log-log analysis.

Fig. 5.12 shows the data loss during the early time of pressure buildup of BUP3, and **Fig. 5.13** illustrates its effect. The effect of the data interruption at this stage is significant and masks the determination of all well-related parameters, such as skin and WBS. Determining the permeability thickness product kh may still be achieved in mild cases, and determining boundaries will be less impacted for such cases.

In the case of data loss in the middle time of the pressure buildup period (**Fig. 5.14**), the effect impacts the determination of the kh level more than well-related parameters or boundary effects, as shown in **Fig. 5.15**.

Data loss in the late time of the pressure buildup period (**Fig. 5.16**) affects only the determination of reservoir boundaries, as shown in **Fig 5.17**.

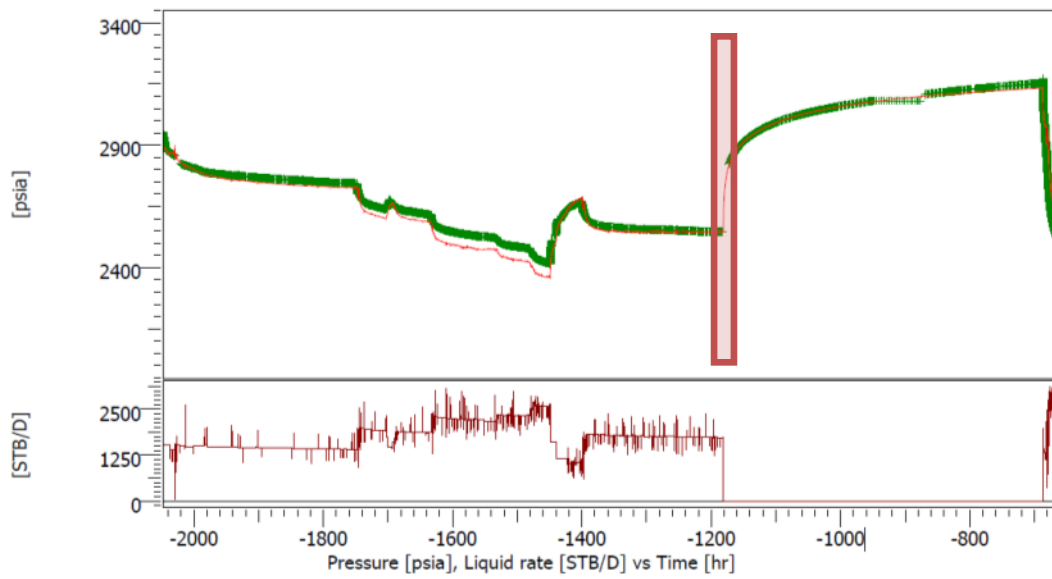


Figure 5.12: Data loss in the early time of pressure buildup

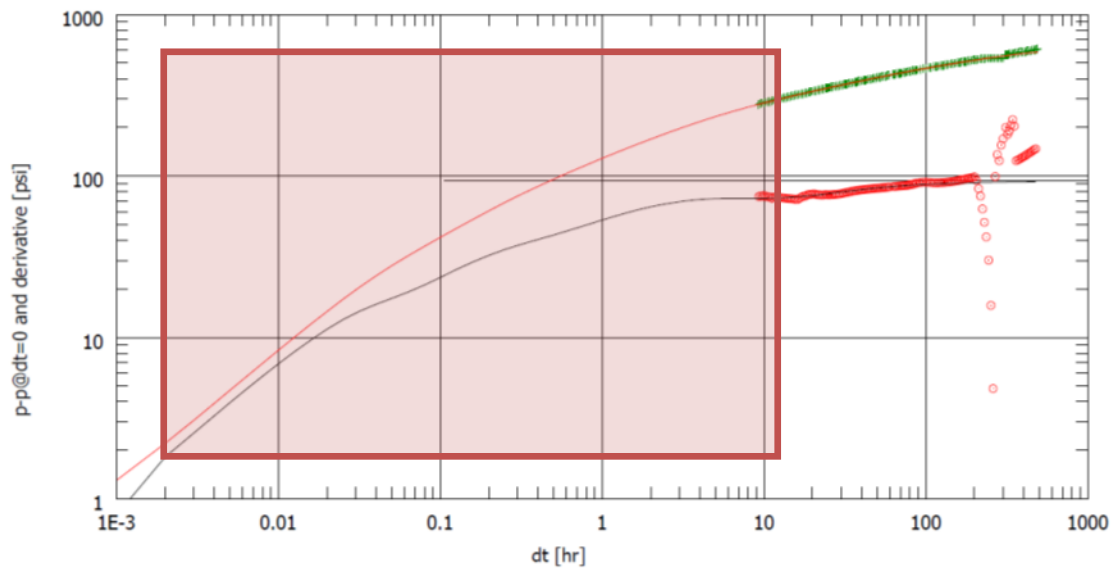


Figure 5.13: Effect on log-log analysis of data loss in the early time of pressure buildup

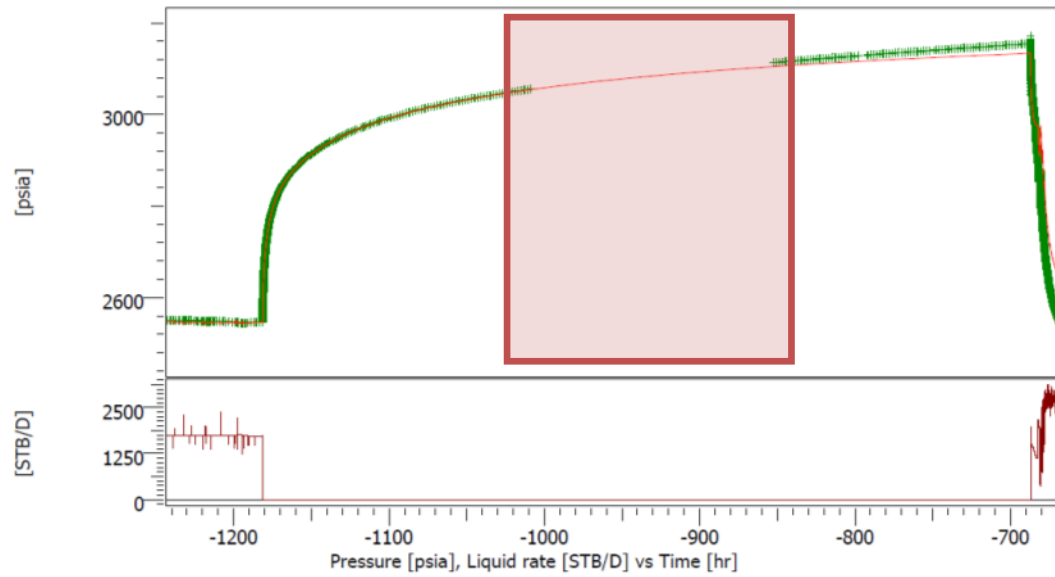


Figure 5.14: Data loss in the middle time of pressure buildup

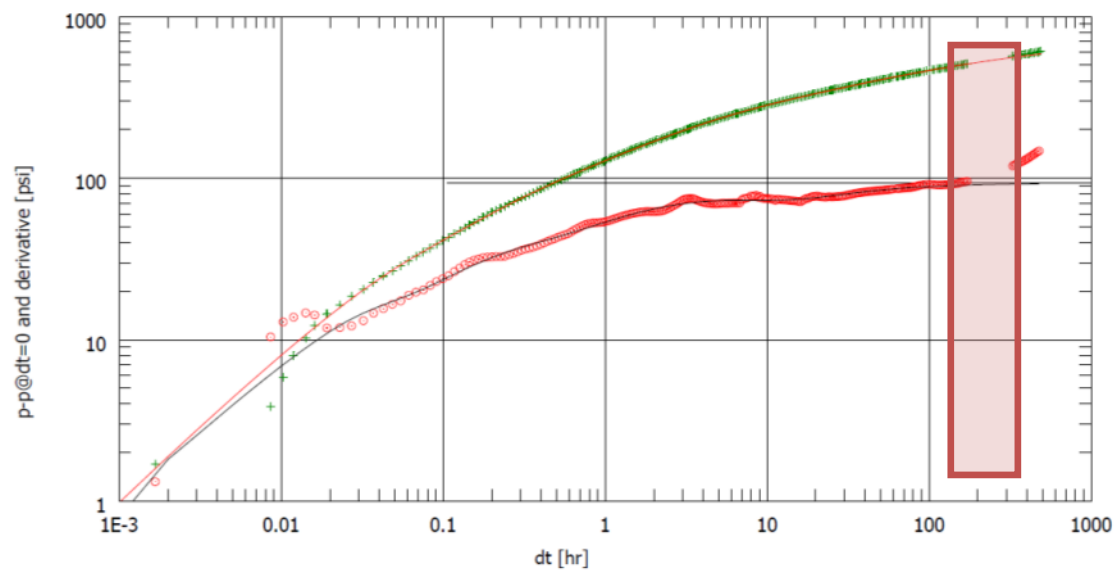


Figure 5.15: Effect on log-log analysis of data loss in the middle time of pressure buildup

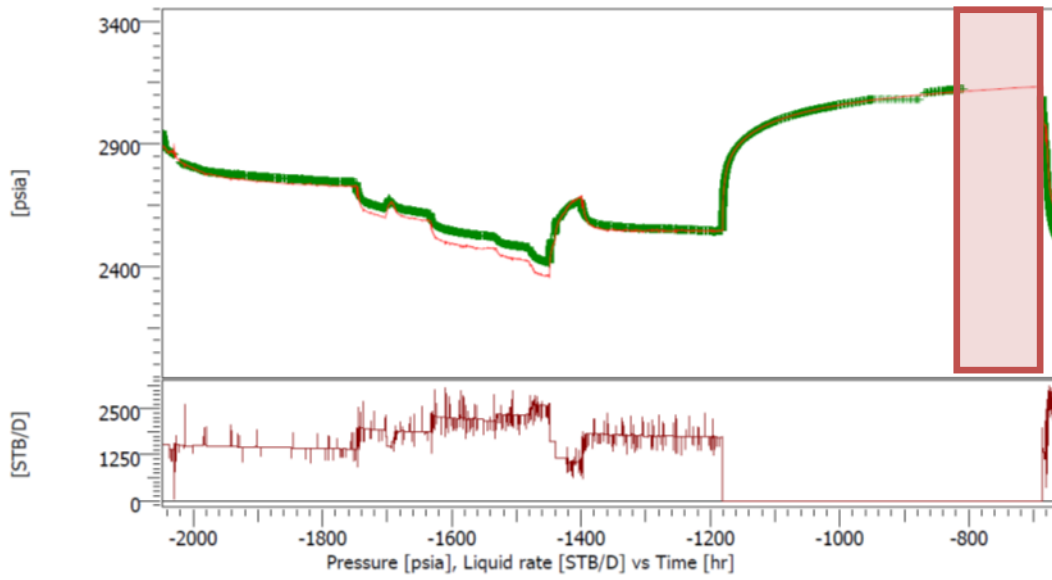


Figure 5.16: Data loss in the late time of pressure buildup

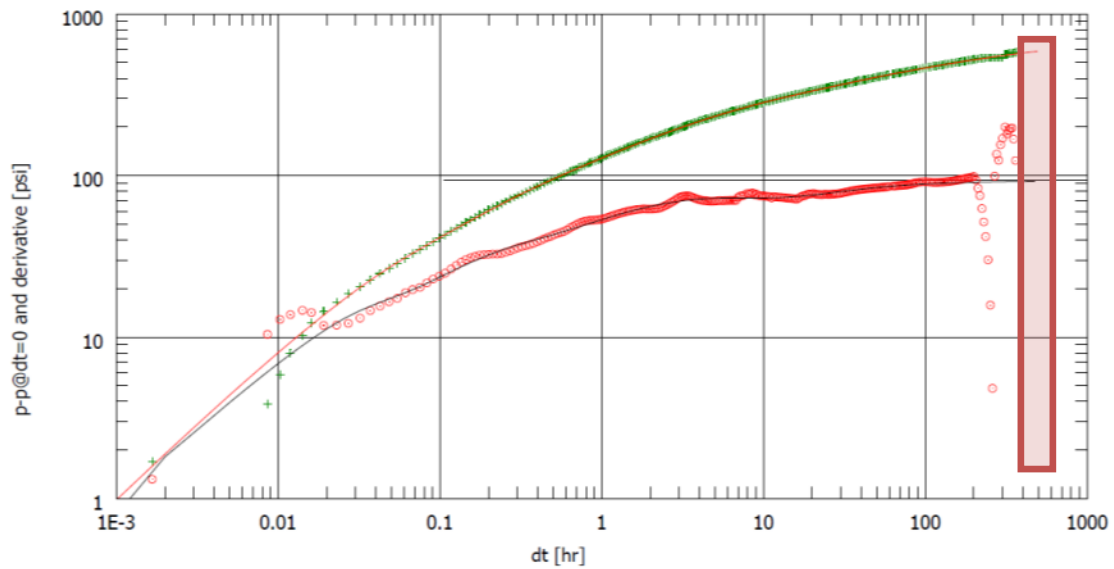


Figure 5.17: Effect on log-log analysis of data loss in the late time of pressure buildup

5.2 Case 2: Y-2

5.2.1 Field Description

This field is a north-south–trending asymmetrical anticline. The eastern flank is slightly steeper than the regional dip, averaging approximately 2° , while the western flank steepens to a maximum dip of 8.7° . The length of the field is approximately 90 km, and the width of the field ranges from 5 to 17 km. There are three oil-bearing reservoirs: Arab-D, Hanifa, and Lower Fadhili, all of which are non-communicating carbonate formations.

5.2.2 Well Description

Well Y-2 was completed in May 2008 as an open hole horizontal producer in Arab-D. **Fig. 5.18** shows Y-2 formation analysis logs. The well is equipped with an electrical submersible pump (ESP) and a Y-tool on 4½-in. tubing. It also has a PDHMS for reservoir monitoring. **Fig. 5.29** shows a cross section of Y-2. This well was a subject to well acid stimulation, at the interval of Arab-D shown in Fig. 5.19.

5.2.3 Data

Fig. 5.20 shows the downhole pressure and rate reading after applying the filtration. These data cover a period of 1,800 hours [75 days] with 12,541 pressure points and 574 rate points.

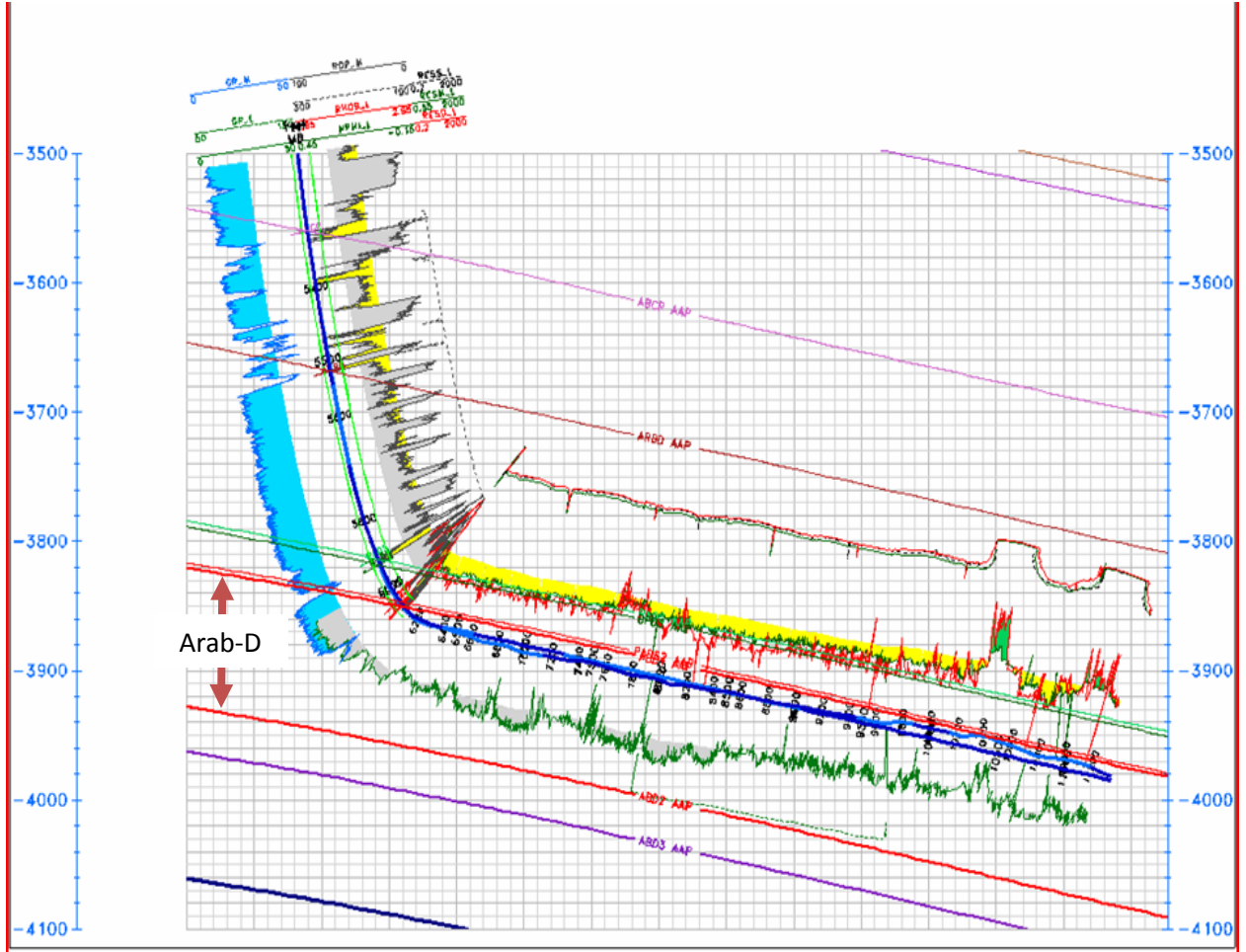


Figure 5.18: Y-2 well trajectory, formation tops, and formation analysis logs

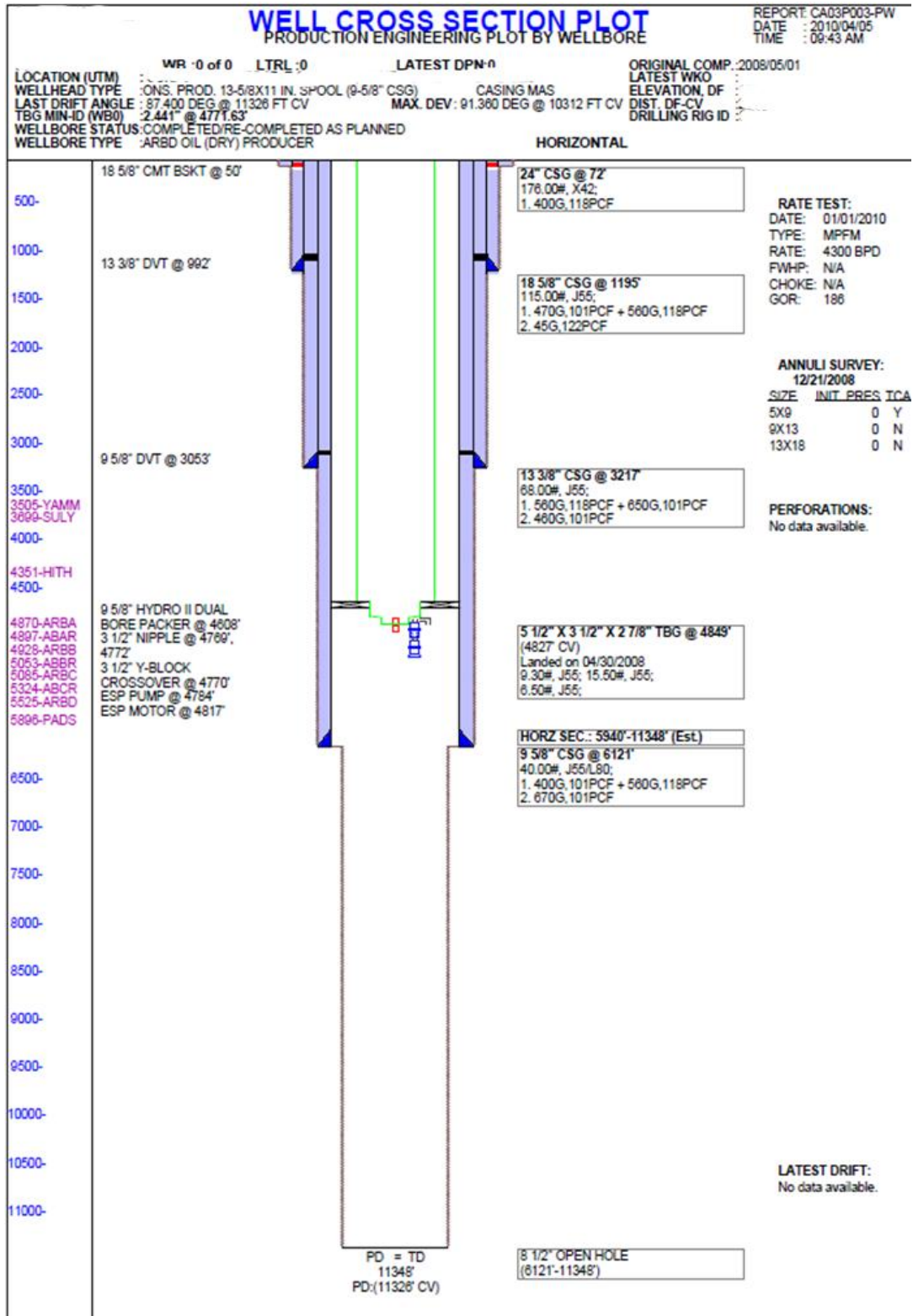


Figure 5.19: Y-2 well cross section

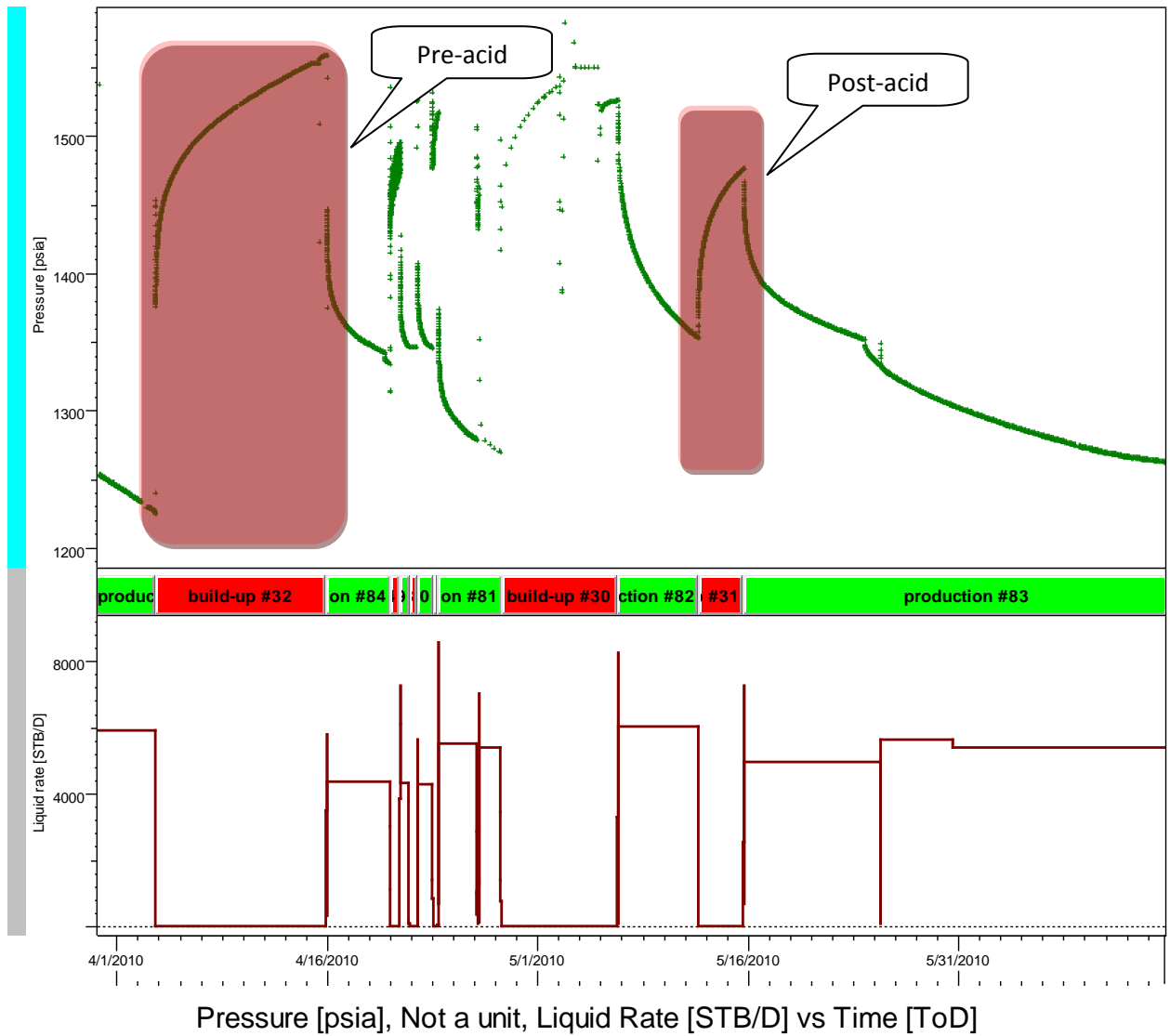


Figure 5.20: Rate and pressure data obtained from well Y-2

5.2.4 Analysis

Using **Table 5.1** we calculate the vertical permeability, K_z , from data in the early-radial or hemiradial flow regimes; its calculation requires that we have independent knowledge of K_x . We cannot obtain an explicit expression for K_z alone.

To calculate the permeability in the K_y direction from data obtained from the pseudoradial flow regime; its calculation requires that we know K_x , the permeability in the direction perpendicular to the wellbore.

To calculate the value of K_x alone if we have data in the early linear or late-linear flow regimes.

To determine K_x from the early-linear flow regime data, we must know the effective completed wellbore length, L_w ; to determine K_x from the late-linear flow regime, we must know the reservoir length, b_H , parallel to the wellbore. Estimating these quantities can be difficult.

To calculate the effective well bore length, L_w , from data in the early-linear flow regime if we have an independent estimate of K_x .

The length of the boundary, b_H , parallel to the wellbore can be calculated from data in the late-linear flow regime if K_x is known.

If some data (such as L_w or b_H) are unknown or if some of the flow regimes are missing, the analysis procedures based on identifying those flow regimes and making the kinds of calculations that we have been discussing is iterative at best and will result in non unique results. Checks on expected durations of flow regimes using tentative results from the analysis of the buildup and drawdown tests are helpful to minimize ambiguity in these results.

It can be assume $K_x = K_y = K_z$ and simplify the analysis in many cases, but the validity of this assumption is questionable.

The best solution is to use information from the various flow regimes to determine the best estimates possible for reservoir and well properties and then use regression analysis and solutions to the flow equations for horizontal wells (available on most commercial well-test-analysis software) to try to improve the estimates of parameters. Alternatively, we may find that numerical models are required to take into account the non ideal effects of reservoir heterogeneities that are not included in analytical models.

Dimensionless coordinates are used to remove the effects of case specificity on the pressure response, defined as (Eqs. 5.2, 5.3, and 5.4)

$$p_D = (p_i - p) \frac{kh}{141.2Q\mu},$$

$$t_D = 0.0002637 \frac{kt}{\phi\mu C_t r_w^2},$$

$$r_D = \frac{r}{r_w},$$

where

t = time (hours)

ϕ = porosity (pore volume/bulk volume)

C_t = total system compressibility (per psi)

r_w = wellbore radius (ft).

Skin effect, which is a dimensionless parameter that represents the additional (positive or negative) pressure drop, suffered at the sand face by the reservoir fluids flowing into the well on account of near-wellbore flow restriction or flow enhancement, calculated in oilfield units as (Eq. 5.4)

$$S = \frac{kh}{141.2qB\mu} \Delta p_s.$$

The wellbore storage coefficient C is a parameter used to quantify the volume of fluid that the wellbore itself will produce due to a unit drop in pressure, described as (Eq. 5.5)

$$C = \frac{V}{\Delta p}$$

where

V =volume produced (bbl)

Δp = pressure drop (psi).

From the expressions of the dimensionless coordinates t_D , C_D , and P_D and from the pressure match, permeability thickness product kh can be calculated as (Eq. 5.6)

$$kh = 141.2Q\mu M_p$$

where

M_p = pressure match.

From the time match, the WBS constant C can be calculated as (Eq. 5.7)

$$C = 0.000295 \frac{kh}{\mu M_t}$$

where

M_t = time match.

Then, the value of C_D can be calculated from the WBS constant C as (Eq. 5.8)

$$C_D = 0.08936 \frac{C}{\phi C_t h r_w^2}$$

From the skin match M_s , the skin factor can be calculated as (Eq. 5.9)

$$S = \frac{1}{2} \ln \frac{M_s}{C_D}$$

Given the following conditions, a horizontal well model was used to match the data with changing WBS in an infinite-boundary homogeneous reservoir with no flow from the top and bottom.

Reservoir and well data:

- porosity $\phi = 18\%$
- well radius $r_w = 0.3542$ ft
- pay zone $h = 110$ ft
- fluid type is oil
- volume factor $B = 1.168$ B/STB
- viscosity $\mu = 1.83$ cp

- total compressibility $c_t = 1.11 \times 10^{-5} \text{ psi}^{-1}$

The main model parameters obtained from the matched model are as follows (**Fig. 5.21**):

- $M_t = 0.292 \text{ hr}^{-1}$
- $M_p = 0.0058 \text{ psi}^{-1}$
- $C = 5.83 \text{ bbl/psi}$
- total skin $= -0.228$
- $kh_{\text{total}} = 10,600 \text{ md.ft}$
- $k_{\text{avg}} = 96.1 \text{ md}$
- $P_i = 1,665.77 \text{ psi}$
- effective well length $L_w = 1,1816.09 \text{ ft}$
- $Z_w = 55 \text{ ft}$

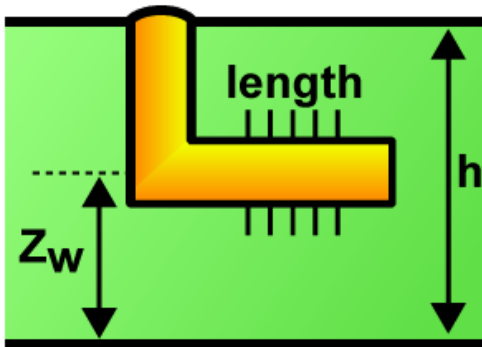


Figure 5.21: Well parameters

The reservoir and boundary parameters obtained from the matched model are as follows (**Fig. 5.22**):

- $h = 110 \text{ ft}$
- $kh = 10,600 \text{ md.ft}$
- $k = 96.1 \text{ md}$
- $kz/kr = 0.421$
- radius of investigation $R_{\text{inv}} = 785 \text{ ft}$

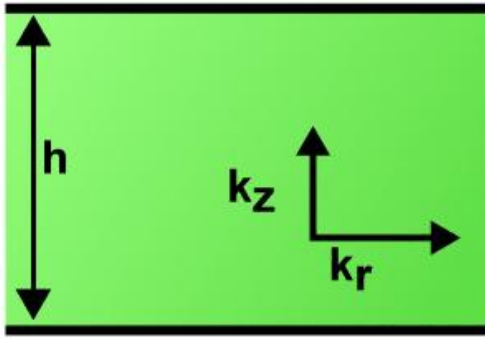
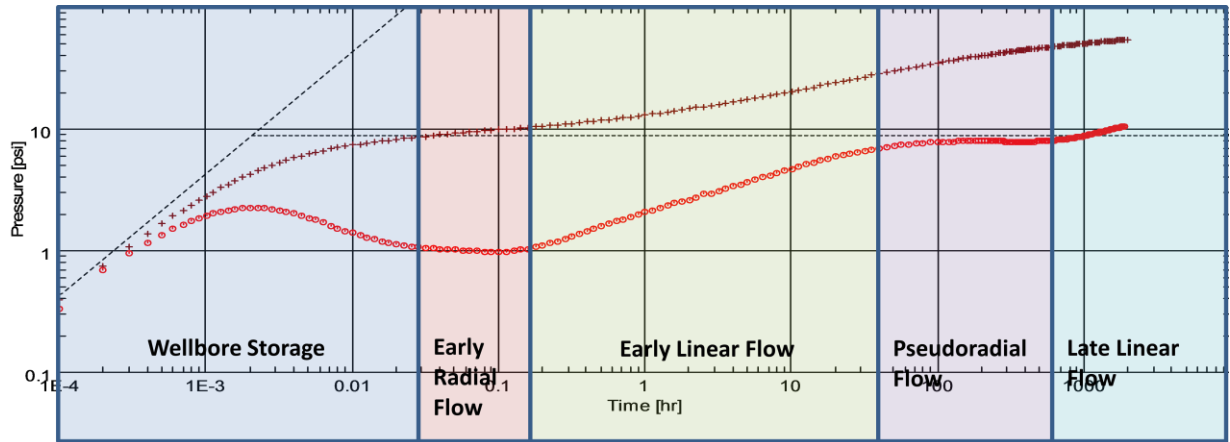
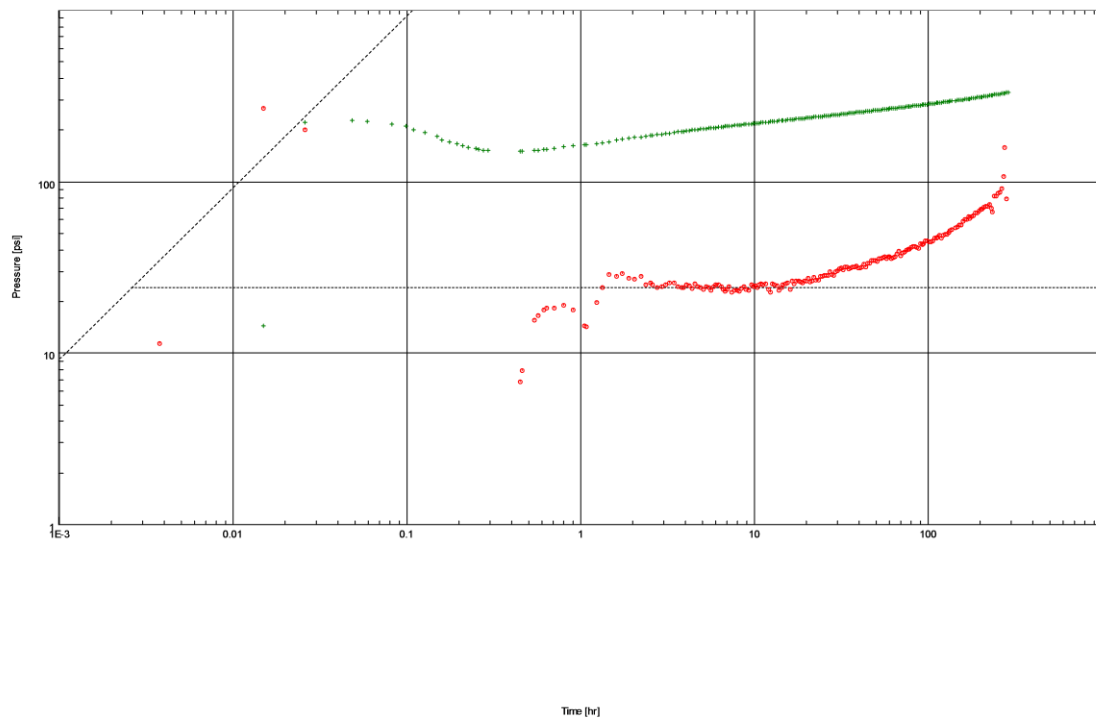


Figure 5.22: Reservoir parameters

The log-log analysis of the pre-stimulation buildup (**Fig. 5.23**) is compared with the log-log analysis of the post-stimulation period (**Fig. 5.24**), where the test data were matched to a horizontal well model in a homogeneous reservoir with changing WBS. Results of this analysis are compared with the pre-acid results to assess the effectiveness of the acid treatment in **Fig 5.25**. The model match indicates an effective horizontal length L_e of 1,816 ft, which is a significant improvement over the previous value, 1,286 ft, determined from the pre-acid test. The flow capacity was determined to be 10,600 md. ft. The results also show a skin factor of -2.4 compared with the pre-acid value of -0.1 . The productivity index more than doubled to 49 BPD/psi from 20.2 BPD/psi in pre-acid analysis. Analysis of the test data indicates a very successful acid treatment and highlights the value of pressure transient analysis of PDHMS data in providing a reliable means to diagnosing the well and characterizing the reservoir. Detailed analysis for this case is presented Appendix A.



Log-Log plot: $p-p@dt=0$ and derivative [psi] vs dt [hr]



Log-Log plot: $p-p@dt=0$ and derivative [psi] vs dt [hr]

Figure 5.23: Pre-stimulation log-log analysis for Y-2 (bottom) compared to ideal horizontal well behavior (top)

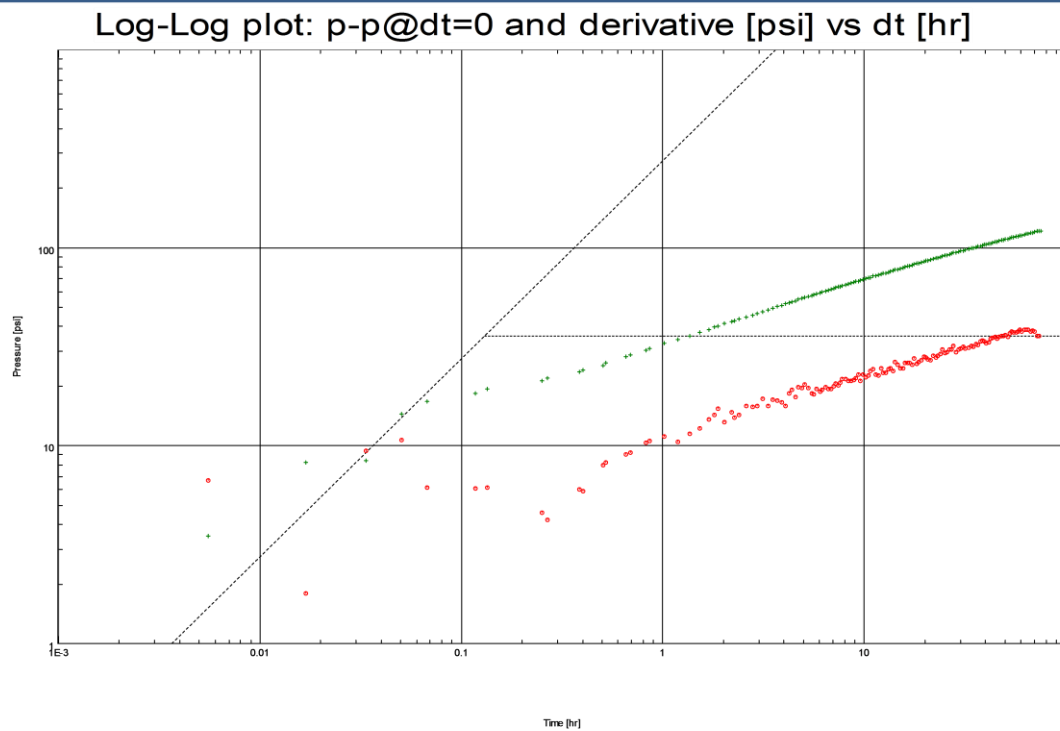
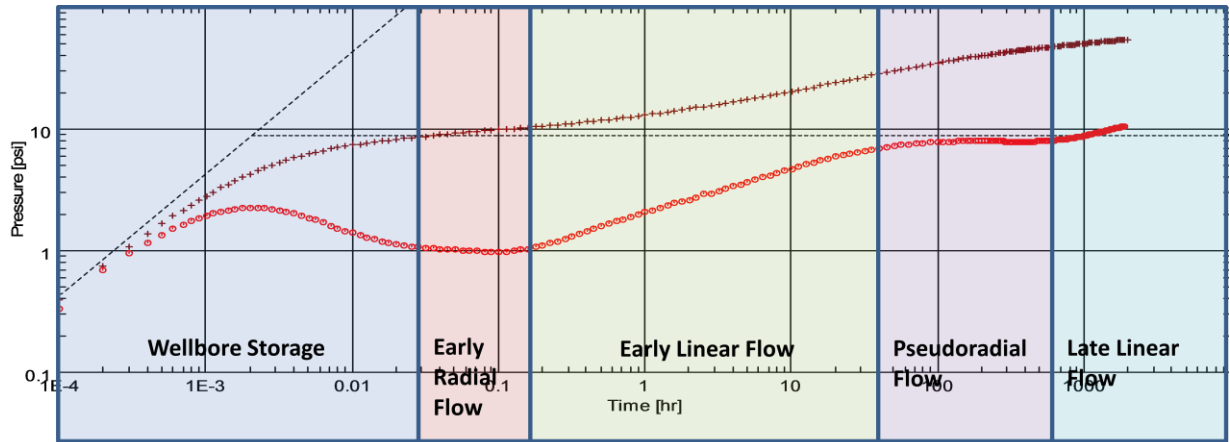
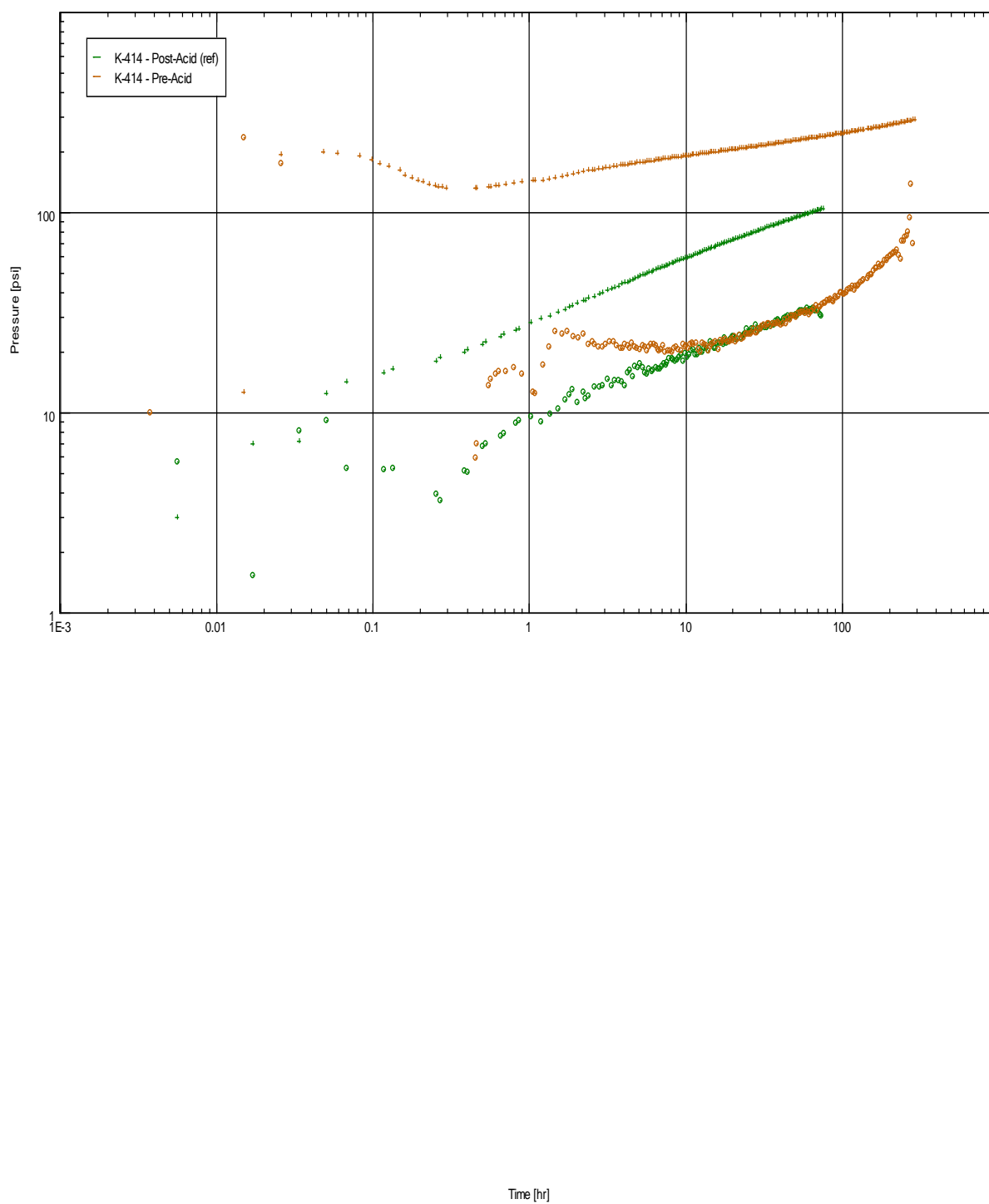


Figure 5.24: Post-stimulation log-log analysis for Y-2 (bottom) compared to ideal horizontal well behavior (top)



Compare files: Log-Log plot (dp and dp' normalized [psi] vs dt)

Figure 5.25: Comparison of pre- and post-stimulation log-log analysis for Y-2

5.2.5 Assessment of Long Rate Stabilization Effects

Considering the pre-acid buildup period, well production rates over a period of 30 days changed quite aggressively, as illustrated in **Fig. 5.26**, for which the log-log analysis is illustrated in **Fig. 5.23**.

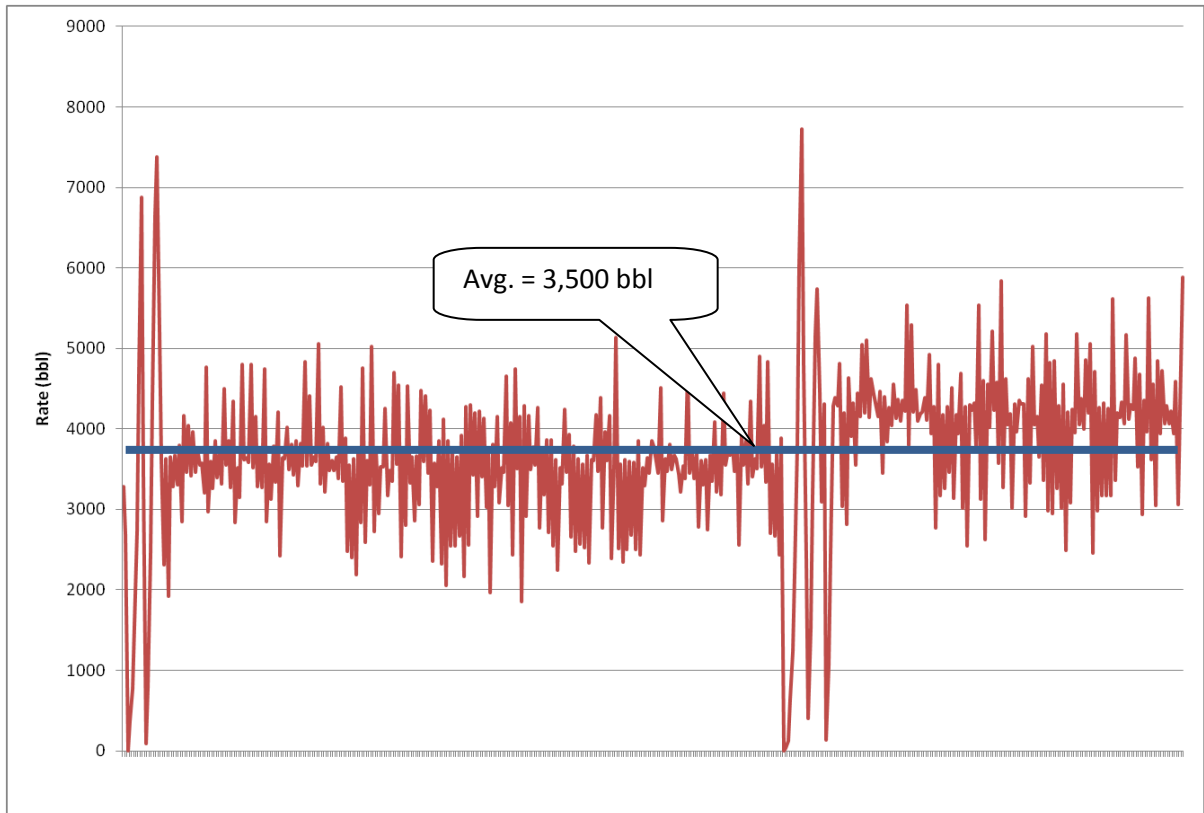
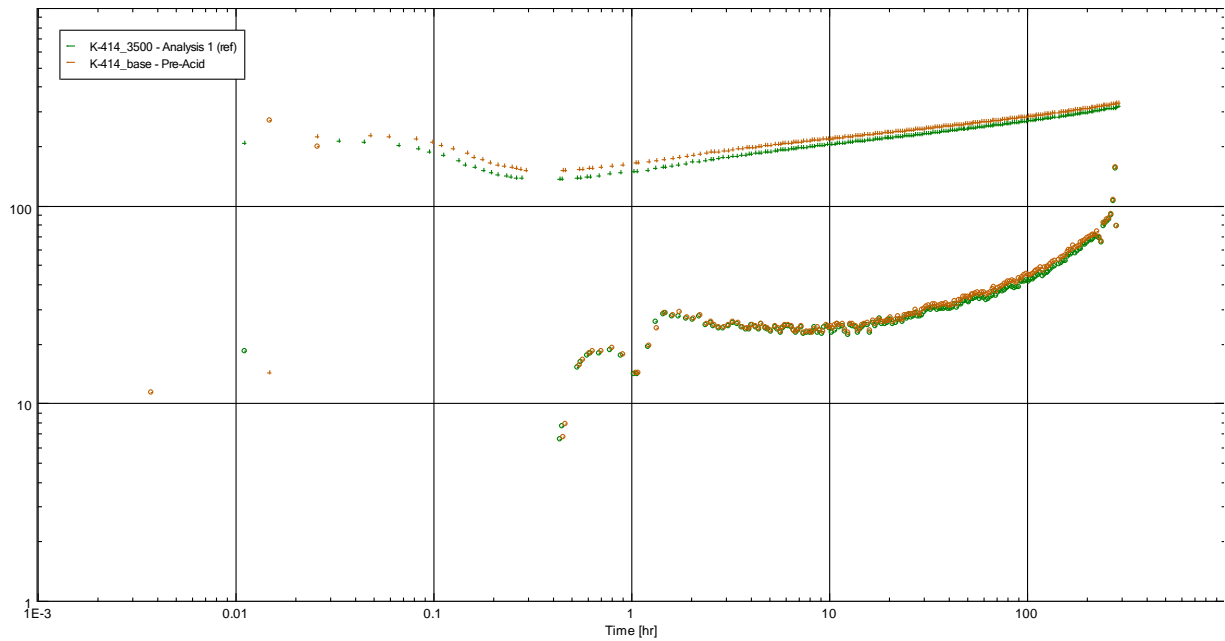


Figure 5.26: Rate changes on Y-2 before shut-in for pre-acid pressure buildup

In theory, rate stabilization will decrease the span of analyzable buildup data. The classic approaches to semi log procedures for analyzing pressure buildup data were derived using a superposition equation, which assumes that production is at a constant flow rate (Miller et al., 1950; Horner, 1951). In log-log analysis, however, there has been no effect when replacing the whole history and stabilizing it with a single rate of 3,500 bbl, as illustrated in **Fig. 5.27**.



Compare files: Log-Log plot (p-p@dt=0 and derivative [psi] vs dt [hr])

Figure 5.27: Y-2 log-log analysis overlay of original case vs. stabilized rate

5.2.6 Assessment of Minimum Duration Effects

Considering the post-acid buildup period, well production rates over preceding this build up changed quite frequently, as illustrated in **Fig. 5.27**, for which the log-log analysis is illustrated in **Fig. 5.24**. For the purpose of assessing the effect on the analysis, rate history was only limited to the last production rate, as illustrated in **Fig. 5.28**. The effect on the log-log analysis when compared with the total rate history inclusion is illustrated in **Fig 5.29**.

It can be concluded in this case that considering the total history will not yield to much improvement in the analysis over including the last rate before shut-in.

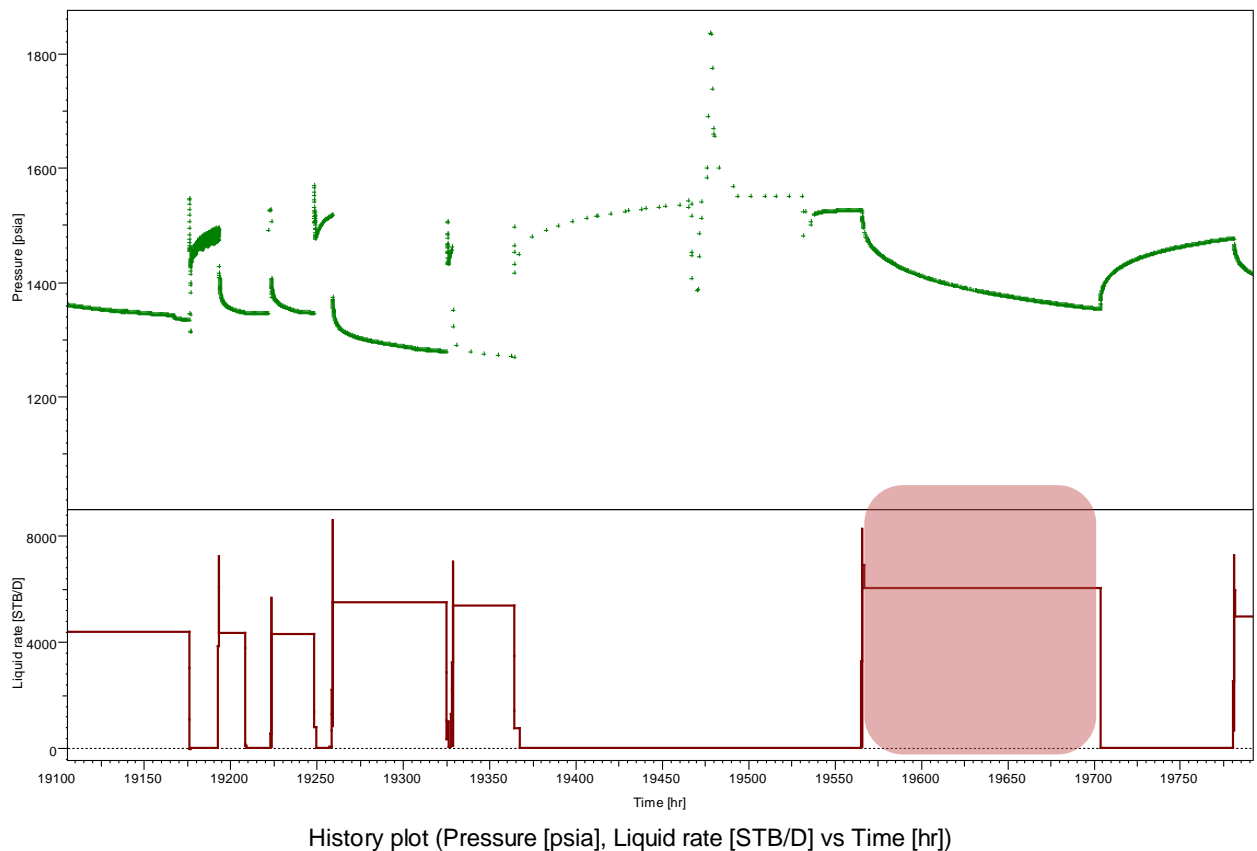
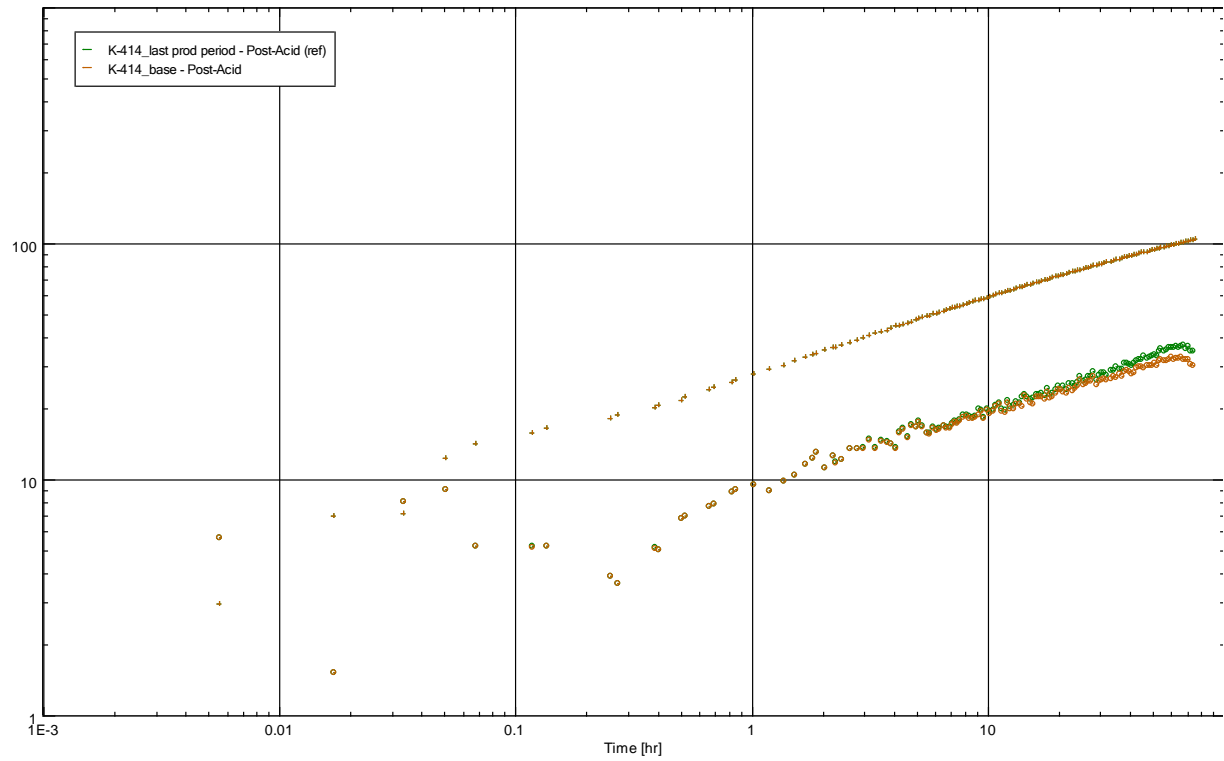


Figure 5.28: Rate changes on Y-2 before shut-in for post-acid pressure buildup, with last production period highlighted



Compare files: Log-Log plot (dp and dp' normalized [psi] vs dt)

Figure 5.29: Y-2 log-log analysis overlay of original case vs. last production rate

5.3 Case 3: Z-3

5.3.1 Field Description

This field measures 23 km in length and 10 km in width. It was discovered in March 1940, with first production in 1961. The field has eight oil-bearing reservoirs: Arab-A and -B, Post Arab-B Stringer, Arab-C, Hanifa, Hadriya, and Upper and Lower Fadhili. Arab-C reservoir produces Arab Medium crude, and the other five reservoirs produce Arab Light crude. Depths of the reservoirs range from 8,600 ft in the Arab reservoir to 10,000 ft in the Fadhili reservoir. In general, the reservoir quality is moderate to good, especially in the crestal area. The reservoir quality in the Hadriya reservoir deteriorates toward the flank.

5.3.2 Well Description

Well Z-3 was completed in June 1973 as vertical producer. It was recompleted in March 2007 as an open hole vertical producer in the Hadriya reservoir lifted with ESP. **Fig. 5.30** shows formation analysis logs for Z-3. It was equipped with an ESP system and a PDHMS for artificial lift and reservoir monitoring, respectively. **Fig. 5.31** shows a well cross section of Z-3. This well was subjected to well acid stimulation before the buildup test interval.

5.3.3 Data

Fig. 5.32 shows the downhole pressure and rate readings after applying the filtration. These data cover a period of 5,500 hours [230 days] with 46,367 pressure points and 104 rate points.

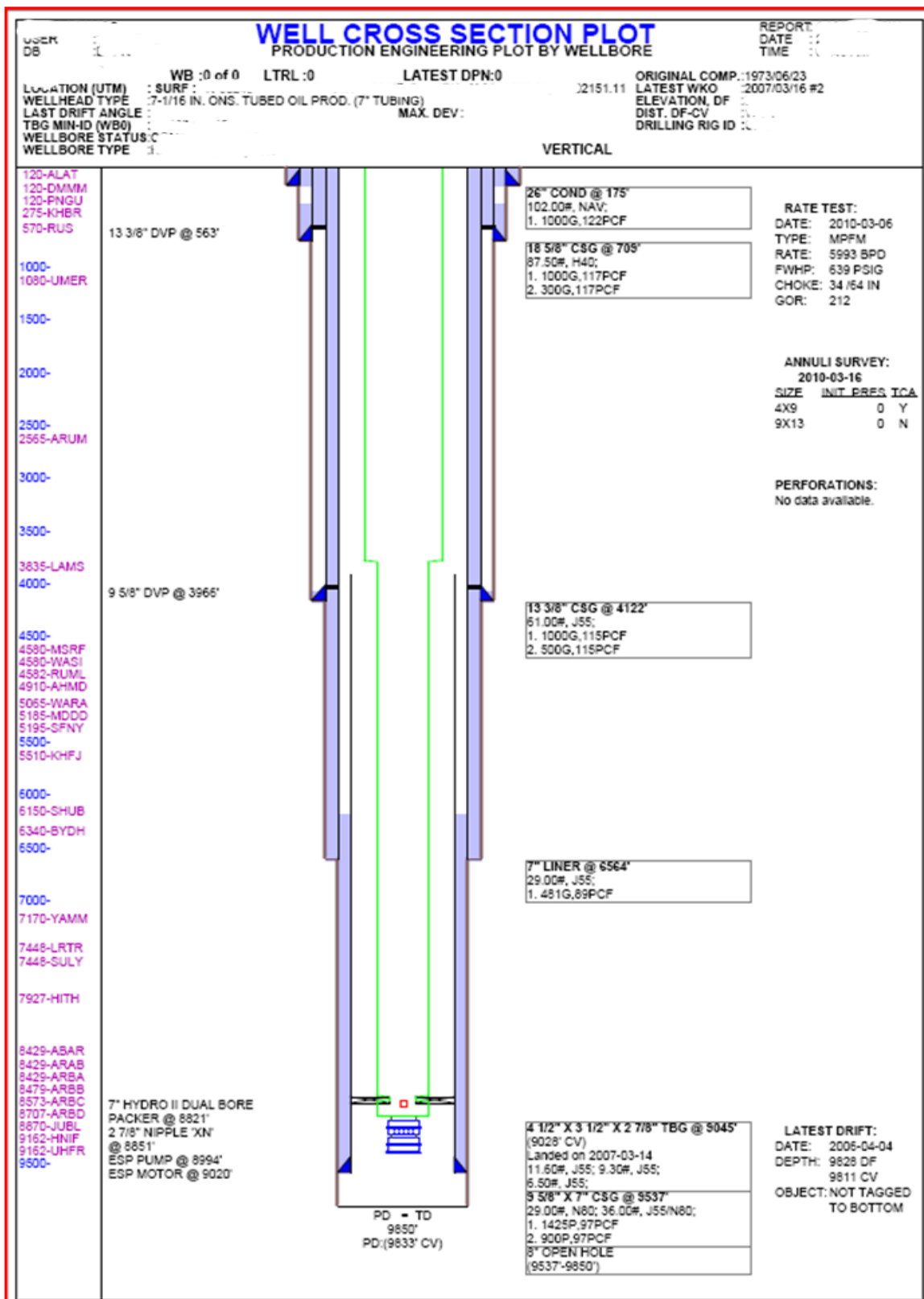
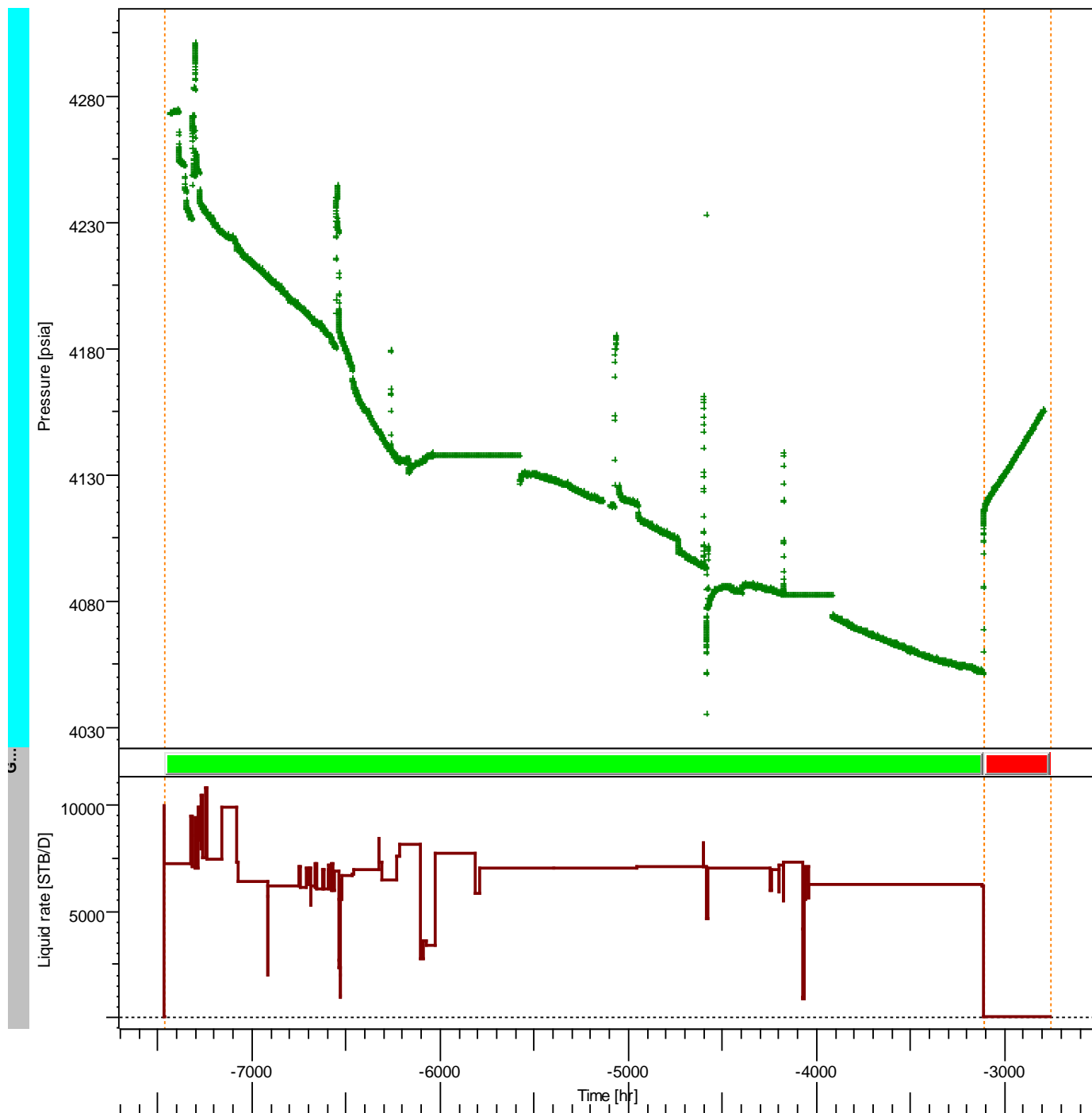


Figure 5.31: Z-3 well cross section



Pressure [psia], Not a unit, Liquid rate [STB/D] vs Time [hr]

Figure 5.32: Rate and pressure data obtained from well Z-3

5.3.4 Analysis

In this dataset, the focus is in the last buildup period. The line source solution for the pressure at time t after the startup of flow into the source and at distance r from the well is, in oilfield units,

$$p_{(r,t)} = p_i - 141.2 \frac{Qu}{kh} \left[-0.5Ei \left(\frac{-\phi\mu C_t r^2}{kt} \right) \right].$$

Dimensionless coordinates are used to remove the effects of case specificity on the pressure response, defined as (Eqs. 5.2, 5.3, and 5.4)

$$p_D = (p_i - p) \frac{kh}{141.2Q\mu},$$

$$t_D = 0.0002637 \frac{kt}{\phi\mu C_t r_w^2},$$

$$r_D = \frac{r}{r_w},$$

where

t = time (hours)

ϕ = porosity (pore volume/bulk volume)

c_t = total system compressibility (per psi)

r_w = wellbore radius (ft).

Skin effect, which is a dimensionless parameter that represents the additional (positive or negative) pressure drop, suffered at the sand face by the reservoir fluids flowing into the well on account of near-wellbore flow restriction or flow enhancement, calculated in oilfield units as (Eq. 5.4)

$$S = \frac{kh}{141.2qB\mu} \Delta p_s.$$

The wellbore storage coefficient C is a parameter used to quantify the volume of fluid that the wellbore itself will produce due to a unit drop in pressure, described as (Eq. 5.5)

$$C = \frac{V}{\Delta p},$$

where

V =volume produced (bbl)

Δp = pressure drop (psi).

From the expressions of the dimensionless coordinates t_D , C_D , and P_D and from the pressure match, permeability thickness product kh can be calculated as (Eq. 5.6)

$$kh = 141.2Q\mu M_p,$$

where

M_p = pressure match.

From the time match, the WBS constant C can be calculated as (Eq. 5.7)

$$C = 0.000295 \frac{kh}{\mu M_t},$$

where

M_t = time match.

Then, the value of C_D can be calculated from the WBS constant C as (Eq. 5.8)

$$C_D = 0.08936 \frac{C}{\phi C_t h r_w^2}.$$

From the skin match M_s , the skin factor can be calculated as (Eq. 5.9)

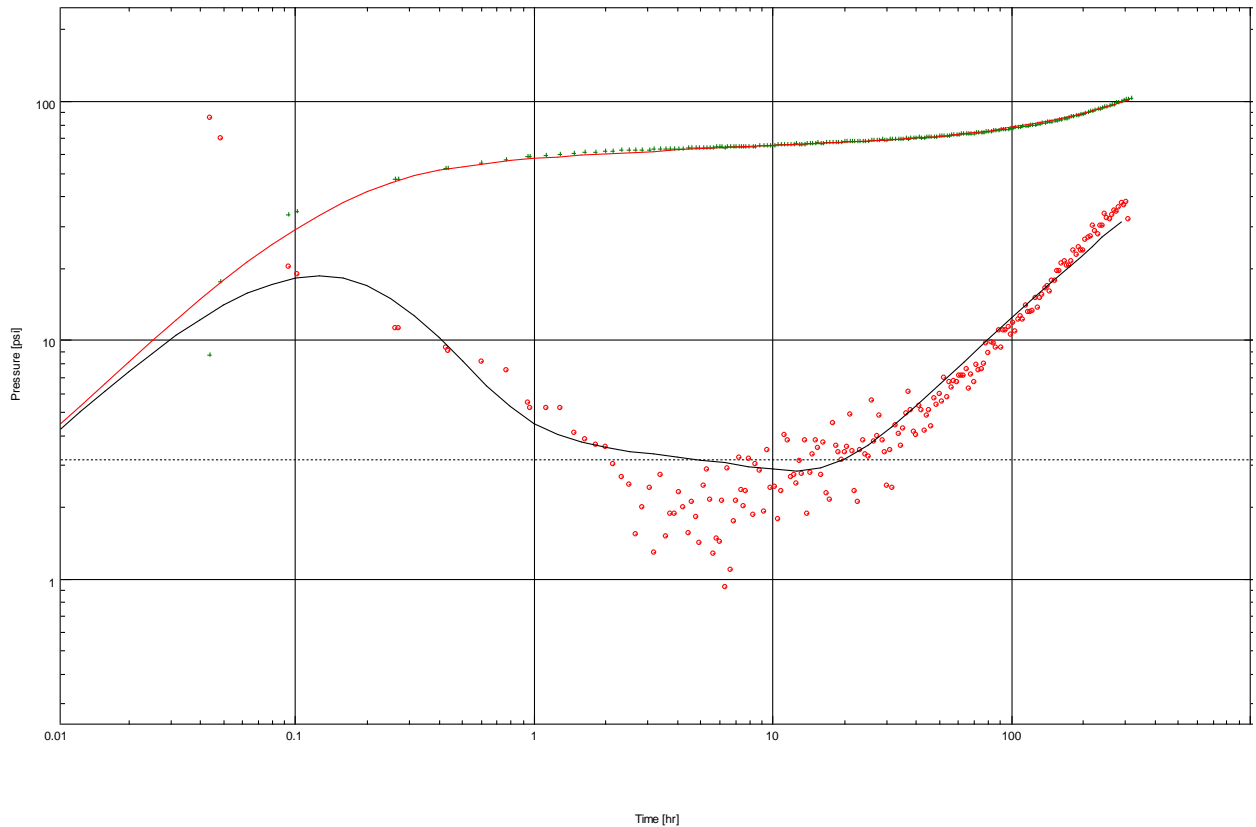
$$S = \frac{1}{2} \ln \frac{M_s}{C_D}.$$

Fig 5.33 shows the log-log analysis of the last buildup period using PDHMS real-time data.

Given the following conditions, a vertical well model was used to match the data with constant WBS in an infinite-boundary radial composite reservoir.

- porosity $\phi = 18\%$

- well radius $r_w = 0.33$ ft
- pay zone $h = 210$ ft
- fluid type is oil
- volume factor $B_o = 1.19$ B/STB
- viscosity $\mu_o = 0.75$ cp
- total compressibility $c_t = 1.76 \times 10^{-5}$ psi⁻¹

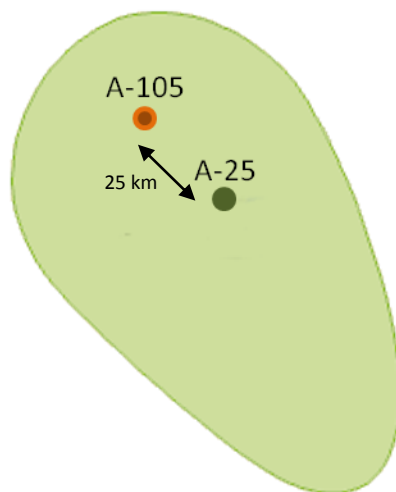
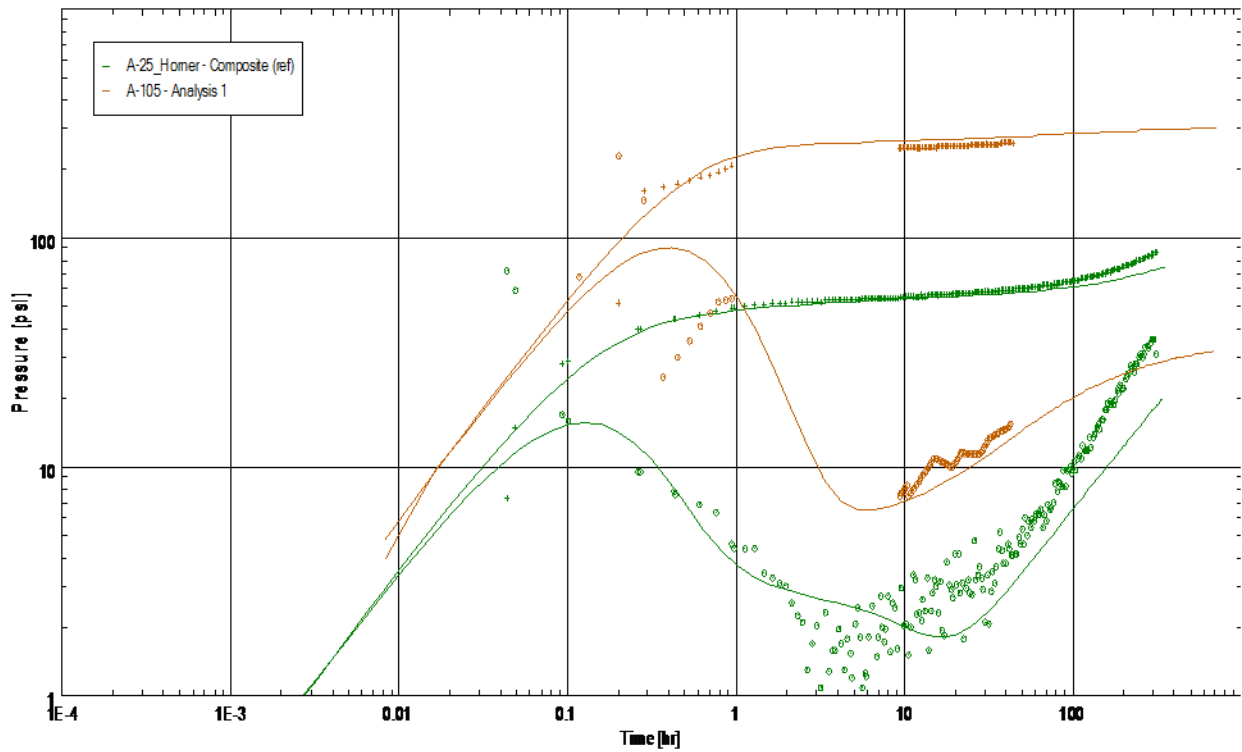


Log-Log plot: p-p@dt=0 and derivative [psi] vs dt [hr]

Figure 5.33: Z-3 log-log analysis

The pressure derivative data exhibit a sharp upward turn at late time, indicating possible degradation in reservoir quality, boundary effect, or interference from a nearby well. Attempts to simulate possible interference from nearby did not yield a match of the pressure history. Also, the geology of the area does not indicate the existence of faults. Therefore, the rise in the derivative was attributed to degradation in reservoir quality. This is supported by the nearby well A-105, completed in the same reservoir, that demonstrated

similar signature of sharp upward turn at late time**Fig5.34**. Note that this analysis included complete rate history.



Compare files: Log-Log plot (dp and dp' normalized [psi] vs dt)

Figure 5.34: Comparison between Z-3 log-log analyses with nearby well A-105

The main model parameters obtained from the matched model are as follows (**Fig. 5.35**):

- $M_t = 71.2 \text{ hr}^{-1}$
- $M_p = 0.159 \text{ psi}^{-1}$
- $C = 0.681 \text{ bbl/psi}$
- total skin = 1.33
- $kh_{\text{total}} = 123,000 \text{ md.ft}$
- $k_{\text{avg}} = 587 \text{ md}$
- $P_i = 4,510.86 \text{ psi}$
- $Z_w = 55 \text{ ft}$

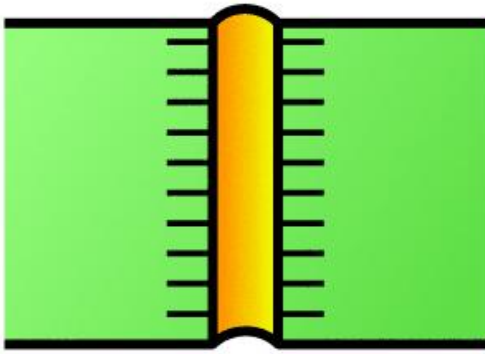


Figure 5.35: Well parameters

The reservoir and boundary parameters obtained from the matched model are as follows

(**Fig. 5.36**):

- $h = 210 \text{ ft}$
- $kh = 123,000 \text{ md.ft}$
- $k = 587 \text{ md}$
- $R_i = 5,210 \text{ ft}$
- $M = 40.3$ *Mobility ratio, (k/μ of inner zone over k/μ of outer zone)*
- $D = 2.18$ *Diffusivity ratio, ($k/\phi\mu.ct$ of innerzone over $k/\phi\mu.ct$ of outer zone)*

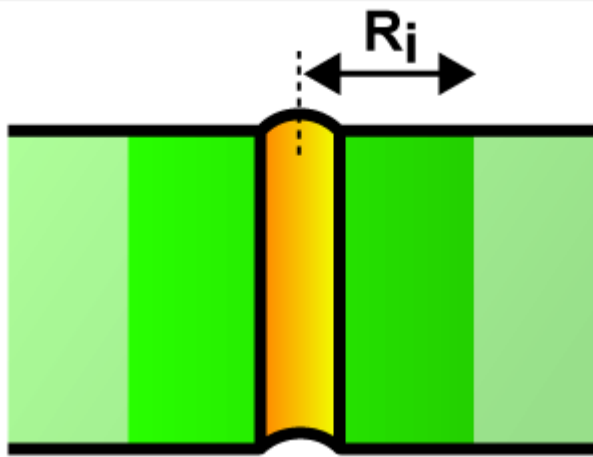


Figure 5.36: Reservoir parameters

Results indicate a good match of the buildup data, with a permeability contrast at approximately 1.5 km away from the well. The flow capacity for this well is estimated at 123,000md.ft, while the productivity index is 60Bbl/psi. Results also indicate a skin factor damage of 1.3. Detailed analysis for this case is presented Appendix A.

5.3.5 Assessment of Minimum Duration Effects

As with the quality of pressure measurements, a focus on flow rate history will yield better model identifications and correct well and reservoir parameter estimations. This is particularly true with the pressure derivative method, which is a very powerful tool, but at the same time is more sensitive to the accuracy and completeness of rate and pressure data that preface the buildup or fall-off periods. The need to take into account the entire rate history has been investigated in the past, and several methods have been proposed to account for production history effects, such as Horner equivalent time or the introduction of a modified rate and time when the production has not been stabilized prior to shut-in (Daungkaew, 2000).

In Horner equivalent time, the rate history is simplified and reduced to one single drawdown, with a rate q_{last} equal to the last rate value prior to shut-in and with a duration t_{pe} equal to the correct cumulative production Q , divided by that last rate:

$$t_{pe} = \frac{24Q}{q_{last}}.$$

In this case of $t_{pe} = 4,812.29\text{hr}$, **Fig.5.37** shows the Horner plot of Z-3 pressure vs. superposition time.

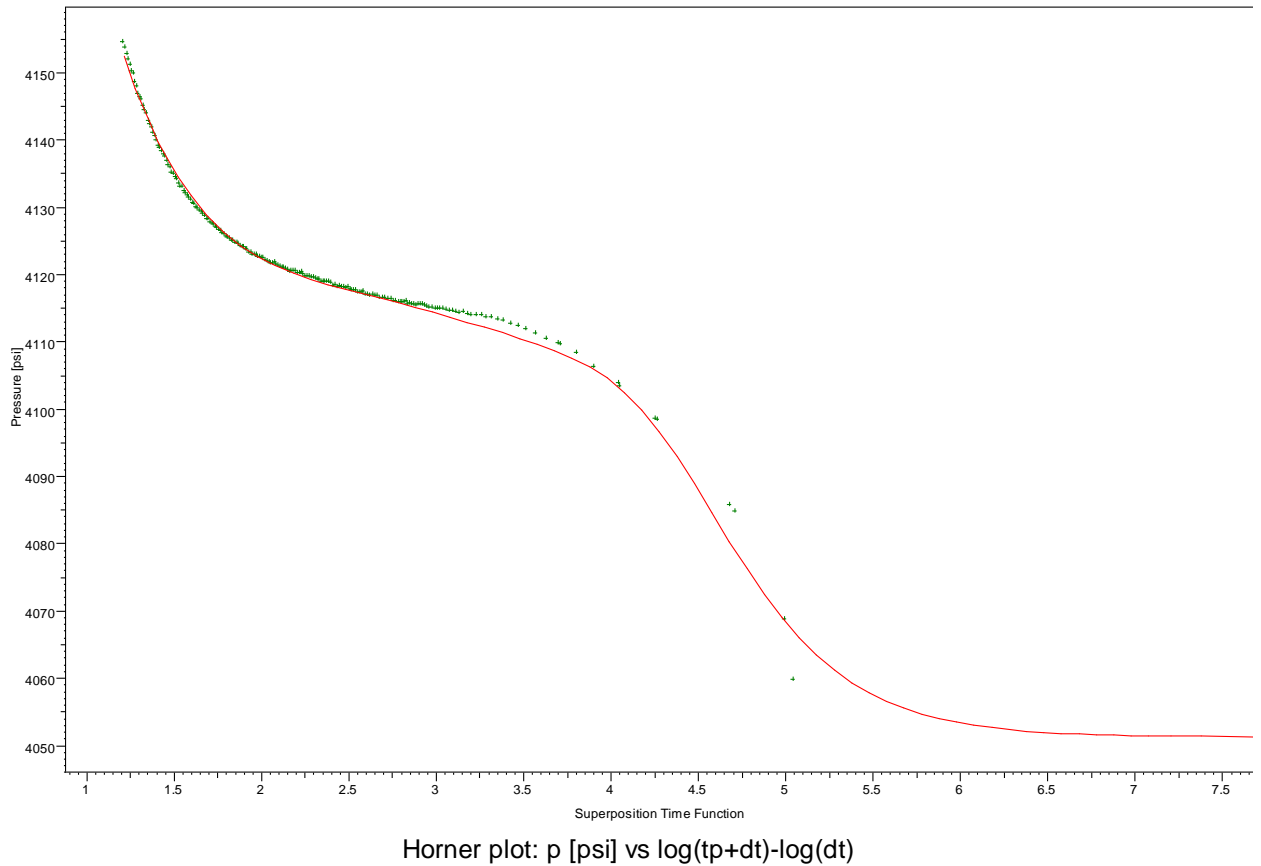
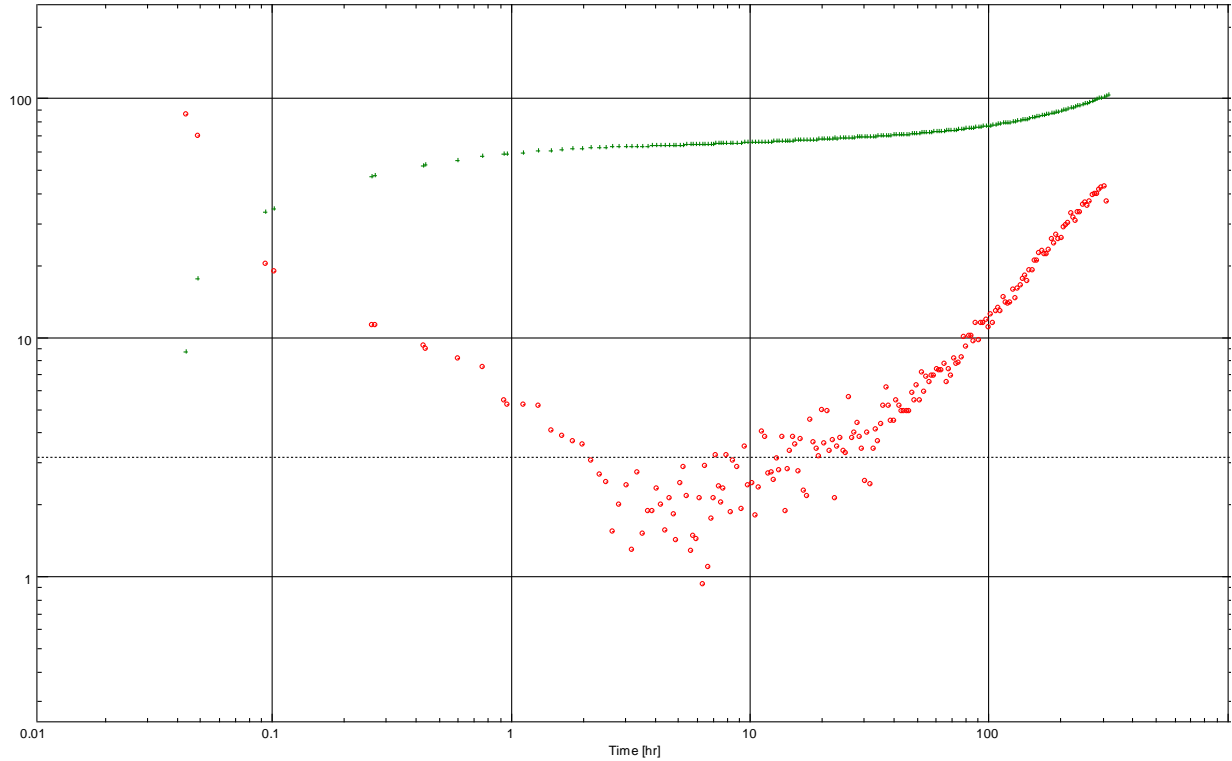


Figure 5.37: Z-3 Horner plot

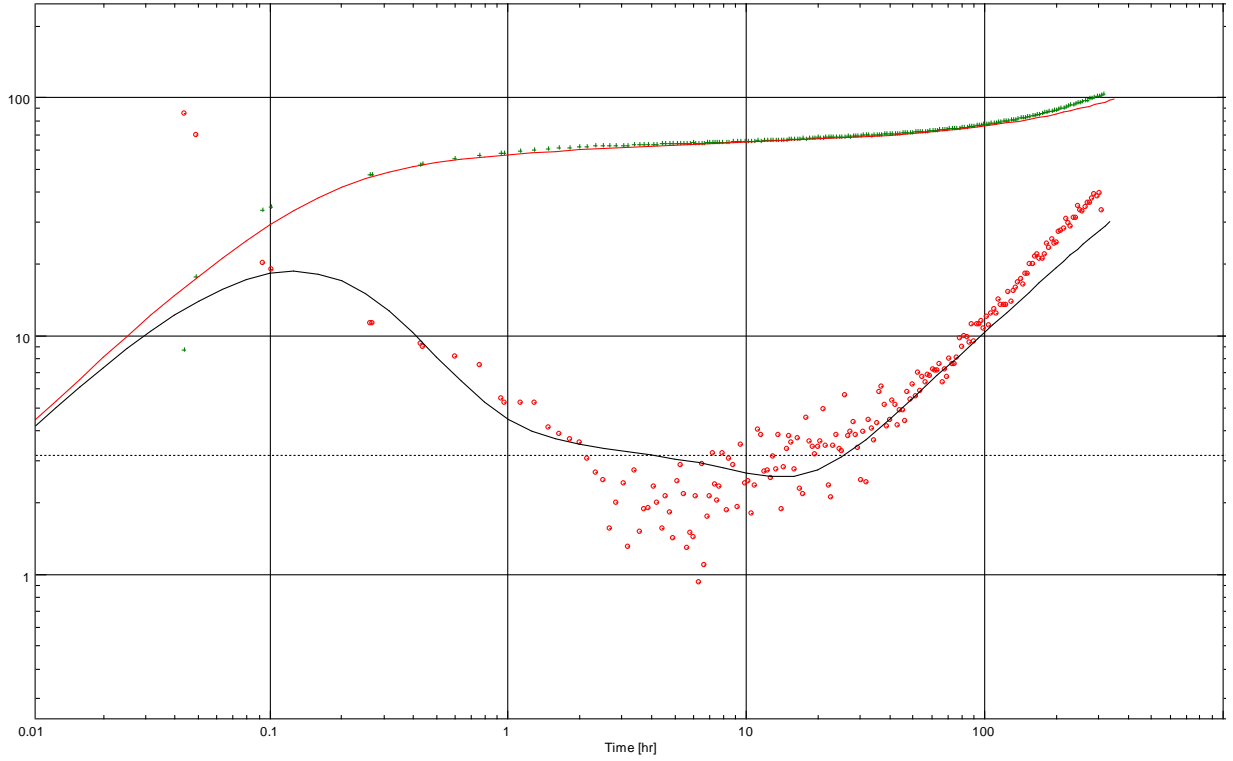
With this approach, the Z-3 model was regenerated with a reduced history up to t_{pe} . **Fig 5.38** shows the resultant log-log plot.



Log-Log plot: p-p@dt=0 and derivative [psi] vs dt [hr]

Figure 5.38: Log-log analysis of Z-3 with Horner approximation

Cinco-Ley and Samaniego (1989) suggest a new rate history approximation that combines a Horner equivalent time with a detailed history for some part of the production history before the test. Using this approach, Daungkaew et al. (2000) investigate different combinations and concludes that rates should be described accurately for the last 40% of the cumulative production, with the first 60% being approximated with a Horner equivalent time $40\% + t_{pe}$. Applying this to the Z-3 case resulted in the log-log graph shown in **Fig. 5.39**.



Log-Log plot: $p-p@dt=0$ and derivative [psi] vs dt [hr]

Figure 5.39: Log-log analysis of Z-3, with the Cinco-Ley-and-Samaniego approximation
40% + $\llbracket t \rrbracket_{pe}$

Due to the nature of the permanent data capturing that exists in the digital oilfields, which avails production history and, in this case, an extended shut-in period of more than 16 days, the effect of eliminating part of the production history using either Horner or Cinco-Ley-and-Samaniego approximations is hardly felt in the analysis. **Fig. 5.40** shows an overlay of the log-log analysis of the base case, Horner, and Cinco-Ley-and-Samaniego approaches.

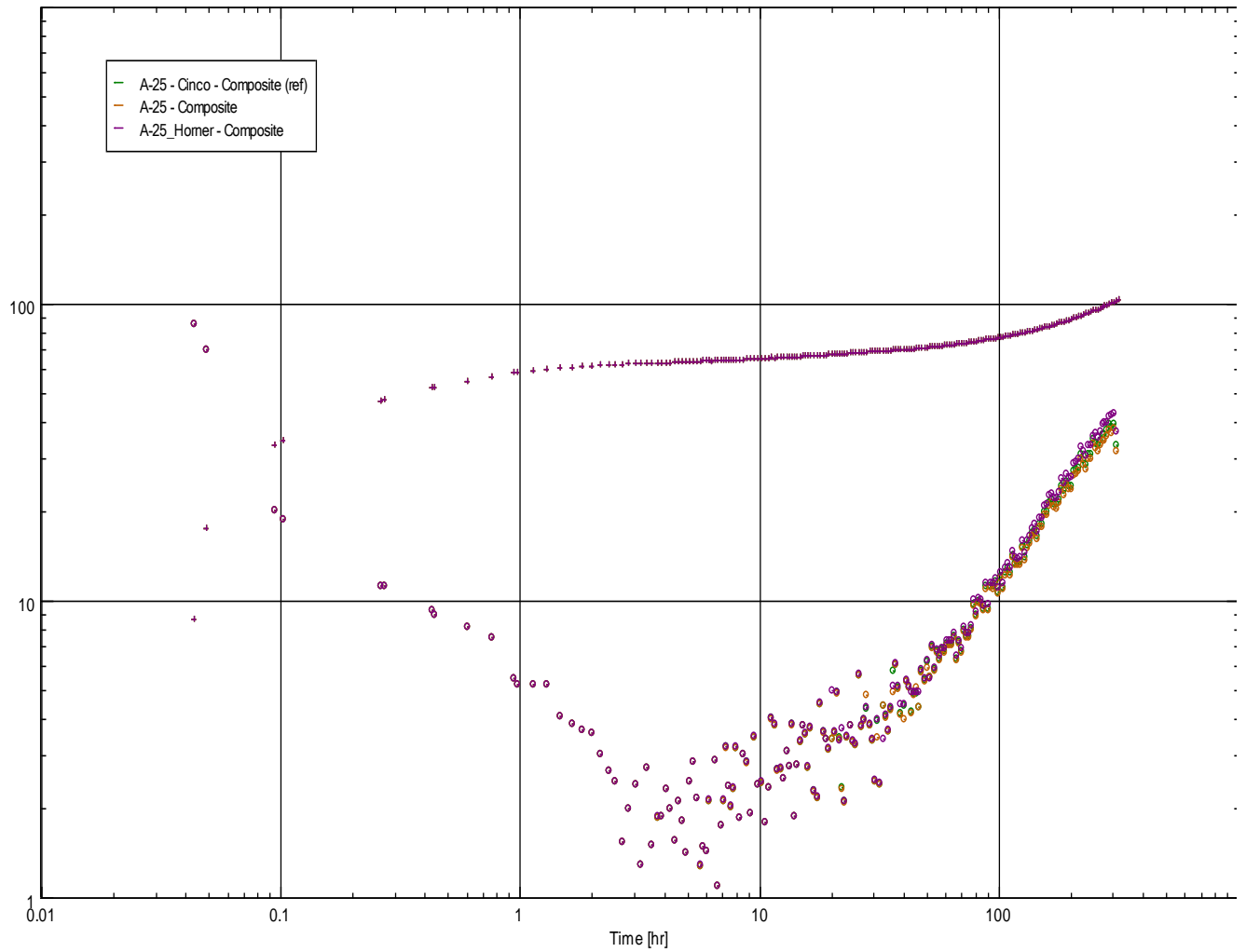


Figure 5.40: Z-3 log-log analysis of the base case, Horner, and Cinco-Ley–and–Samaniego approaches

Only when we consider a far shorter rate history—in this case, equivalent to the buildup period—we start to notice some effects. **Fig. 5.41** shows this effect compared with previous approximations. This concludes that the Horner equivalent time approximation is safe and valid to use in such an analysis.

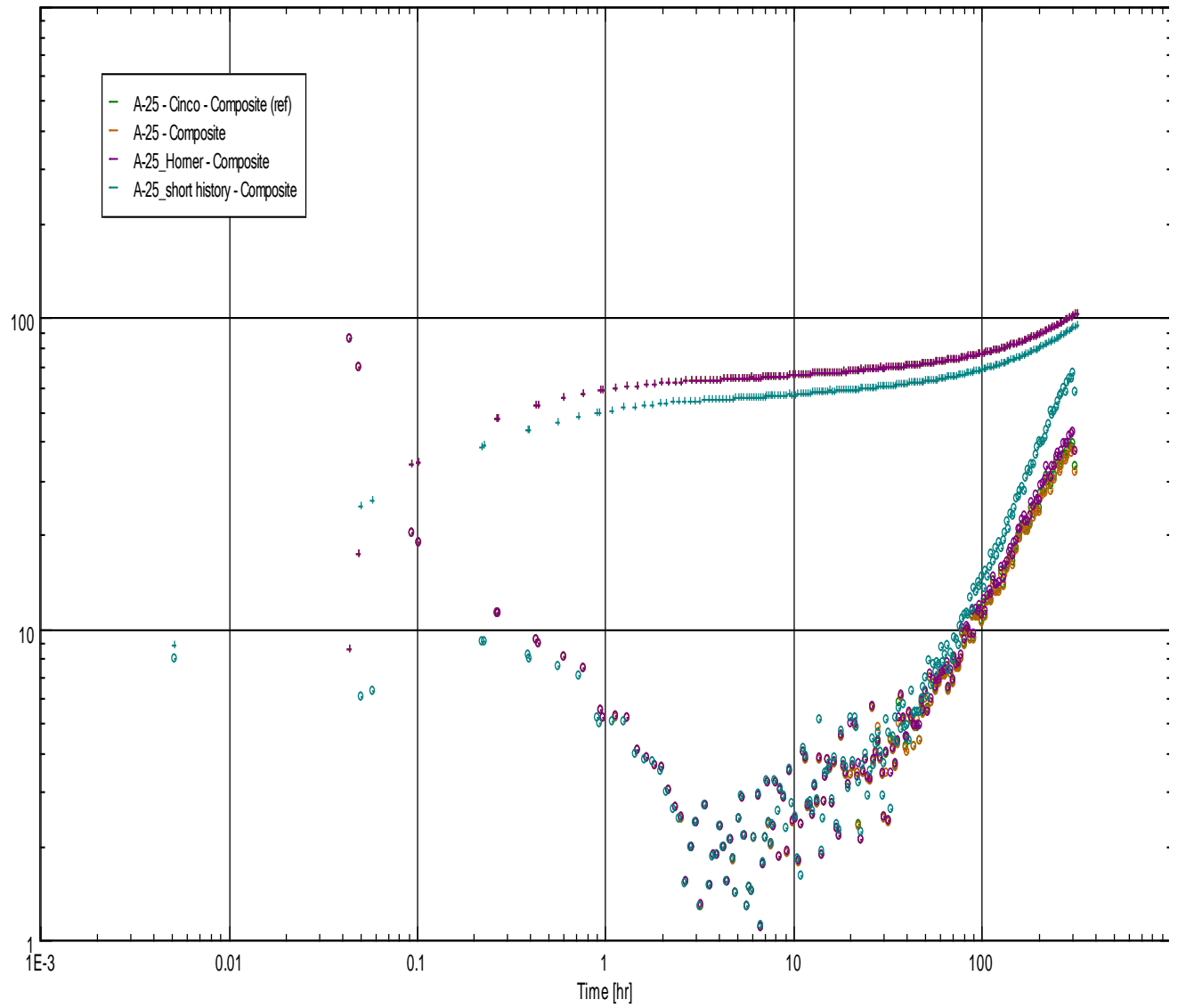


Figure 5.41: Z-3 log-log analysis of the base case, Horner, and Cinco-Ley–and–Samaniego approaches, compared with a shorter rate history

CHAPTER 6

CONCLUSION

In this study, we have presented dynamic pressure transient analysis workflows to utilize permanent downhole gauges availed by the new “Intelligent Field” initiatives in the industry. These workflows leverage the massive investments in instrumentation, data acquisition, and storage to enable dynamic characterization of hydrocarbon reservoirs. Several challenges in on establishing reliable analysis using these data were discussed in this study; including minimum duration, long stabilization, and data interruptions. The utilization of this data in pressure transient analysis will result in significant cost savings due to a reduction in the number of planned shut-ins for pressure buildup tests which would normally require well shut-in and, consequently, loss of production from a few days to a few weeks. In addition, the use of long production history data captured by PDHMSs enables the determination of reservoir boundaries, hydrocarbons in place, and permeability.

REFERENCES

1. Aghar, H., Carie, M., Elshahawi, H., Gomez, J.R., Saeedi, J., Young, C., Pinguet, B., Swainson, K., Takla, E., and Theuveny, B. 2007. The Expanding Scope of Well Testing. *Oilfield Review***19** (1): 44–59.
2. Al-Dhubaib, T.A., Almadi, S.M., Shenqiti, M.S., and Mansour, A.M. 2008a. I-Field Data Acquisition and Delivery Infrastructure: Case Study. Paper SPE 112201 presented at the SPE Intelligent Energy Conference and Exhibition, Amsterdam, The Netherlands, 25–27 February. doi: 10.2118/112201-MS.
3. Al-Dhubaib, T.A., Issaka, M.B., Barghouty, M.F., Mubarak, S., Dowais, A.H., Shenqiti, M.S., and Ansari, N.H. 2008b. Saudi Aramco Intelligent Field Development Approach: Building the Surveillance Layer. Paper SPE 112106 presented at the SPE Intelligent Energy Conference and Exhibition, Amsterdam, The Netherlands, 25–27 February. doi: 10.2118/112106-MS.
4. Athichanagorn, S., Horne, R.N., and Kikani, J. 1999. Processing and Interpretation of Long-Term Data Acquired from Permanent Pressure Gauges. *SPE Res Eval&Eng***5** (5): 384–391. SPE-80287-PA. doi:10.2118/80287-PA.
5. Chorneyko, D.M. 2006. Real-Time Reservoir Surveillance Utilizing Permanent Downhole Pressures - An Operator's Experience. Paper SPE 103213 presented at the SPE Annual Technical Conference and Exhibition, San Antonio, Texas, 24–27 September. doi: 10.2118/103213-MS.
6. Cinco-Ley, H. and Samaniego, V.F. 1989. Use and Misuse of the Superposition Time Function in Well Test Analysis. Paper SPE 19817 presented at the 64th Annual Technical Conference and Exhibition, San Antonio, Texas, USA, 8–11 October. doi: 10.2118/19817-MS.
7. Daungkaew, S., Hollaender, F., and Gringarten, A.C. 2000. Frequently Asked Questions in Well Test Analysis. Paper SPE 63077 presented at the SPE Annual Technical Conference and Exhibition, Dallas, Texas, USA, 1–4 October. doi: 10.2118/63077-MS.

8. de Oliveira Silva, M.I. and Kato, E.T. 2004. Reservoir Management Optimization Using Permanent Downhole Gauge Data. Paper SPE 90973 presented at the SPE Annual Technical Conference and Exhibition, Houston, Texas, USA, 26–29 September. doi: 10.2118/90973-MS.
9. Horne, R.N. 1990. *Modern Well Test Analysis: A Computer-Aided Approach*. Palo Alto, California: Petroway.
10. Horne, R.N. 2007. Listening to the Reservoir—Interpreting Data from Permanent Downhole Gauges. *J Pet Technol* **59** (12): 78–86. SPE-103513-MS.
11. Horner, D.R. 1951. Pressure Build-Up in Wells. Paper WPC 4135 presented at the 3rd World Petroleum Congress, The Hague, The Netherlands, May 28– June 6.
12. Houzé, O., Viturat, D., and Fjaere, O.S. 2008. *Dynamic Flow Analysis*. KAPPA Engineering.
13. Miller, C.C., Dyes, A.B., and Hutchinson Jr., C.A. 1950. The Estimation of Permeability and Reservoir Pressure From Bottom Hole Pressure Build-Up Characteristics. SPE-950091-G. *Trans. AIME* **189**: 91–104.
14. Nestlerode, W.A. 1963. The Use of Pressure Data from Permanently Installed Bottom Hole Pressure Gauges. Paper SPE 590 presented at the SPE Rocky Mountain Joint Regional Meeting, Denver, Colorado, USA, May 27–28. doi: 10.2118/590-MS.
15. Ortiz, C.E.P., Auguiar, R.B., and Pires, A.P. 2009. Wavelet Filtering of Permanent Downhole Gauge Data. Paper SPE 123028 presented at the SPE Latin America and Caribbean Petroleum Conference, Catagena, Colombia, 31 May–3 June. doi: 10.2118/123028-MS.
16. Ouyang, L.B. and Kikani, J. 2002. Improving Permanent Downhole Gauge (PDG) Data Processing via Wavelet Analysis. Paper SPE 78290 presented at the 13th Europe Petroleum Conference, Aberdeen, Scotland, UK, 29–31 October. doi: 10.2118/78290-MS.

17. Omotosho, R.J. 2004. Permanent Downhole Sensors in Today's Petroleum Industry: Current Trends, Problems and Case Studies. MS Thesis, U. of Texas, Texas.
18. Reynolds Jr., A.C. 1986. Errors Involved in Pressure Buildup Analysis. SPE-15903-MS.
19. Saleri, N.G., Al-Kaabi, A.O., and Muallem, A.S. 2006. Haradh III: A Milestone for Smart Fields. *J Pet Technol* **58** (11).
20. Suzuki, S. and Chorneyko, D. 2009. Automatic Detection of Pressure-Buildup Intervals from Permanent Downhole Pressure Data Using Filter Convolution. Paper SPE 125240 presented at the SPE Annual Technical Conference and Exhibition, New Orleans, Louisiana, USA, 4–7 October. doi: 10.2118/125240-MS.
21. Van Gisbergen, S.J.C.H.M and Vandeweyer, A.A.H. 2001. Reliability Analysis of Permanent Downhole Monitoring Systems. *SPE Drill & Compl* **16** (1): 60–63. SPE-57057-PA. doi: 10.2118/57057-PA.

APPENDIX A

Data and Detailed Analysis Results

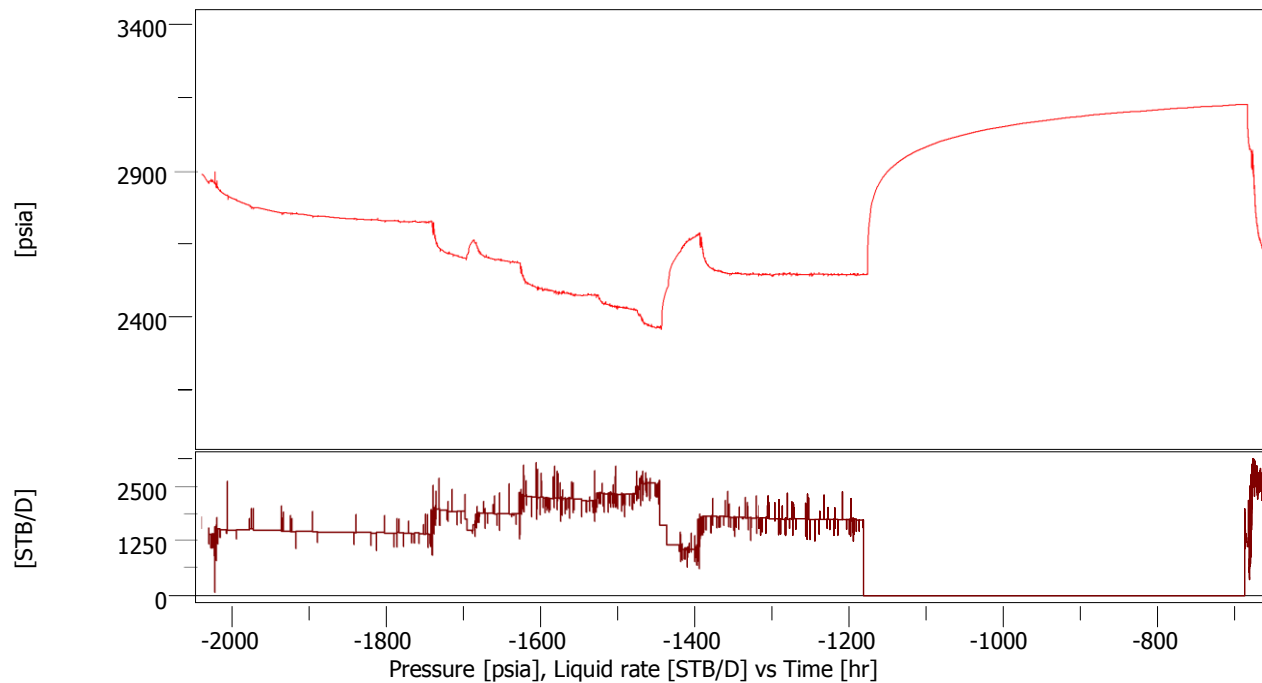
Case # 1

Well: X-1 Detailed PTA Analysis



History plot

Final

Company MMB Thesis
Well 1Field X
Test Name / # X-1 Real-Time BU Test

Fltd data S1 build-up #3
Rate 0 STB/D
Rate change 1727.49 STB/D
P@dt=0 2546.02 psia
Pi 3256.03 psia
Smoothing 0.1

Default values are used!
Selected Model
Model Option Standard Model
Well Horizontal, Changing Storage (Hegeman)
Reservoir Homogeneous
Boundary Infinite
Top/Bottom No flow/No flow

Main Model Parameters
TMatch 4.7 [hr]⁻¹
PMatch 0.00535 [psia]⁻¹
C 0.136 bbl/psi
Total Skin -6.14
k.h, total 785 md.ft
k, average 8.72 md
Pi 3256.03 psia

Model Parameters
Well & Wellbore parameters (1)
C 0.136 bbl/psi
Ci/Cf 0.809
delta_t 0.167 hr
Skin -2.89
Geometrical Skin -3.25
well length 1024.51 ft
Zw 75.4184 ft

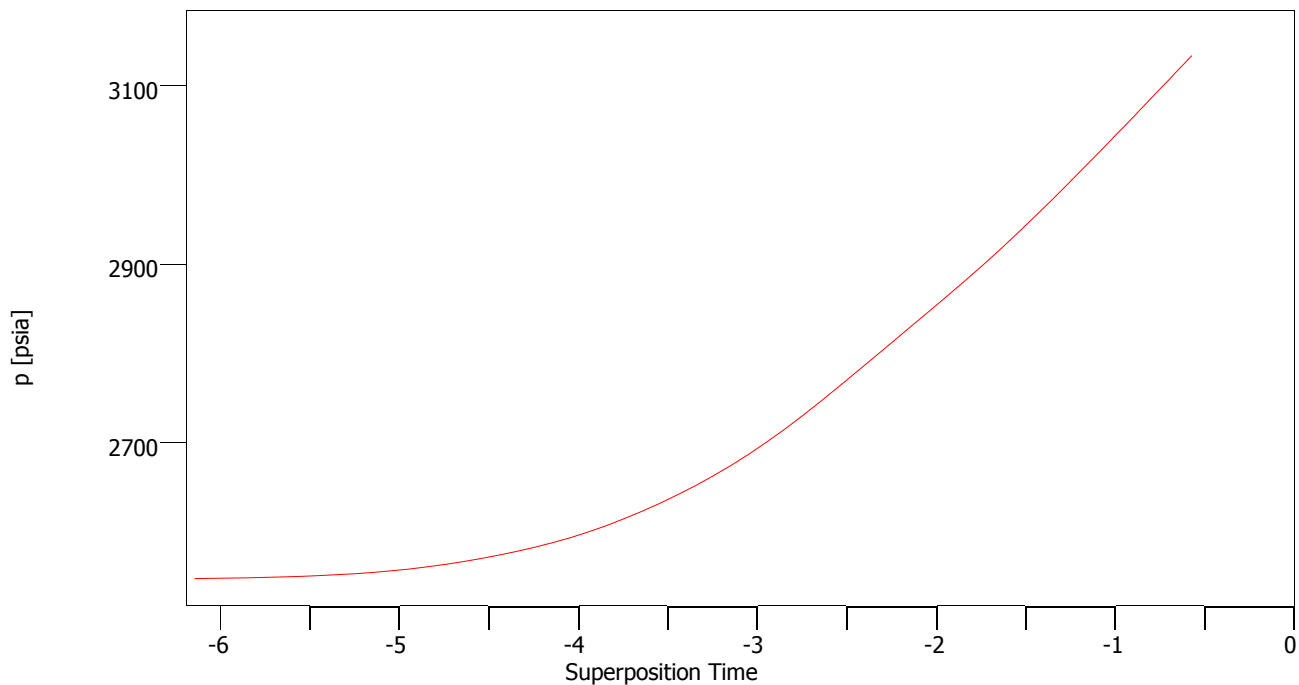
Reservoir & Boundary parameters
h 90 ft
Pi 3256.03 psia
k.h 785 md.ft
k 8.72 md
kz/kr 0.0146

Derived & Secondary Parameters
Rinv 4410 ft
Test. Vol. 166.814 MMB
Delta P (Total Skin) -1147.29 psi
Delta P Ratio (Total Skin) -1.9519 Fraction



Semi-Log plot

Final

Company MMB Thesis
Well 1Field X
Test Name / # X-1 Real-Time BU Test

Fltd data S1 build-up #3
Rate 0 STB/D
Rate change 1727.49 STB/D
P@dt=0 2546.02 psia
Pi 3256.03 psia
Smoothing 0.1

Default values are used!

Selected Model

Model Option Standard Model
Well Horizontal, Changing Storage (Hegeman)
Reservoir Homogeneous
Boundary Infinite
Top/Bottom No flow/No flow

Main Model Parameters

TMatch 4.7 [hr]⁻¹
PMatch 0.00535 [psia]⁻¹
C 0.136 bbl/psi
Total Skin -6.14
k.h, total 785 md.ft
k, average 8.72 md
Pi 3256.03 psia

Model Parameters

Well & Wellbore parameters (1)

C 0.136 bbl/psi
Ci/Cf 0.809
delta_t 0.167 hr
Skin -2.89
Geometrical Skin -3.25
well length 1024.51 ft
Zw 75.4184 ft

Reservoir & Boundary parameters

h 90 ft
Pi 3256.03 psia
k.h 785 md.ft
k 8.72 md
kz/kr 0.0146

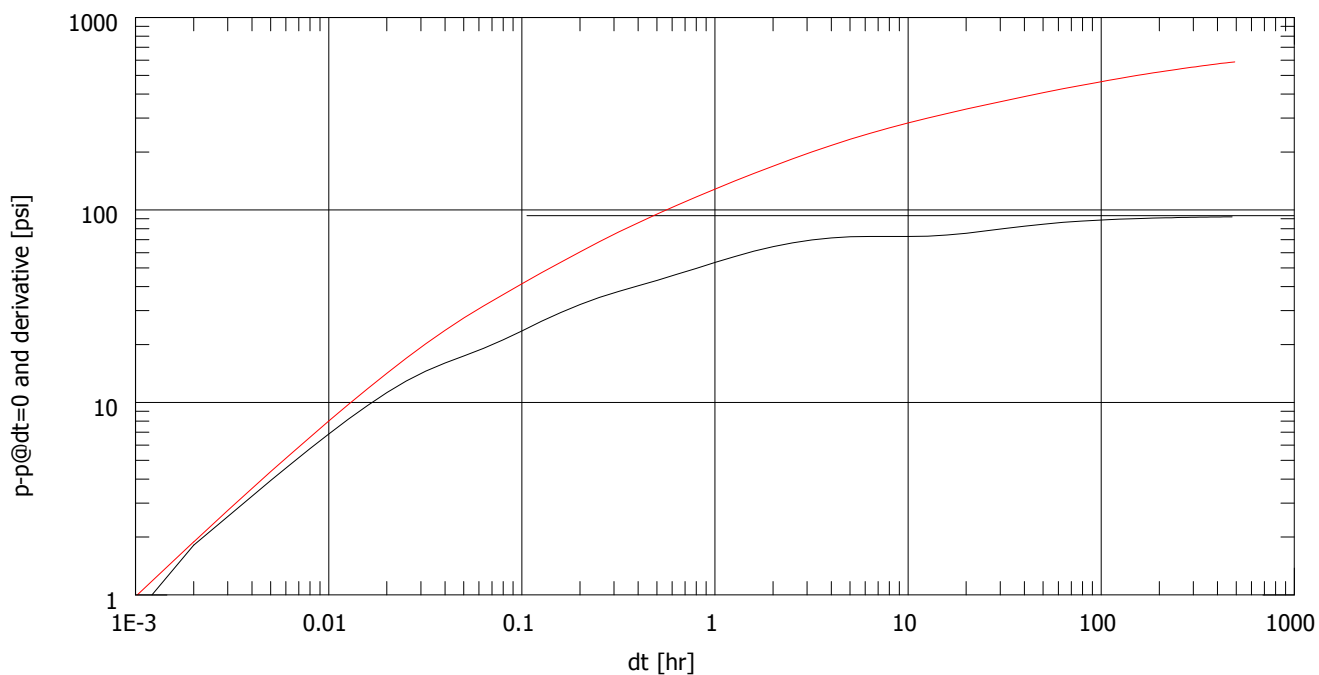
Derived & Secondary Parameters

Rinv 4410 ft
Test. Vol. 166.814 MMB
Delta P (Total Skin) -1147.29 psi
Delta P Ratio (Total Skin) -1.9519 Fraction



Log-Log plot

Final

Company MMB Thesis
Well 1Field X
Test Name / # X-1 Real-Time BU Test



Fltd data S1 build-up #3
Rate 0 STB/D
Rate change 1727.49 STB/D
P@dt=0 2546.02 psia
Pi 3256.03 psia
Smoothing 0.1

Default values are used!
Selected Model
Model Option Standard Model
Well Horizontal, Changing Storage (Hegeman)
Reservoir Homogeneous
Boundary Infinite
Top/Bottom No flow/No flow

Main Model Parameters
TMatch 4.7 [hr]⁻¹
PMatch 0.00535 [psia]⁻¹
C 0.136 bbl/psi
Total Skin -6.14
k.h, total 785 md.ft
k, average 8.72 md
Pi 3256.03 psia

Model Parameters
Well & Wellbore parameters (1)
C 0.136 bbl/psi
Ci/Cf 0.809
delta_t 0.167 hr
Skin -2.89
Geometrical Skin -3.25
well length 1024.51 ft
Zw 75.4184 ft
Reservoir & Boundary parameters
h 90 ft
Pi 3256.03 psia
k.h 785 md.ft
k 8.72 md
kz/kr 0.0146

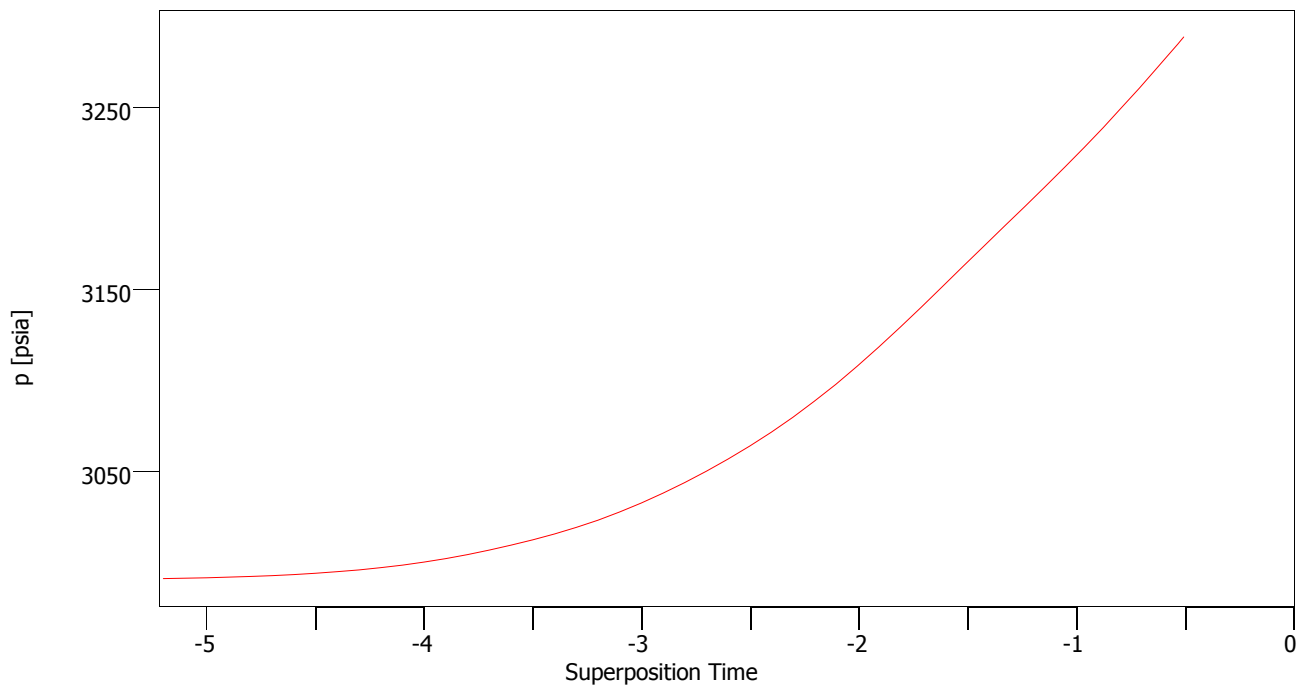
Derived & Secondary Parameters
Rinv 4410 ft
Test. Vol. 166.814 MMB
Delta P (Total Skin) -1147.29 psi
Delta P Ratio (Total Skin) -1.9519 Fraction

	Main results	Final	
	Company MMB Thesis Well 1	Field X Test Name / # X-1 Real-Time BU Test	
<p>Test date / time</p> <p>Formation interval</p> <p>Perforated interval</p> <p>Gauge type / #</p> <p>Gauge depth</p> <p>Analyzed by</p> <p>Analysis date / time</p>			
TEST TYPE Standard			
<p>Porosity Phi (%) 17</p> <p>Well Radius rw 0.3 ft</p> <p>Pay Zone h 90 ft</p>			
Fluid type Oil			
<p>Volume Factor B 1.66 B/STB</p> <p>Viscosity 0.362 cp</p> <p>Total Compr. C_t 2.22E-5 psi-1</p>			
Default values are used!			
Selected Model			
Model Option Standard Model			
Well Horizontal, Changing Storage (Hegeman)			
Reservoir Homogeneous			
Boundary Infinite			
Top/Bottom No flow/No flow			
Main Model Parameters			
TMatch 4.7 [hr]-1			
PMatch 0.00535 [psia]-1			
C 0.136 bbl/psi			
Total Skin -6.14			
k.h, total 785 md.ft			
k, average 8.72 md			
Pi 3256.03 psia			
Model Parameters			
Well & Wellbore parameters (1)			
C 0.136 bbl/psi			
Ci/Cf 0.809			
delta_t 0.167 hr			
Skin -2.89			
Geometrical Skin -3.25			
well length 1024.51 ft			
Zw 75.4184 ft			
Reservoir & Boundary parameters			
h 90 ft			
Pi 3256.03 psia			
k.h 785 md.ft			
k 8.72 md			
kz/kr 0.0146			
Derived & Secondary Parameters			
Rinv 4410 ft			
Test. Vol. 166.814 MMB			
Delta P (Total Skin) -1147.29 psi			
Delta P Ratio (Total Skin) -1.9519 Fraction			



Semi-Log plot

BU1

Company MMB Thesis
Well 1Field X
Test Name / # X-1 Real-Time BU Test

Fltd data S1 build-up #1
Rate 0 STB/D
Rate change 1211.68 STB/D
P@dt=0 2989.76 psia
Pi 3363 psia
Smoothing 0.1

Default values are used!
Selected Model
Model Option Standard Model
Well Horizontal, Changing Storage (Hegeman)
Homogeneous
Boundary Infinite
Top/Bottom No flow/No flow

Main Model Parameters
TMatch 4.7 [hr]⁻¹
PMatch 0.00763 [psia]⁻¹
C 0.136 bbl/psi
Total Skin -6.14
k.h, total 785 md.ft
k, average 8.72 md
Pi 3363 psia

Model Parameters
Well & Wellbore parameters (1)
C 0.136 bbl/psi
Ci/Cf 0.809
delta_t 0.167 hr
Skin -2.89
Geometrical Skin -3.25
well length 1024.51 ft
Zw 75.4184 ft

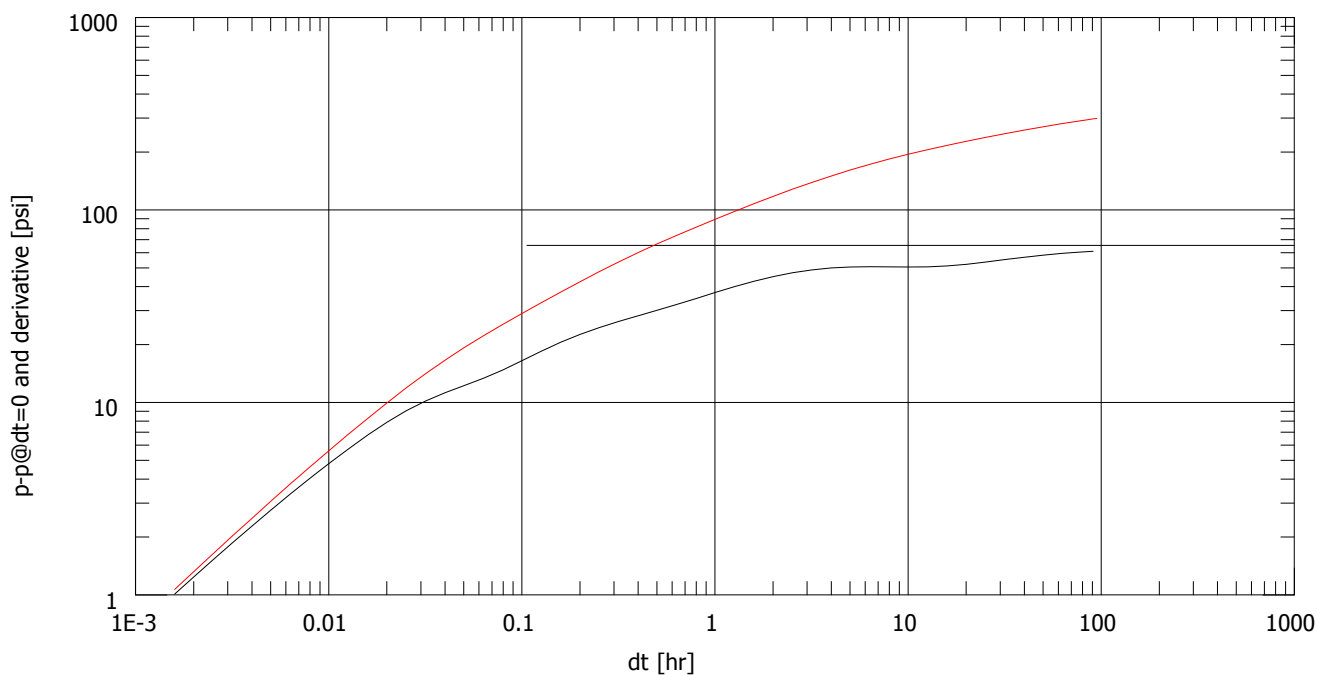
Reservoir & Boundary parameters
h 90 ft Reservoir
Pi 3363 psia
k.h 785 md.ft
k 8.72 md
kz/kr 0.0146

Derived & Secondary Parameters
Rinv 1940 ft
Test. Vol. 32.2881 MMB
Delta P (Total Skin) -804.72 psi
Delta P Ratio (Total Skin) -2.69257 Fraction



Log-Log plot

BU1

Company MMB Thesis
Well 1Field X
Test Name / # X-1 Real-Time BU Test

Fltd data S1 build-up #1
Rate 0 STB/D
Rate change 1211.68 STB/D
 $P@dt=0$ 2989.76 psia
 P_i 3363 psia
Smoothing 0.1

Default values are used!
Selected Model
Model Option Standard Model
Well Horizontal, Changing Storage (Hegeman)
Homogeneous
Boundary Infinite
Top/Bottom No flow/No flow

Main Model Parameters
TMatch 4.7 [hr]⁻¹
PMatch 0.00763 [psia]⁻¹
C 0.136 bbl/psi
Total Skin -6.14
k.h, total 785 md.ft
k, average 8.72 md
 P_i 3363 psia

Model Parameters
Well & Wellbore parameters (1)
C 0.136 bbl/psi
C_i/C_f 0.809
 Δt 0.167 hr
Skin -2.89
Geometrical Skin -3.25
well length 1024.51 ft
Z_w 75.4184 ft

Reservoir & Boundary parameters
h 90 ft Reservoir
 P_i 3363 psia
k.h 785 md.ft
k 8.72 md
kz/kr 0.0146

Derived & Secondary Parameters
R_{inv} 1940 ft
Test. Vol. 32.2881 MMB
 ΔP (Total Skin) -804.72 psi
 ΔP Ratio (Total Skin) -2.69257 Fraction



Main results

BU1

Company MMB Thesis
Well 1Field X
Test Name / # X-1 Real-Time BU TestTest date / time
Formation interval
Perforated interval
Gauge type / #
Gauge depth
Analyzed by
Analysis date / time

TEST TYPE Standard

Porosity Phi (%) 17
Well Radius rw 0.3 ft
Pay Zone h 90 ft

Fluid type Oil

Volume Factor B 1.66 B/STB
Viscosity 0.362 cp
Total Compr. C_t 2.22E-6 psi-1

Default values are used!

Selected Model

Model Option Standard Model
Well Horizontal, Changing Storage (Hegeman)
Reservoir Homogeneous
Boundary Infinite
Top/Bottom No flow/No flow

Main Model Parameters

TMatch 4.7 [hr]-1
PMatch 0.00763 [psia]-1
C 0.136 bbl/psi
Total Skin -6.14
k.h, total 785 md.ft
k, average 8.72 md
Pi 3363 psia

Model Parameters

Well & Wellbore parameters (1)

C 0.136 bbl/psi
Ci/Cf 0.809
delta_t 0.167 hr
Skin -2.89
Geometrical Skin -3.25
well length 1024.51 ft
Zw 75.4184 ft

Reservoir & Boundary parameters

h 90 ft
Pi 3363 psia
k.h 785 md.ft
k 8.72 md
kz/kr 0.0146

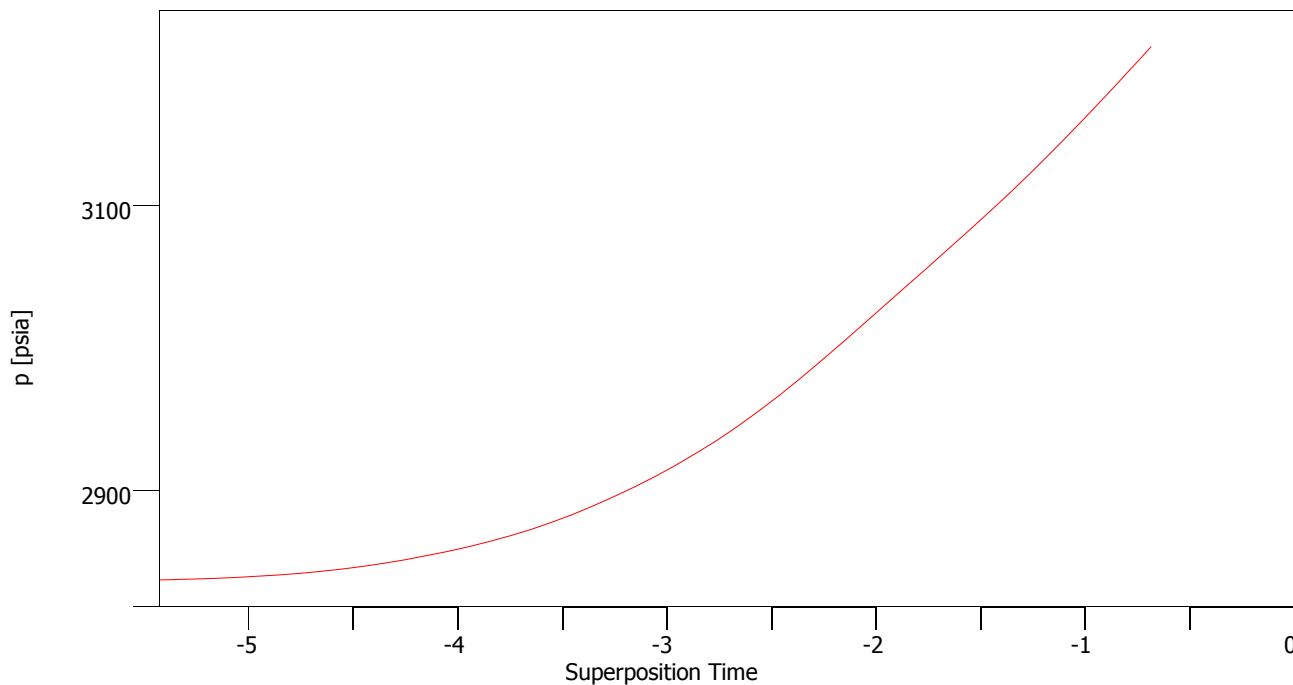
Derived & Secondary Parameters

Rinv 1940 ft
Test. Vol. 32.2881 MMB
Delta P (Total Skin) -804.72 psi
Delta P Ratio (Total Skin) -2.69257 Fraction



Semi-Log plot

BU2

Company MMB Thesis
Well 1Field X
Test Name / # X-1 Real-Time BU Test

Fltd data S1 build-up #2
Rate 0 STB/D
Rate change 1346.3 STB/D
P@dt=0 2835.21 psia
Pi 3324.41 psia
Smoothing 0.1

Default values are used!
Selected Model
Model Option Standard Model
Well Horizontal, Changing Storage (Hegeman)
Reservoir Homogeneous
Boundary Infinite
Top/Bottom No flow/No flow

Main Model Parameters
TMatch 4.7 [hr]⁻¹
PMatch 0.00687 [psia]⁻¹
C 0.136 bbl/psi
Total Skin -6.14
k.h, total 785 md.ft
k, average 8.72 md
Pi 3324.41 psia

Model Parameters
Well & Wellbore parameters (1)
C 0.136 bbl/psi
Ci/Cf 0.809
delta_t 0.167 hr
Skin -2.89
Geometrical Skin -3.25
well length 1024.51 ft
Zw 75.4184 ft

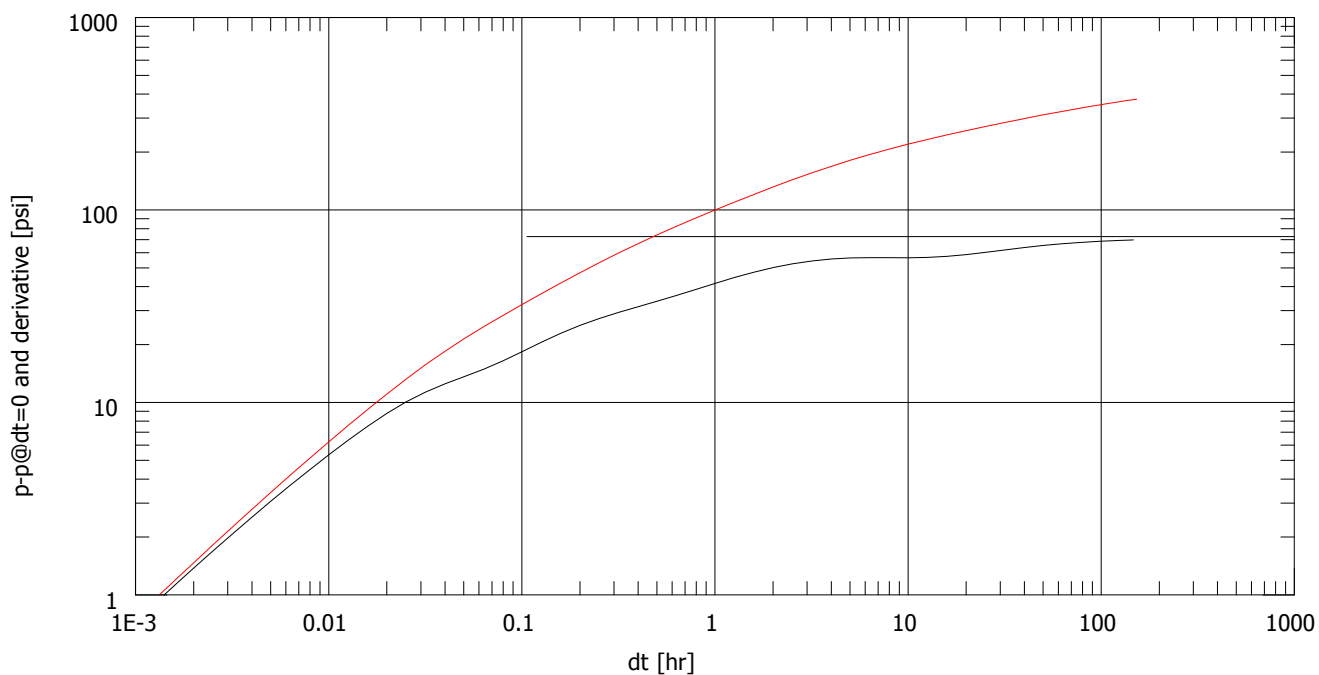
Reservoir & Boundary parameters
h 90 ft
Pi 3324.41 psia
k.h 785 md.ft
k 8.72 md
kz/kr 0.0146

Derived & Secondary Parameters
Rinv 2460 ft
Test. Vol. 51.726 MMB
Delta P (Total Skin) -894.128 psi
Delta P Ratio (Total Skin) -2.37702 Fraction



Log-Log plot

BU2

Company MMB Thesis
Well 1Field X
Test Name / # X-1 Real-Time BU Test

Fltd data S1 build-up #2
Rate 0 STB/D
Rate change 1346.3 STB/D
 $P@dt=0$ 2835.21 psia
 P_i 3324.41 psia
Smoothing 0.1



Default values are used!
Selected Model
Model Option Standard Model
Well Horizontal, Changing Storage (Hegeman)
Reservoir Homogeneous
Boundary Infinite
Top/Bottom No flow/No flow

Main Model Parameters
TMatch 4.7 [hr]⁻¹
PMatch 0.00687 [psia]⁻¹
C 0.136 bbl/psi
Total Skin -6.14
k.h, total 785 md.ft
k, average 8.72 md
 P_i 3324.41 psia

Model Parameters
Well & Wellbore parameters (1)
C 0.136 bbl/psi
C_i/C_f 0.809
 Δt 0.167 hr
Skin -2.89
Geometrical Skin -3.25
well length 1024.51 ft
Z_w 75.4184 ft

Reservoir & Boundary parameters
h 90 ft
 P_i 3324.41 psia
k.h 785 md.ft
k 8.72 md
kz/kr 0.0146

Derived & Secondary Parameters
R_{inv} 2460 ft
Test. Vol. 51.726 MMB
 ΔP (Total Skin) -894.128 psi
 ΔP Ratio (Total Skin) -2.37702 Fraction

	Main results	BU2	
	Company MMB Thesis Well 1	Field X Test Name / # X-1 Real-Time BU Test	
<div> <div> Test date / time Formation interval Perforated interval Gauge type / # Gauge depth Analyzed by Analysis date / time </div> <div> TEST TYPE Standard </div> <div> Porosity Phi (%) 17 Well Radius rw 0.3 ft Pay Zone h 90 ft </div> <div> Fluid type Oil </div> <div> Volume Factor B 1.66 B/STB Viscosity 0.362 cp Total Compr. C_t 2.22E-6 psi-1 </div> <div> Default values are used! Selected Model Model Option Standard Model Well Horizontal, Changing Storage (Hegeman) Reservoir Homogeneous Boundary Infinite Top/Bottom No flow/No flow </div> <div> Main Model Parameters TMatch 4.7 [hr]-1 PMatch 0.00687 [psia]-1 C 0.136 bbl/psi Total Skin -6.14 k.h, total 785 md.ft k, average 8.72 md Pi 3324.41 psia </div> <div> Model Parameters Well & Wellbore parameters (1) C 0.136 bbl/psi Ci/Cf 0.809 delta_t 0.167 hr Skin -2.89 Geometrical Skin -3.25 well length 1024.51 ft Zw 75.4184 ft Reservoir & Boundary parameters h 90 ft Pi 3324.41 psia k.h 785 md.ft k 8.72 md kz/kr 0.0146 </div> <div> Derived & Secondary Parameters Rinv 2460 ft Test. Vol. 51.726 MMB Delta P (Total Skin) -894.128 psi Delta P Ratio (Total Skin) -2.37702 Fraction </div> </div>			

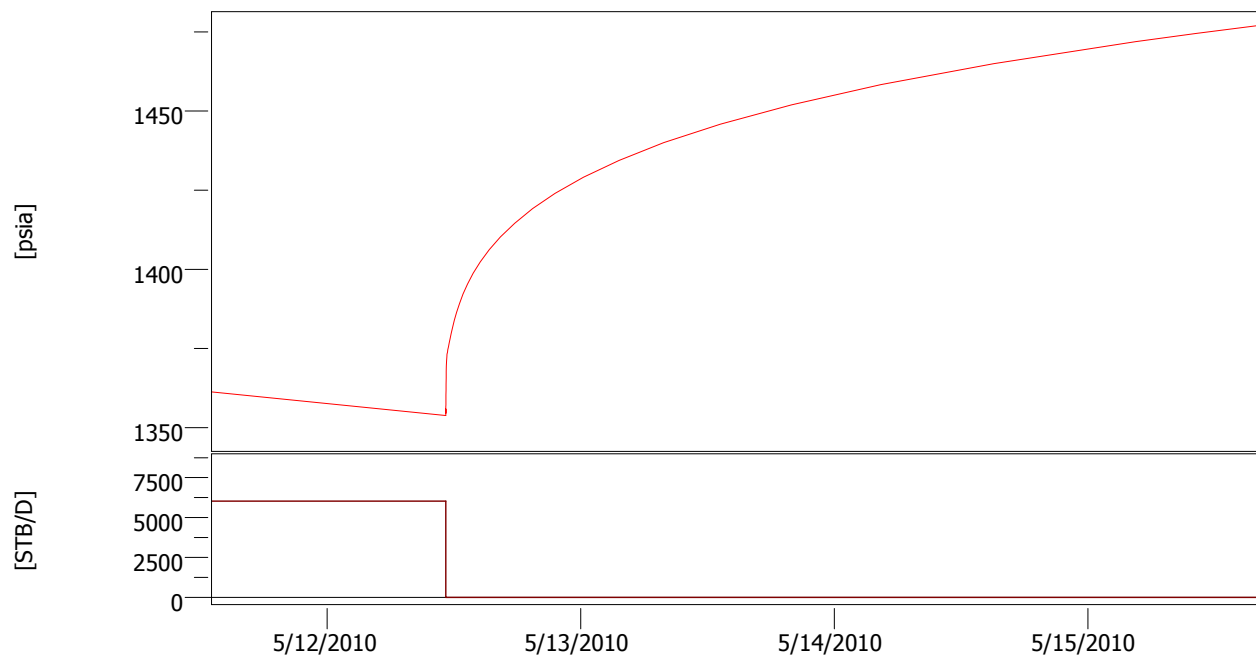
Case # 2

Well: Y-2 Detailed PTA Analysis



History plot

Final

Company MMB Thesis
Well 2Field Y
Test Name / # BU

Pressure [psia], Liquid rate [STB/D] vs Time [ToD]

Fltd data build-up #31
Rate 0 STB/D
Rate change 6032.05 STB/D
P@dt=0 1353.8 psia
Pi 1665.77 psia
Smoothing 0.1

Selected Model
Model Option Standard Model
Well Horizontal, Changing Storage (Hegeman)
Reservoir Homogeneous
Boundary Infinite
Top/Bottom No flow/No flow

Main Model Parameters
TMatch 0.292 [hr]-1
PMatch 0.0058 [psia]-1
C 5.83 bbl/psi
Total Skin -7.01
k.h, total 10600 md.ft
k, average 96.1 md
Pi 1665.77 psia

Model Parameters
Well & Wellbore parameters (2)
C 5.83 bbl/psi
Ci/Cf 0.147
delta_t 0.222 hr
Skin -0.228
Geometrical Skin -6.79
well length 1816.09 ft
Zw 55 ft

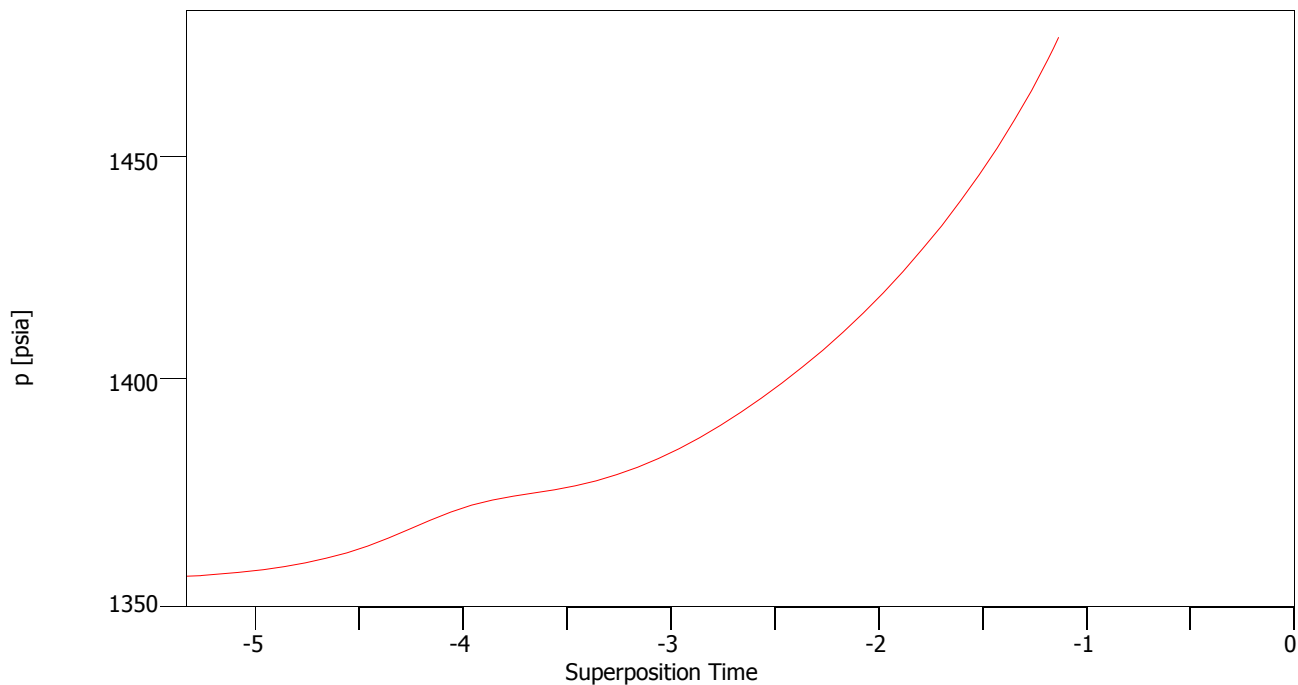
Reservoir & Boundary parameters
h 110 ft
Pi 1665.77 psia
k.h 10600 md.ft
k 96.1 md
kz/kr 0.421

Derived & Secondary Parameters
Rinv 785 ft
Test. Vol. 6.82907 MMB
Delta P (Total Skin) -1208.28 psi
Delta P Ratio (Total Skin) -9.81085 Fraction



Semi-Log plot

Final

Company MMB Thesis
Well 2Field Y
Test Name / # BU

Fltd data build-up #31
Rate 0 STB/D
Rate change 6032.05 STB/D
P@dt=0 1353.8 psia
Pi 1665.77 psia
Smoothing 0.1

Selected Model
Model Option Standard Model
Well Horizontal, Changing Storage (Hegeman)
Reservoir Homogeneous
Boundary Infinite
Top/Bottom No flow/No flow

Main Model Parameters
TMatch 0.292 [hr]⁻¹
PMatch 0.0058 [psia]⁻¹
C 5.83 bbl/psi
Total Skin -7.01
k.h, total 10600 md.ft
k, average 96.1 md
Pi 1665.77 psia

Model Parameters
Well & Wellbore parameters (2)
C 5.83 bbl/psi
Ci/Cf 0.147
delta_t 0.222 hr
Skin -0.228
Geometrical Skin -6.79
well length 1816.09 ft
Zw 55 ft

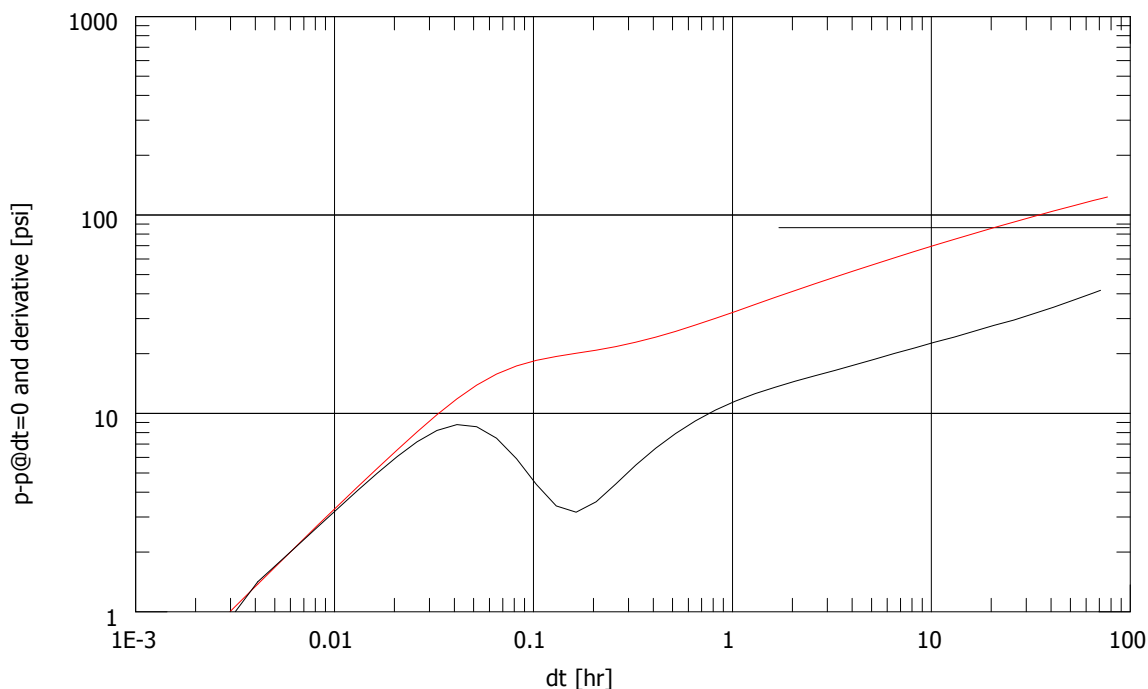
Reservoir & Boundary parameters
h 110 ft
Pi 1665.77 psia
k.h 10600 md.ft
k 96.1 md
kz/kr 0.421

Derived & Secondary Parameters
Rinv 785 ft
Test. Vol. 6.82907 MMB
Delta P (Total Skin) -1208.28 psi
Delta P Ratio (Total Skin) -9.81085 Fraction



Log-Log plot

Final

Company MMB Thesis
Well 2Field Y
Test Name / # BU

Fltd data build-up #31
Rate 0 STB/D
Rate change 6032.05 STB/D
P@dt=0 1353.8 psia
Pi 1665.77 psia
Smoothing 0.1



Selected Model
Model Option Standard Model
Well Horizontal, Changing Storage (Hegeman)
Reservoir Homogeneous
Boundary Infinite
Top/Bottom No flow/No flow



Main Model Parameters
TMatch 0.292 [hr]⁻¹
PMatch 0.0058 [psia]⁻¹
C 5.83 bbl/psi
Total Skin -7.01
k.h, total 10600 md.ft
k, average 96.1 md
Pi 1665.77 psia

Model Parameters
Well & Wellbore parameters (2)
C 5.83 bbl/psi
Ci/Cf 0.147
delta_t 0.222 hr
Skin -0.228
Geometrical Skin -6.79
well length 1816.09 ft
Zw 55 ft

Reservoir & Boundary parameters
h 110 ft
Pi 1665.77 psia
k.h 10600 md.ft
k 96.1 md
kz/kr 0.421

Derived & Secondary Parameters
Rinv 785 ft
Test. Vol. 6.82907 MMB
Delta P (Total Skin) -1208.28 psi
Delta P Ratio (Total Skin) -9.81085 Fraction

	Main results	Final	
	Company MMB Thesis Well 2	Field Y Test Name / # BU	
<p>Test date / time</p> <p>Formation interval</p> <p>Perforated interval</p> <p>Gauge type / #</p> <p>Gauge depth</p> <p>Analyzed by</p> <p>Analysis date / time</p>			
TEST TYPE Standard			
<p>Porosity Phi (%) 18</p> <p>Well Radius rw 0.3542 ft</p> <p>Pay Zone h 110 ft</p>			
Fluid type Oil			
<p>Volume Factor B 1.168 B/STB</p> <p>Viscosity 1.83 cp</p> <p>Total Compr. C_t 1.11E-5 psi-1</p>			
Selected Model			
Model Option Standard Model			
Well Horizontal, Changing Storage (Hegeman)			
Reservoir Homogeneous			
Boundary Infinite			
Top/Bottom No flow/No flow			
Main Model Parameters			
TMatch 0.292 [hr]-1			
PMatch 0.0058 [psia]-1			
C 5.83 bbl/psi			
Total Skin -7.01			
k.h, total 10600 md.ft			
k, average 96.1 md			
Pi 1665.77 psia			
Model Parameters			
Well & Wellbore parameters (2)			
C 5.83 bbl/psi			
Ci/Cf 0.147			
delta_t 0.222 hr			
Skin -0.228			
Geometrical Skin -6.79			
well length 1816.09 ft			
Zw 55 ft			
Reservoir & Boundary parameters			
h 110 ft			
Pi 1665.77 psia			
k.h 10600 md.ft			
k 96.1 md			
kz/kr 0.421			
Derived & Secondary Parameters			
Rinv 785 ft			
Test. Vol. 6.82907 MMB			
Delta P (Total Skin) -1208.28 psi			
Delta P Ratio (Total Skin) -9.81085 Fraction			

	Main results	Pre-Acid	
	Company MMB Thesis Well 2	Field Y Test Name / # BU	

Test date / time
 Formation interval
 Perforated interval
 Gauge type / #
 Gauge depth
 Analyzed by
 Analysis date / time

TEST TYPE Standard

Porosity Phi (%) 18
 Well Radius rw 0.3542 ft
 Pay Zone h 110 ft

Fluid type Oil

Volume Factor B 1.168 B/STB
 Viscosity 1.83 cp
 Total Compr. C_t 1.11E-5 psi-1

Main Model Parameters
 TMatch 194 [hr]-1
 PMatch 0.0207 [psia]-1
 C 0.0306 bbl/psi
 k.h, total 36700 md.ft
 k, average 334 md
 Pi 1665.77 psia

Derived & Secondary Parameters
 Rinv 2870 ft
 Test. Vol. 91.2843 MMB

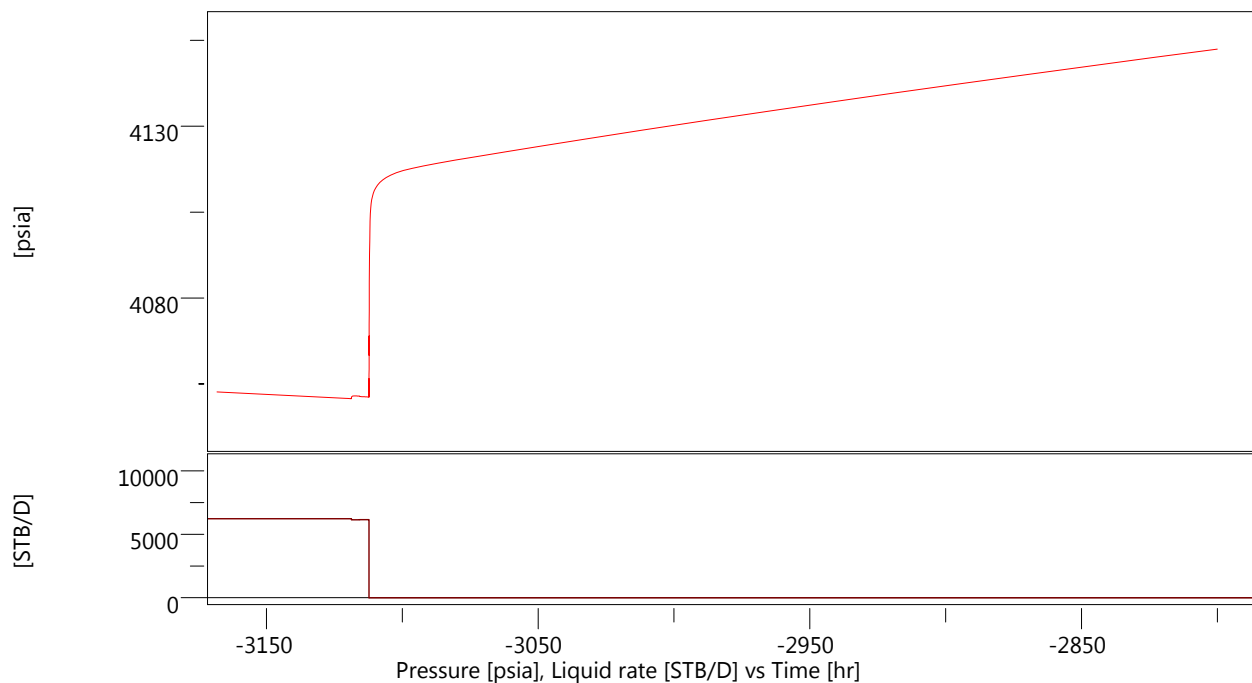
Case # 3

Well: Z-3 Detailed PTA Analysis



History plot

Composite

Company MMB Thesis
Well 3Field Z
Test Name / # BU

Fltd data #3 build-up #1

Rate 0 STB/D
Rate change 6158.73 STB/D
P@dt=0 4051.2 psia
Pi 4510.86 psia
Smoothing 0.1

Selected Model

Model Option Standard Model
Well Vertical
Reservoir Radial composite
Boundary Infinite

Main Model Parameters

TMatch 71.2 [hr]⁻¹
PMatch 0.159 [psia]⁻¹
C 0.681 bbl/psi
Total Skin 1.33
k.h, total 1.23E+5 md.ft
k, average 587 md
Pi 4510.86 psia

Model Parameters

Well & Wellbore parameters (3)

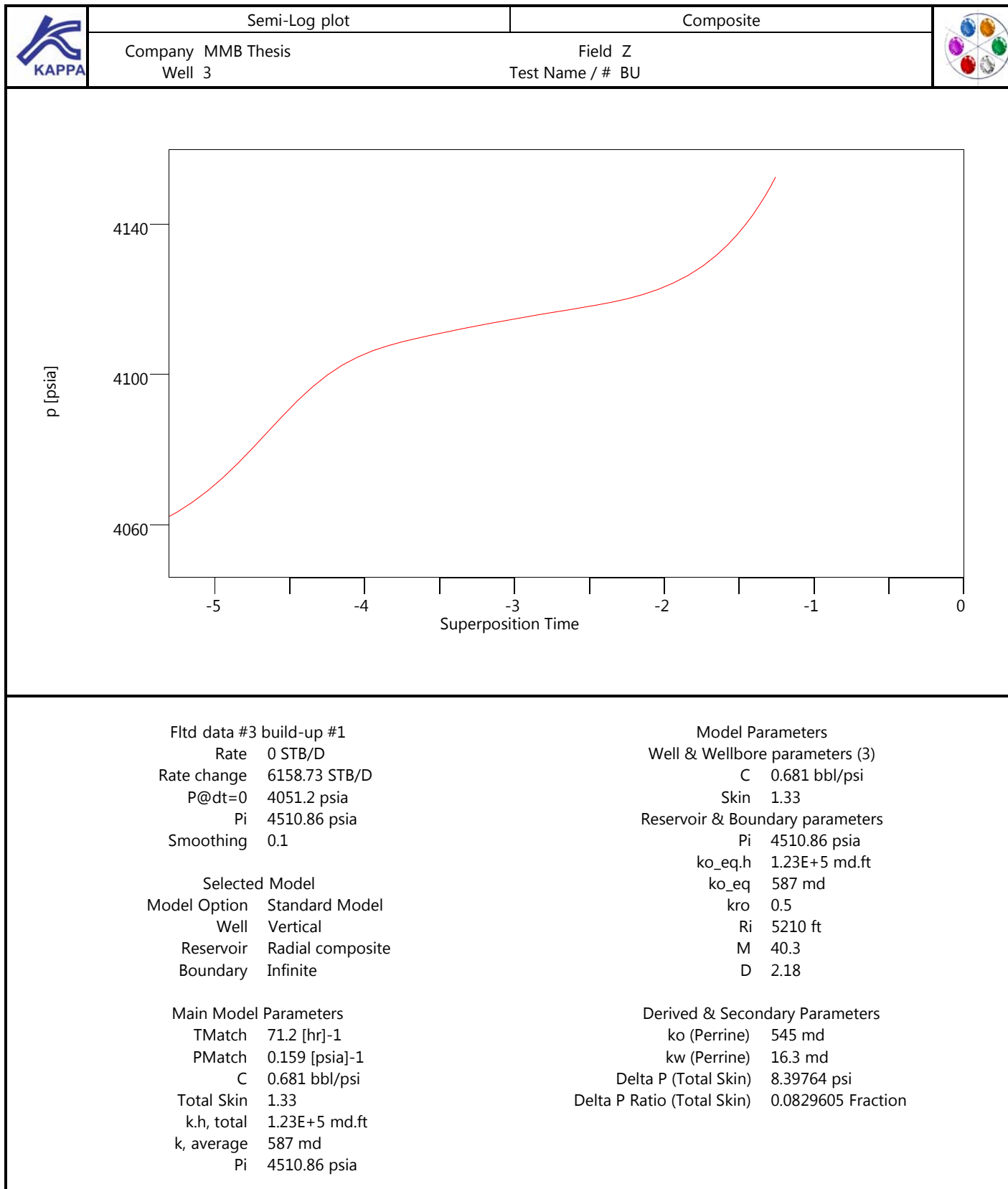
C 0.681 bbl/psi
Skin 1.33

Reservoir & Boundary parameters

Pi 4510.86 psia
ko_eq.h 1.23E+5 md.ft
ko_eq 587 md
kro 0.5
Ri 5210 ft
M 40.3
D 2.18

Derived & Secondary Parameters

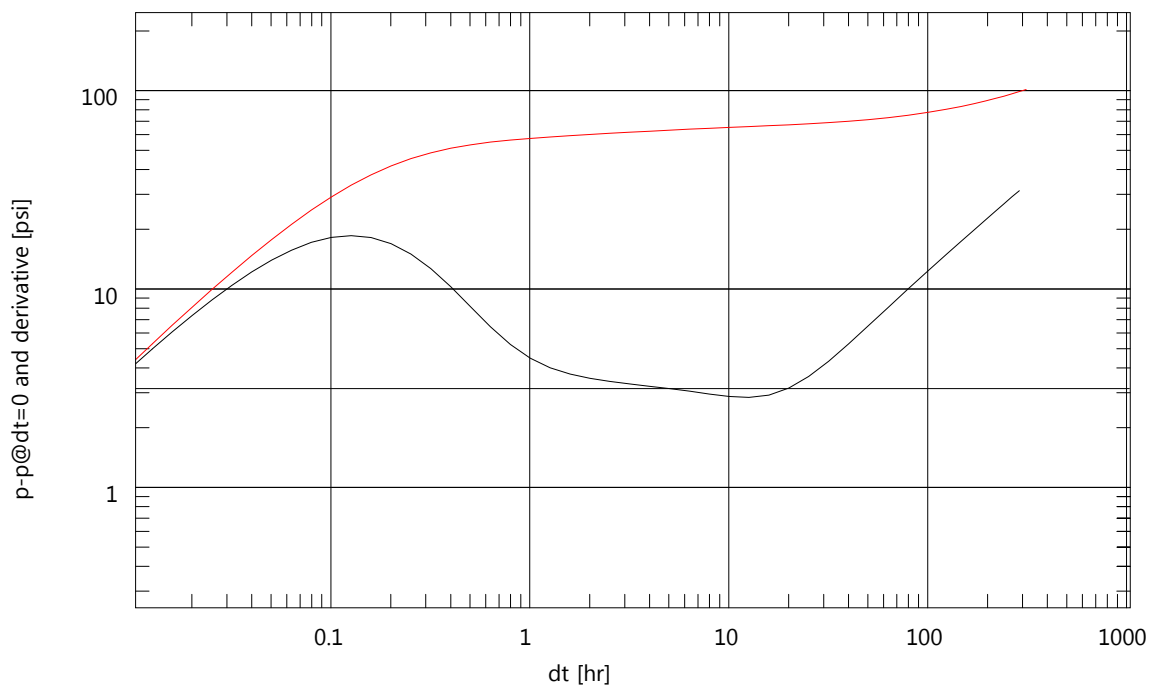
ko (Perrine) 545 md
kw (Perrine) 16.3 md
Delta P (Total Skin) 8.39764 psi
Delta P Ratio (Total Skin) 0.0829605 Fraction





Log-Log plot

Composite

Company MMB Thesis
Well 3Field Z
Test Name / # BU

Fltd data #3 build-up #1

Rate 0 STB/D
Rate change 6158.73 STB/D
P@dt=0 4051.2 psia
Pi 4510.86 psia
Smoothing 0.1

Selected Model

Model Option Standard Model
Well Vertical
Reservoir Radial composite
Boundary Infinite

Main Model Parameters

TMatch 71.2 [hr]⁻¹
PMatch 0.159 [psia]⁻¹
C 0.681 bbl/psi
Total Skin 1.33
k.h, total 1.23E+5 md.ft
k, average 587 md
Pi 4510.86 psia

Model Parameters

Well & Wellbore parameters (3)

C 0.681 bbl/psi
Skin 1.33

Reservoir & Boundary parameters

Pi 4510.86 psia
ko_eq.h 1.23E+5 md.ft
ko_eq 587 md
kro 0.5
Ri 5210 ft
M 40.3
D 2.18

Derived & Secondary Parameters

ko (Perrine) 545 md
kw (Perrine) 16.3 md
Delta P (Total Skin) 8.39764 psi
Delta P Ratio (Total Skin) 0.0829605 Fraction

CURRICULUM VITAE



Name: Meshal Mohammad Al Buraikan

Nationality: Saudi

E-mail: meshal.buraikan@aramco.com

Address: Post Office Box # 5239
Dhahran 31311
Eastern Province, Saudi Arabia

Education: Bachelor of Science in Computer Engineering, 2001
King Fahd University of Petroleum & Minerals,
Dhahran 31261, Saudi Arabia.

Master of Science in Petroleum Engineering, 2011
King Fahd University of Petroleum & Minerals
Dhahran 31261, Saudi Arabia.

Areas of Interest: Well Testing, Reservoir Management

Professional Affiliations: Society of Petroleum Engineers (SPE)

Experience: Joined Saudi Aramco in January 2002. Worked in different organizations within the company including; Simulation Systems, Reservoir Engineering Systems, Reservoir Management, Well Testing Analysis, Well Testing Operations, and lastly in the I-Field and Producing Systems Division as the supervisor of the I-Field Systems Development Group.